



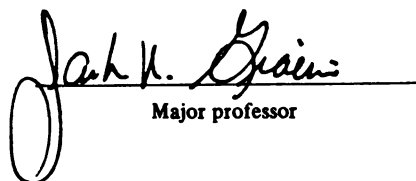
This is to certify that the
thesis entitled
THE PERMEABILITY OF BINARY ORGANIC VAPOR MIXTURES
THROUGH POLYMER MEMBRANES BY A DYNAMIC PURGE AND
TRAP/THERMAL DESORPTION PROCEDURE: THEORETICAL AND
PRACTICAL CONSIDERATIONS

presented by

TEERAPONG LAOHARAVEE

has been accepted towards fulfillment
of the requirements for

MASTER degree in PACKAGING


Major professor

Date FEBRUARY 19, 1998



PLACE IN RETURN BOX
to remove this checkout from your record.
TO AVOID FINES return on or before date due.

| DATE DUE | DATE DUE | DATE DUE |
|----------------------------|----------|----------|
| JAN 11 2000 JAN 11 2000 | | |
| FEB 04 2007 | | |
| | | |
| | | |
| | | |
| | | |

**THE PERMEABILITY OF BINARY ORGANIC VAPOR MIXTURES
THROUGH POLYMER MEMBRANES BY A DYNAMIC PURGE AND
TRAP/THERMAL DESORPTION PROCEDURE: THEORETICAL AND
PRACTICAL CONSIDERATIONS**

By

Teerapong Laoharavee

A THESIS

Submitted to
Michigan State University
In partial fulfillment of the requirements
For the degree of

MASTER OF SCIENCE

School of Packaging

1998

ABSTRACT

THE PERMEABILITY OF BINARY ORGANIC VAPOR MIXTURES THROUGH POLYMER MEMBRANES BY A DYNAMIC PURGE AND TRAP/THERMAL DESORPTION PROCEDURE: THEORETICAL AND PRACTICAL CONSIDERATIONS

By

Teerapong Laoharavee

This study was designed to determine the effect of varying concentrations of organic vapors alone, and in binary mixtures on the barrier properties of an oriented polypropylene film and a high barrier PVdC coated oriented polypropylene film. The permeability tests were carried out at 50°C for OPP and 60°C for PVdC coated OPP film. The results obtained indicated that the permeants; ethyl butyrate, ethyl acetate and d-limonene showed minimal concentration dependency for the mass transfer parameters within the vapor activity ranges studied for the two test membranes. The effect of a co-permeant on the permeability of binary mixtures through OPP film and the PVdC coated OPP film was studied by determining the permeation rate of the constituents of a series of binary mixtures of varying compositions using the dynamic purge and trap/thermal desorption procedure. When combined in a series of binary mixtures, the constituents of the mixtures showed little propensity of altering the transport properties of the co-permeant.

Delicated to My Parents

ACKNOWLEDGMENTS

I would like to express my appreciation, first of all, to Dr. Jack Giacin for his persistent support, guidance, and serving as my thesis advisor. Special thanks also goes to Dr. Susan Selke and Dr. Krishnamurthy Jayaraman for their valuable critical review of this thesis. Acknowledgement is given to CFPPR for financial support, Mobil Chemical Co., Film Division for supplying materials, and MAS Technology Co. for proper advise on the instrument.

In addition, a special thanks to my parents for providing financial support throughout the entire study at Michigan State University.

TABLE OF CONTENTS

| | |
|------------------------------------------------------------------|-------------|
| LIST OF TABLES..... | viii |
| LIST OF FIGURES | x |
| INTRODUCTION | 1 |
| LITERATURE REVIEW | 7 |
| Mathematical Model Describing the Transport Process | 7 |
| Steady State Permeation in a Plane Sheet | 9 |
| Sorption Mechanism through Polymer Membrane | 11 |
| Diffusion Mechanism through Polymer Membrane | 15 |
| Factors Affecting the Permeation Process | 17 |
| Temperature | 17 |
| Concentration | 20 |
| Nature of Penetrant | 22 |
| Nature of Polymer | 24 |
| Permeation of Binary Mixtures | 26 |
| Permeation Measurement Procedure and Technique | 30 |
| Dynamic Purge and Trap/Thermal Desorption Technique | 33 |
| MATERIALS AND METHODS | 35 |
| Materials and Equipment | 36 |

| | |
|-----------------------------------------------------------------------------------------------------------------------------------------------------------|-----------|
| Methods | 38 |
| Calibration Curves of d-Limonene, Ethyl Butyrate, and Ethyl Acetate by Gas Chromatography Analysis: Preparation and Testing | 38 |
| Calibration Curves for Dynamic Purge and Trap/Thermal Desorption Procedure | 41 |
| Permeability Test System | 43 |
| Permeability Measurements | 45 |
| Dynamic Purge and Trap/Thermal Desorption Procedure | 48 |
| Analysis of Test Permeant by Thermal Desorption/Gas Chromatography Procedure | 49 |
| RESULTS AND DISCUSSION | 51 |
| Comparison between MAS2000™ Isostatic Test Procedure and Dynamic Purge and Trap/Thermal Desorption Procedure | 51 |
| Estimation of the Detection Sensitivity Limit Between the Two Procedures | 51 |
| Comparison of Permeability Values Between the MAS 2000™ Isostatic Test Procedure and the Dynamic Purge and Trap/Thermal Desorption Procedure | 52 |
| Effect of Vapor Activity on the Organic Vapor Diffusion and Permeability Analyzed by Isostatic Permeability Test Procedure | 57 |
| The Effect of Binary Mixtures Composition on Co-permeant Permeability | 69 |
| Statistical Analysis of Binary Mixture Permeability Studies | 83 |
| SUMMARY AND CONCLUSIONS | 85 |
| FUTURE STUDY | 87 |
| APPENDICES..... | 89 |
| Gas Chromatograph Calibration Procedure | 89 |
| Dynamic Purge and Trap/Thermal Desorption Calibration Procedure | 93 |

| | |
|--------------------------------------------------------------------------------------------------------------------------------|-----|
| Calibration Curve of Carrier Gas Flow Rate Versus Permeant Vapor Activity ... | 95 |
| Method of Calculating $l^2/4Dt$ for each Value of $(\Delta M/\Delta t)_t/(\Delta M/\Delta t)_\infty$ from Equation 32 | 97 |
| Statistical Analysis of P, D, and S as a Function of Permeant Vapor Activity ... | 98 |
| Statistical Analysis of Binary Mixture Permeability Studies | 102 |
| BIBLIOGRAPHY | 106 |

LIST OF TABLES

| | |
|-----------------------------------------------------------------------------------------------------------------------------------------------------------------------------------------------|----|
| Table 1 - Estimated lowest measurable transmission rate between the two procedures | 52 |
| Table 2 - Permeability coefficient, $\text{kg m/m}^2 \text{ s Pa} \times 10^{-15}$, of limonene through OPP film (50°C) determined by the two procedures | 53 |
| Table 3 - Permeability coefficient, $\text{kg m/m}^2 \text{ s Pa} \times 10^{-15}$, of ethyl butyrate through OPP film (50°C) determined by the two procedures | 53 |
| Table 4 - Permeability coefficient, $\text{kg m/m}^2 \text{ s Pa} \times 10^{-16}$, of ethyl acetate through OPP film (50°C) determined by the two procedures | 53 |
| Table 5 - Permeance, $\text{kg /m}^2 \text{ s Pa} \times 10^{-13}$, of limonene through PVdC coated OPP film (60°C) determined by the two procedures | 56 |
| Table 6 - Permeance, $\text{kg /m}^2 \text{ s Pa} \times 10^{-13}$, of ethyl butyrate through PVdC coated OPP film (60°C) determined by the two procedures | 56 |
| Table 7 - Permeability and diffusion coefficients for limonene through the two test films | 59 |
| Table 8 - Solubility coefficient values for limonene and the estimated % sorbed (v/v) in the two test films | 59 |
| Table 9 - Permeability and diffusion coefficients for ethyl butyrate through the two test films | 59 |
| Table 10 - Solubility coefficient values for ethyl butyrate and the estimated % sorbed (v/v) through the two test films | 60 |
| Table 11 - Permeability, diffusion and solubility coefficient values and the estimated % permeant sorbed for ethyl acetate through OPP film at 50°C | 60 |
| Table 12 - The Hildebrand solubility parameters (δ) values | 68 |
| Table 13 - The permeability coefficient, $\text{kg m/s m}^2 \text{ Pa} \times 10^{-15}$, of limonene through OPP film (50°C) as a single permeant and in binary mixtures with ethyl butyrate | |

| | |
|----------------------------------------------------------------------------------------------------------------------------------------------------------------------------------------------------|----|
| and ethyl acetate | 70 |
| Table 14 - The permeability coefficient, $\text{kg m/s m}^2 \text{ Pa} \times 10^{-15}$, of ethyl butyrate through OPP film (50°C) as a single permeant and in binary mixture with limonene | 70 |
| Table 15 - The permeance, $\text{kg/s m}^2 \text{ Pa} \times 10^{-13}$, of limonene through PVdC coated OPP film (60°C) as a single permeant and in binary mixtures with ethyl butyrate | 71 |
| Table 16 - The permeance, $\text{kg/s m}^2 \text{ Pa} \times 10^{-12}$, of ethyl butyrate through PVdC coated OPP film (60°C) as a single permeant and in binary mixtures with d-limonene | 71 |
| Table 17 - Permeation ratios in OPP film (50°C) for individual components of the binary mixtures..... | 79 |
| Table 18 - Permeation ratios in PVdC coated OPP film (60°C) for individual components of the binary mixtures | 80 |
| Table 19 - The permeability coefficient, $\text{kg m/s m}^2 \text{ Pa} \times 10^{-16}$, of ethyl acetate through OPP film (50°C) in single permeant and in binary mixture with limonene ... | 81 |
| Table 20 - The solution of ethyl butyrate and d-limonene in CCl_4 | 89 |
| Table 21 - Calibration data of ethyl butyrate and d-limonene by gas chromatograph | 89 |
| Table 22 - Calibration data of ethyl acetate by gas chromatograph | 90 |
| Table 23 - Calibration data of ethyl butyrate and d-limonene for dynamic purge and trap/thermal desorption procedure | 92 |
| Table 24 - Calibration data of ethyl acetate for dynamic purge and trap/thermal desorption procedure | 92 |

LIST OF FIGURES

| | |
|------------------------------------------------------------------------------------------------------------------------------------------------------|----|
| Figure 1 - Control Volume Element (taken from Crank, 1975) | 8 |
| Figure 2 - Permeation through a film at steady state | 10 |
| Figure 3 - Characteristic isotherms plots described by Langmuir, Flory Huggins, and BET equations. (taken from Roger, 1985) | 13 |
| Figure 4 - Schematic diagram of permeation test and trap apparatus | 46 |
| Figure 5 - Comparison of permeability of organic vapors through OPP film by MAS2000 TM and DPT/TD procedures (50°C) | 54 |
| Figure 6 - Comparison between MAS2000 TM and DPT/TD procedures: organic vapor permeation through PVdC coated OPP film (60°C) | 55 |
| Figure 7 - Diffusion of organic vapors through OPP film as a function of vapor activity (50°C) | 61 |
| Figure 8 - Apparent diffusion coefficient of organic vapors through PVdC coated OPP as a function of vapor activity | 62 |
| Figure 9 - Solubility coefficient of organic vapors in OPP film as a function of vapor concentration (50°C) | 63 |
| Figure 10 - Solubility coefficient of organic vapors in PVdC coated OPP film as a function of vapor concentration | 64 |
| Figure 11 - Diffusivities of organic vapors through OPP at 50°C as a function of penetrant molar volume | 67 |
| Figure 12 - Effect of ethyl butyrate on permeability of d-limonene through OPP as a function of binary mixture composition (50°C) | 72 |
| Figure 13 - Effect of ethyl butyrate on permeation rate of d-limonene through PVdC/OPP film as a function of binary mixture composition (60°C) | 73 |
| Figure 14 - Effect of d-limonene on the permeation rate of ethyl butyrate through OPP as | |

| | |
|-------------------------------------------------------------------------------------------------------------------------------------------------------------------------------------------------------|----|
| a function of binary mixture composition (50°C) | 74 |
| Figure 15 - Effect of d-limonene on the permeation rate of ethyl butyrate through PVdC/OPP film as a function of binary mixture composition (60°C) | 75 |
| Figure 16 - Transmission profiles of binary mixture composition of d-limonene, a=0.05/ ethyl butyrate a=0.04 and its respective individual permeants through OPP film (50°C) | 77 |
| Figure 17 - Transmission profiles of binary mixture composition of d-limonene, a=0.2 and ethyl butyrate a=0.2 and its respective individual permeants through PVdC coated OPP film (60°C) | 78 |
| Figure 18 - Calibration curve of ethyl butyrate for setting vapor activity | 90 |
| Figure 19 - Calibration curve of d-limonene for setting vapor activity | 91 |
| Figure 20 - Calibration curve of ethyl acetate for setting vapor activity | 91 |
| Figure 21 - Calibration curve of ethyl butyrate for dynamic purge and trap/thermal desorption procedure | 93 |
| Figure 22 - Calibration curve of d-limonene for dynamic purge and trap/thermal desorption procedure | 93 |
| Figure 23 - Calibration curve of ethyl acetate for dynamic purge and trap/thermal desorption procedure | 94 |
| Figure 24 - Calibration curve of carrier gas flow rate versus limonene vapor activity ... | 95 |
| Figure 25 - Calibration curve of carrier gas flow rate versus ethyl butyrate and ethyl acetate vapor activity | 96 |

INTRODUCTION

The use of polymeric materials in food packaging has been increasing in the past few decades and is expected to continue to increase into the next century. Unlike paper, glass, or metal, polymeric materials are capable of tailor-made properties to provide light weight, coupled with strength, lower costs, and flexible shaped packages. Optimal packaging design requires not only protection from the surrounding environment but also compatibility with specific foods to prolong changes in product color, texture, surface structure, aroma, smell and taste, until the time of consumption (Koszinowski, 1987).

Because of their molecular nature, polymeric materials can allow relatively high rates of diffusion of gases and vapors through the package, resulting in degradation of the contained food product. The shelf life of certain food products, based solely on the prevention of individual permanent gases, such as oxygen and carbon dioxide permeating both into and out of packages, can be successfully described and predicted by a simple shelf life model (Salame, 1996). This is due to the well defined transport behavior of a permanent gas, a gas that is not easily condensable and small, as compared to the monomer unit of a polymer. The non-interactive nature of permanent gases with a polymer results in their diffusion and solubility coefficients being independent of concentration. These two parameters are related to the permeability coefficient, by the relationship $P = D \times S$, where D and S are the diffusion and solubility coefficients, respectively. The permeability coefficient, P , is defined as the amount of substance

passing through a polymer film of unit thickness, per unit time, per unit area, and at a unit pressure difference across the film. The diffusion coefficient is a kinetic term that describes how fast a permeant molecule moves through a unit area of a polymer film or slab. The solubility coefficient is a thermodynamic term that describes the amount of a substance that will be sorbed by a polymer. Both experimental data and techniques for estimating these parameters for permanent gases and small organic molecules in various polymers have been reported in the literature (Van Krevelen, 1976; Brandrup, 1975; Salame, 1986).

Today, the packaging of a food product to prevent deterioration of its original flavor and aroma presents a challenging problem to packaging engineers. Flavors are either composed of the same organic compounds with different proportions, or are specific and dependent on distinctive chemical entities and structures for their characteristic profile (Rohan, 1970). These molecules are usually present in extremely low quantities; often less than one part per million, but are responsible for the unique flavor of a particular food (Strandburg et. al., 1991). The interaction of these organic molecules with a polymeric packaging structure, through permeation and/or sorption, can cause an imbalance in concentration of certain organic compounds, leading to an off-flavor taste and resulting in a shorter shelf life for the product. The prediction of shelf life, based on the flavor and aroma retention in food packaging, is complicated due to the strong interaction between these organic compounds and a polymeric packaging structure. Thus, making it difficult to monitor a flavor profile in plastic packages.

Permeation of gases and organic vapors through polymer membranes includes diffusion and sorption mechanisms, which are dependent upon a number of parameters. According to Fujita (1968), the diffusion of permanent gases (i.e. O₂, H₂, etc.) is independent of sorbed permeant concentration, because the small molecular size and chemical inertness of these compounds allow them to move freely within the polymer matrix, without requiring segmental mobility of the polymer chain. The diffusion mechanism for molecules that have a size comparable to the monomer unit of a polymer, on the other hand, requires a co-operative movement by the micro-Brownian motion of several monomer units to take place. As a result, their diffusion coefficients are primarily controlled by the mobility of the polymer segmental unit. Factors that enhance polymer segmental mobility, increase the average interchain distance, and weaken the molecular interaction between neighboring polymer molecules, lead to an increase in permeant diffusion. Therefore, the diffusion coefficient of organic vapors in polymer membranes generally increases with increasing sorbed permeant concentration and temperature.

Sorption of permeant molecules in a polymer may be described by one or more different types of sorption modes occurring concurrently, such as those that can be described by Henry's law, the Langmuir equation, the Flory-Huggins equation and the Brunauer, Emmett, Teller (BET) equation. Henry's law is the common sorption mode for permanent gases and small organic vapor molecules at a partial pressure up to 1 atmospheric (Stannett, 1968). It is the simplest case, where the solubility coefficient is independent of sorbed penetrant concentration and does not violate the $P=D \times S$ relationship. In general, temperature, sorbed permeant concentration, polymer

morphology and the functionality of the polymer, as well as the size and functional groups of the permeant molecule, affect the sorption and diffusion processes.

A study by Hensley et al.(1991) involving the permeation of ethyl acetate/limonene binary mixtures through an oriented polypropylene film showed that the permeation rate for the mixture was significantly higher than the sum of the transmission rates for the individual pure components. At the lower activity levels, the increased permeation rate was attributed to the transmission rate of ethyl acetate, which increased significantly in the presence of limonene. The transmission rate of limonene only showed a significant increase, as compared to the permeability of pure limonene at a similar activity level, when the vapor activity level of ethyl acetate, as a co-permeant, was at a high vapor activity level ($a=0.48$).

In a recent study on the sorption of ethyl acetate/limonene binary mixtures by oriented polypropylene, Nielson and Giacin (1994) reported that for ethyl acetate/limonene binary mixtures, limonene as a co-penetrant appears to have little or no effect on the solubility of ethyl acetate in oriented polypropylene film, while significantly changing the inherent mobility of ethyl acetate within the polymer bulk phase. This accounts for the observed increase in the transmission rates for ethyl acetate through the OPP film in the presence of limonene, as reported by Hensley et al. (1991).

While not fully understood, Nielson and Giacin proposed that there may be co-penetrant induced relaxation effects occurring during the diffusion of ethyl acetate/limonene binary mixtures in the oriented polypropylene film investigated. Such relaxation processes, which occur over a longer time-scale than diffusion, may be related to a structural reordering of the free volume elements in the polymer. Such processes are

believed to provide additional sites of appropriate size and frequency of formation, which promote diffusion and account for the observed increase in the permeation rate of ethyl acetate in the presence of limonene as a co-permeant.

A review of the literature shows a paucity of data on the permeation of multi-component mixtures of organic liquids and vapors through barrier membranes (Li et al., 1965; Huang and Lin, 1968; Weinberg, 1976; Michelson et al., 1985; Hensley et al., 1991). This lack of data can be attributed to the complexities involved with organic vapor mixtures exposed to plastics, as well as to the lack of commercial instrumentation that allows the separation and detection of individual components of multi-component penetrant mixtures. DeLassus et al. (1988) alluded briefly to the transport of apple aroma in polymer films, where the permeation of binary organic vapor mixtures in low density polyethylene was studied. Such studies would be more representative of an actual product/package system, where the product aroma profile contains numerous volatile components.

In addition to the lack of data on the permeability of organic vapor mixtures through barrier films, only Hensley et al. (1991) have reported on the concentration dependency of the permeability of organic vapor mixtures, and the effect of the relative concentration of individual components of the vapor mixture on the transport of each particular penetrant comprising the mixture.

The present study therefore focuses specifically on developing a methodology for determining the permeability of binary organic vapor mixtures of varying composition through a polymeric barrier film, and considers the non-ideality of the mass transfer process, as indicated by the permeation ratio.

The specific objectives of the study include:

- 1) Evaluate and compare the permeability data from a dynamic purge and trap/thermal desorption procedure to the data obtained from the MAS 2000™ organic permeability tester.
- 2) Evaluate the concentration dependence of the transport process of the individual permeants selected for study.
- 3) Evaluate the effect of co-permeants on the diffusivity of the respective individual penetrants through the test barrier polymer structures.
- 4) Utilize data obtained from the permeability studies to develop a better understanding of the mechanism and the variables, which affect the diffusivity of organic penetrants in barrier polymer films. In particular, the effect of penetration (i.e. sorption) of the barrier polymers by a constituent of the binary organic vapor mixture, on the transport properties of the polymer will be addressed, as indicated by the permeation ratio.

The significance of this study is that it is applicable to permeation of flavor and aroma components in food, since they are present at very low vapor pressures. The data from this study can be used to make a relative comparison of barrier properties of polymeric packaging materials to organic permeants of varying molecular structure and polarity. In the future, therefore, a means of designing an appropriate barrier structure for a specific end use application would be available to researchers. In terms of theoretical importance, the data from this study may assist in better understanding and developing a model to accurately predict the permeation profile of different flavor compounds of food in plastic packages.

LITERATURE REVIEW

Mathematical Model Describing the Transport Process

The transport of molecules through a polymer membrane is based on random molecular motions as described by Fick's laws of diffusion (Fick, 1855). Fick's first law states that the rate of transfer of a diffusing substance through an isotropic membrane is proportional to the concentration gradient normal to the section.

$$F_x = -D\left(\frac{\partial C}{\partial x}\right) \quad (1)$$

F, flux, is the amount of a substance diffusing across a unit area in unit time, C is the concentration of diffusing substance, x is the space coordinate measured normal to the section, and D is the diffusion coefficient. The first law only applies to steady state diffusion, where concentration is not varying with time.

Fick's second law describes the non-steady state diffusion where the concentration of the diffusing substance is changing with time. The mathematical treatment of Fick's second law, taken from Crank (1975), is briefly summarized as follows.

Assuming a unit square box

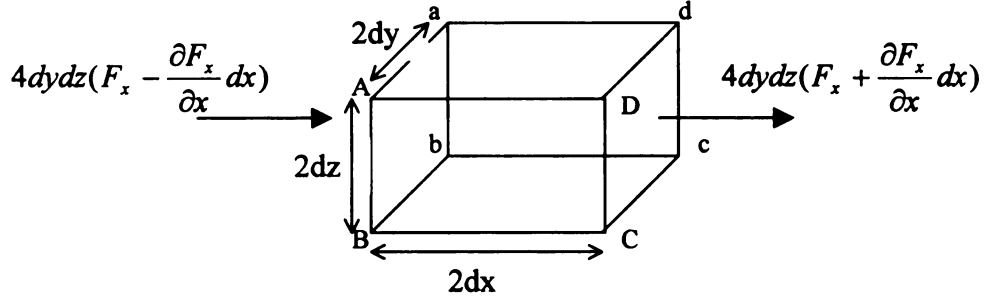


Figure 1. Control Volume Element (taken from Crank, 1975)

as a control element with a size of 2 on each length, width, and height, the rate of diffusing substance entering the plane AabB is $4 dydz (F_x - (dF_x/dx))$ and that of leaving the plane CcDd is $4 dydz(F_x + (dF_x/dx))$ (see Figure 1). Thus, the rate of a diffusing substance accumulating in the volume element in the x direction, R_x , is

$$R_x = -8 \, dx dy dz \left(\frac{\partial F_x}{\partial x} \right) \quad (2)$$

A similar approach is used to derive the rate of accumulation in the y and z directions.

$$R_y = -8 \, dx dy dz \left(\frac{\partial F_y}{\partial y} \right) \quad (3)$$

$$R_z = -8 \, dx dy dz \left(\frac{\partial F_z}{\partial z} \right) \quad (4)$$

Thus, the rate of concentration increase in the volume element is given by

$$\frac{\partial c}{\partial t} = \frac{R_x + R_y + R_z}{8 \, dx dy dz} \quad (5)$$

By substituting equations 2,3 and 4 into 5

$$\frac{\partial c}{\partial t} = -\partial \frac{F_x}{\partial x} - \partial \frac{F_y}{\partial y} - \partial \frac{F_z}{\partial z} \quad (6)$$

Differentiating the flux gradient of equation 1 and substituting into equation 6, the change in concentration can be rewritten as

$$\frac{\partial c}{\partial t} = D \left(\frac{\partial^2 c}{\partial x^2} + \frac{\partial^2 c}{\partial y^2} + \frac{\partial^2 c}{\partial z^2} \right) \quad (7)$$

When the diffusion is restricted only in the x direction, as in the sheet film, equation 7 simplifies to

$$\frac{\partial c}{\partial t} = D \frac{\partial^2 c}{\partial x^2} \quad (8)$$

Equation 8 is referred to as Fick's second law of diffusion, where the concentration of the diffusing substance is at nonsteady state. The diffusion coefficient in Fick's first and second laws, written in the form of equations 1 and 8, is assumed to be a constant and independent of direction, time, and concentration. In cases where D depends on these three variables, the mathematical treatment can be found elsewhere (Crank, 1975).

Steady State Permeation in a Plane Sheet.

For steady state in one dimensional diffusion through a plane sheet with thickness,

l, the concentration at surfaces $x = 0$ and $x = l$ are maintained at constant concentration C_1 and C_2 respectively, as shown in Figure 2 (Crank, 1975).

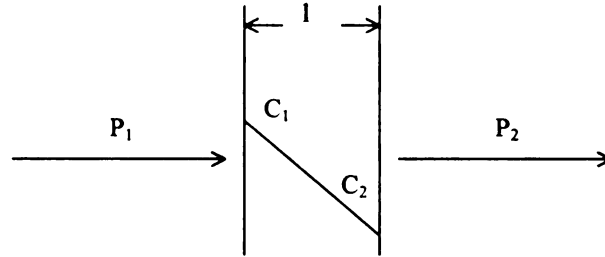


Figure 2. Permeation through a Film at Steady State

Here, the permeant concentration at all points in the sheet remains constant and equation 8 becomes $d^2C/dx^2 = 0$. Further integration with respect to x and restricted boundary conditions of $C = C_1$ at $x = 0$ and $C = C_2$ at $x = l$ gives:

$$\frac{C - C_1}{C_2 - C_1} = \frac{x}{l} \quad (9)$$

This shows that the concentration changes linearly from C_1 to C_2 through the sheet. The rate of transfer of the diffusing substance can be written as

$$F = -D \frac{dC}{dx} = \frac{D(C_1 - C_2)}{l} \quad (10)$$

In permeability experiments, the surface concentrations C_1 and C_2 are unknown and so equation 10 is replaced by

$$F = \frac{P(p_1 - p_2)}{l} \quad (11)$$

where P is the amount of diffusing substance permeated through the film of thickness, l , per exposed film area, time, and partial pressure difference across the film. It is referred to as the permeability constant with SI unit of $\text{kg m/m}^2 \text{ s Pa}$. When the partial pressure of the permeant varies linearly with its equilibrium concentration on the surface of the film, Henry's law states that

$$C = Sp \quad (12)$$

where S is the solubility coefficient of the permeant with the film. Substituting equation 12 into equation 11, one can derive the relationship:

$$P = DxS \quad (13)$$

This equation states that permeation is dependent on both solubility and diffusion parameters. According to Stannett (1968), the permeation process through a homogeneous membrane was described as the condensation and solution of a gas or vapor at one surface followed by diffusion through the barrier membrane, in the form of a liquid, and evaporation of the penetrant to the gaseous state at the other surface. Thus, the permeation process can be discussed in terms of a diffusion and sorption mechanism.

Sorption Mechanism through Polymer Membrane

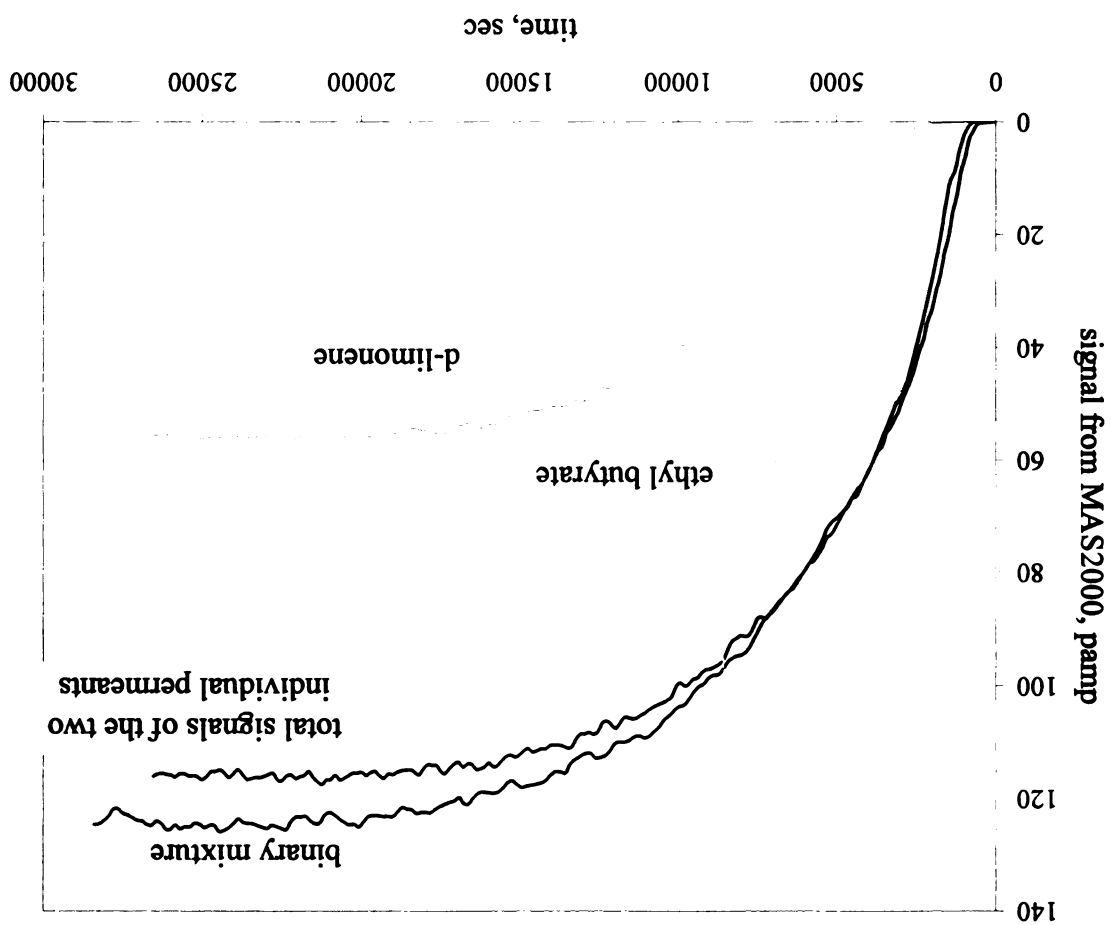


Figure 16. Transmission profiles of binary mixture composition of d-limonene, $a = 0.05$ /ethyl butyrate $a = 0.04$ and its respective individual permeants through OPP film (50°C)

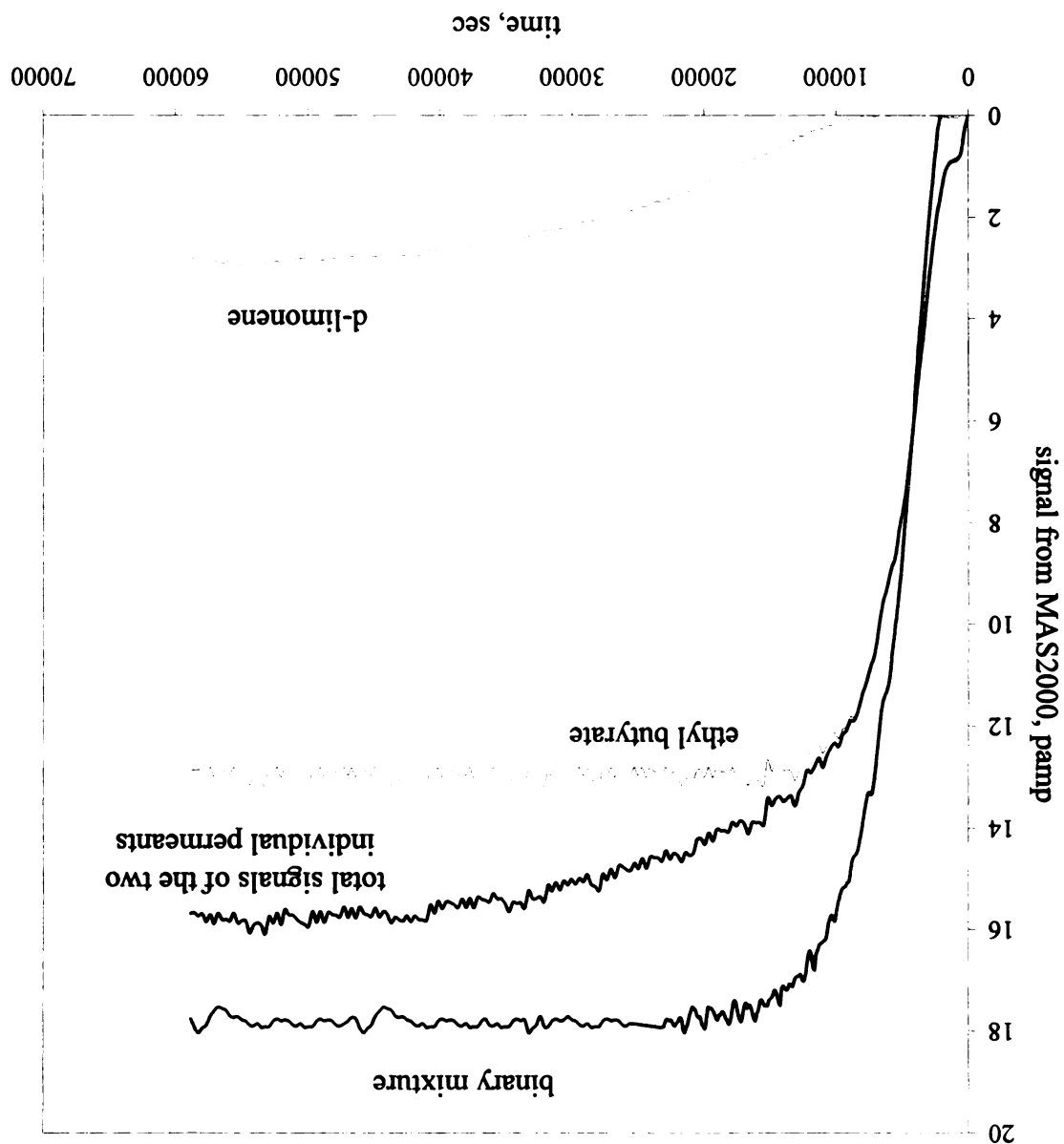


Figure 17. Transmission profiles of binary mixture composition of d-limonene, $a=0.2$ and ethyl butyrate $a=0.2$ and its respective individual permeants through PVdC coated OPP film (60°C)

limonene $a = 0.2$) and as a binary mixture (ethyl butyrate $a = 0.2$ / d-limonene $a = 0.2$) are presented.

Table 17. Permeation ratios in OPP film (50°C) for individual components of the binary mixtures

| Binary mixture compositions | | | | Permeation ratio | |
|-----------------------------|----------------------|----------------|----------------------|-------------------------------|-----------------------------------|
| d-Limonene | | Ethyl butyrate | | $\theta_A(\text{d-limonene})$ | $\theta_B(\text{ethyl butyrate})$ |
| Vapor activity | Vapor Pressure, (Pa) | Vapor activity | Vapor Pressure, (Pa) | | |
| 0.3 | 93 | 0.12 | 241 | 1.08 | 1.25 |
| | | 0.04 | 73 | 0.98 | 1.49 |
| 0.2 | 62 | 0.2 | 404 | 1.29 | 1.08 |
| | | 0.12 | 241 | 1.18 | 1.09 |
| | | 0.04 | 73 | 1.06 | 1.19 |
| 0.13 | 41 | 0.2 | 404 | 1.13 | 0.87 |
| | | 0.12 | 241 | 1.12 | 0.99 |
| | | 0.04 | 73 | 1.07 | 1.17 |
| | 16 | 0.2 | 404 | 1.23 | 0.93 |
| 0.05 | | 0.12 | 241 | 1.17 | 1.04 |
| | | 0.04 | 73 | 1.23 | 1.24 |

The permeation ratio value (equations 29 and 30), which is defined as the ratio of the transmission rate of the individual components in the binary mixture to the single component transmission rate at equivalent concentration, indicates the effect of mixture composition on the transport process of the individual components. A permeation ratio value equivalent to unity suggests that the transmission rate of the permeant is not affected by the presence of a co-permeant in the mixture. Tables 17 and 18 summarize the permeation ratio of limonene and ethyl butyrate in the binary mixture through the OPP and PVdC coated OPP films, respectively. As shown, all of the permeation ratio values obtained for both limonene and ethyl butyrate and the respective test membranes

are close to 1, indicating that the limonene/ethyl butyrate binary mixtures exhibit ideal Fickian permeation behavior through OPP and PVdC coated OPP film, under the test conditions evaluated.

Table 18. Permeation ratios in PVdC coated OPP film (60°C) for individual components of the binary mixtures

| Binary mixture compositions | | | | Permeation ratio | |
|-----------------------------|--------------|----------------|--------------|-------------------------------|-----------------------------------|
| d-Limonene | | Ethyl butyrate | | $\theta_A(\text{d-limonene})$ | $\theta_B(\text{ethyl butyrate})$ |
| Vapor activity | Pressure, Pa | Vapor activity | Pressure, Pa | | |
| 0.20 | 62 | 0.20 | 404 | 1.06 | 1.20 |
| | | 0.12 | 241 | 0.85 | 1.10 |
| | | 0.04 | 73 | 0.75 | 1.17 |
| 0.13 | 41 | 0.20 | 404 | 0.99 ^(a) | 1.17 |
| | | 0.12 | 241 | 1.05 ^(a) | 1.02 |
| | | 0.04 | 73 | 1.17 ^(a) | 1.30 |

(a) The permeation rate of the single limonene permeant at vapor activity of $a = 0.09$ instead of $a = 0.13$ was used to calculate the permeation ratio.

Table 19 summarizes the results of studies carried out to evaluate the effect of d-limonene on the permeability of ethyl acetate vapor through OPP film. Permeability studies were carried out at ethyl acetate vapor activity levels of $a = 0.3$, $a = 0.14$ and $a = 0.04$, respectively. A limonene vapor activity level of $a = 0.2$ was evaluated in binary mixtures, with the respective ethyl acetate vapor concentrations. Statistical analysis indicated that the permeability of ethyl acetate showed a statistically significant increase at a 95% confidence level, for combinations of ethyl acetate $a = 0.3/\text{limonene } a = 0.2$ and ethyl acetate $a = 0.14/\text{limonene } a = 0.2$, as compared to the permeability values obtained for ethyl acetate in the absence of d-limonene at comparable vapor activity levels.

Whenever a gas is in contact with a solid, there will be an equilibrium established between the molecules in the gas phase and those which are bound to the surface of the solid. The amount of gas molecules sorbed onto the surface will depend on the pressure of the gas above the surface and the temperature of the system. Higher temperatures tend to increase the internal energy of the sorbate molecules, thus decreasing their sorption by the polymer membrane. Increasing gas pressure increases collision rates of the sorbate molecules into the polymer membrane and increases the amount sorbed. Henry's law, Langmuir, Flory-Huggin, and Brunauer, Emmett and Teller (BET) equations are some of the common equations used to describe the behavior of gas sorption into a polymer membrane, as a function of its pressure at fixed temperature. Characteristic isotherms described by each respective equation are shown in Figure 3. The derivations, assumptions, as well as treatments for each equation can be found in *Physical Chemistry of Surfaces* (1997).

The Langmuir equation, developed in 1916, was found to fit the experimental data for a variety of sorbate and substrate systems. As show in Figure 3, the polymer provides some kind of specific sites to sorb the penetrant in the initial stage, such that the sorbed concentration is linearly proportion to the pressure. When the sites on the surface layer are nearly all occupied, a small amount of penetrant dissolves in a more or less random distribution until a single monolayer saturated uptake is reached. In the initial sorption state, where the pressure is less than 1 or 2 atmospheres, the solubility coefficient is constant (Stannett, 1968). At high pressure the solubility decreases. In glassy polymers, where polymer chains have long relaxation times, a two-mode sorption process can occur, due to a combination of Langmiur and Henry's law sorption modes. This so-called dual-

mode sorption model has been successfully used to describe the sorption behavior of carbon dioxide in PET (Stern et al., 1990).

When the sorbate interacts strongly with a solid, such as organic vapors in polymers, the sorbed vapors have a tendency to plasticize and loosen the polymer structure, causing subsequent sorbate molecules to cluster within the polymer matrix . Thus, the observed solubility coefficient is initially constant but significantly increases as pressure increases, causing multiple uptake into the bulk polymer. This type of sorption is described by the Flory- Huggins equation and is observed in some organic vapor/polymer systems, as well as for water vapor sorption by hydrophobic polymers. (Stern, et al., 1973)

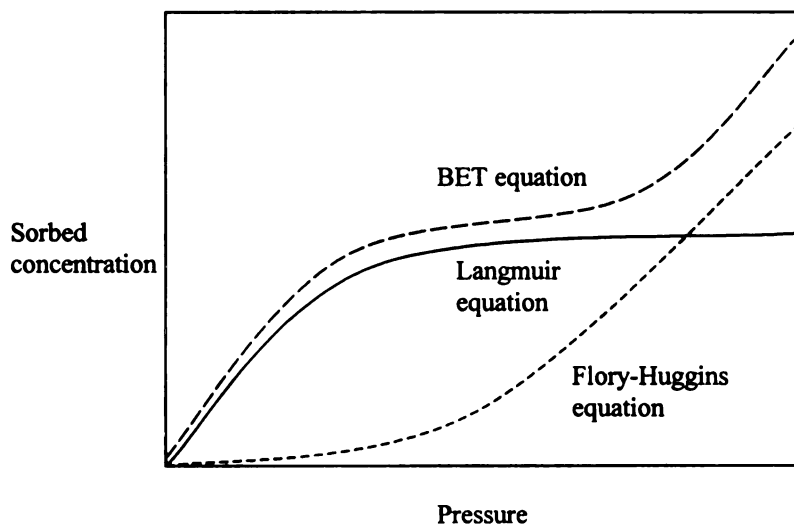


Figure 3. Characteristic isotherms plots described by Langmuir, Flory Huggins, and BET equations (taken from Roger, 1985)

The BET equation can be thought of as a combination of monolayer sorption, as in Langmuir, and a multilayer sorption, as in Flory-Huggins sorption. Depending on the

interaction between the sorbate and the polymer, pressure of the sorbate, and temperature of the system, the sorbate may experience more than one concurrent or sequential modes of sorption in the polymer materials, according to Henry's law, Langmuir, and Flory-Huggins equations.

The degree of interaction between the sorbate and the polymeric material can be characterized by the solubility parameter, δ , of the sorbate and polymeric material, which is defined as the square root of the cohesive energy density. Solubility can be expected if δ values for the sorbate and that of the polymer are less than about $2 \text{ (cal/cm}^3\text{)}^{1/2}$, provided that there are no strong polar or hydrogen-bonding interactions in either the polymer or solvent (Rudin, 1982). In general, the closer the values of the solubility parameters, the more soluble the sorbate will be in the polymer. Experimental values and estimation techniques of common solvents and polymers can be found in the literature. (Rudin, 1982, Van Krevelen, 1976).

The barrier properties of a polymer may be seriously impaired by the presence of organic vapors, which penetrate and plasticize the polymer. Henry's law is usually observed for sorption of permanent gases and some low molecular weight organic vapors by polymer membranes, where the pressure is less than about 1 atmosphere (Rogers, 1985). When the sorption behavior does not follow Henry's law, the substitution of $C = S p$ into equation 11 is in doubt, and the relationship described by equation 13, $P = D \times S$, is violated. Studying the sorption behavior would allow one to predict the effect of penetrant plasticization on the transport behavior of the penetrant.

Diffusion Mechanism through Polymer Membrane

The hole theory of diffusion states that the rate of diffusion will depend on (a) the number and size of distribution of pre-existing holes, and (b) the ease of hole formation (Fujita, 1968). The diffusion process can be thought of as the permeant molecule, in a series of random “hops” or “jump”, moving through the polymer membrane from an environment where the concentration of permeant molecules is high, to an environment where the concentration is low. The unit diffusion involves rearrangement of the permeant molecule and its surrounding polymer chain segments. For the movement of permeant to occur, a certain number of van der Waals type or other interactions between the component molecules and chain segments must be broken to allow a rearrangement of the local structure. The amount of energy required for this rearrangement or ‘hole formation’ will increase as the size and shape of the permeant molecule increases (Fujita, 1968).

The diffusion mechanism for permanent gases (i.e. hydrogen, argon, nitrogen and carbon dioxide), that have a molecular size much smaller than the monomer unit of a given polymer, is such that a limited rotational oscillation of only one or two monomer units would be sufficient to give a cross-section area for the diffusant molecule to jump thermally from one position to a neighboring one, due to a weak thermodynamic interaction between the penetrants and the polymers. This mechanism follows both Fick’s linear diffusion law and Henry’s law, and the diffusion coefficient is independent of concentration.

The diffusion mechanism for molecules with a size larger than the monomer unit

of a polymer, on the otherhand, requires a cooperative movement by the micro-Brownian motion of several monomer units to take place. Such a complicated mechanism is observed for permeants such as water or organic vapors, which interact strongly with the polymer. As a result, their diffusion coefficient is primarily controlled by the mobility of the polymer segmental unit. Factors that enhance polymer segment mobility and thus increase average interchain distance and weaken the molecular interaction between neighboring polymer molecules leads to an increase in diffusion. Therefore, diffusion coefficients of vapors in polymer generally increase with increasing penetrant concentration and temperature (Fujita, 1968).

Crank and Park (1951) postulated that polymer molecules rearrange their conformation toward a new equilibrium conformation with the sorbed state, when they absorb a vapor. The change toward this new conformation also changes the free volume within the polymer matrix. Therefore, the level at concentration of sorbed vapor needed to cause changes in polymer conformation, as well as the time for the polymer chain to rearrange toward a new conformation, affects the diffusion rate. Furthermore, internal stresses built up by swelling of the polymer structure during the sorption process cause a change in polymer conformation to relieve those stresses. For these reasons, diffusion is believed to be time-dependent (Crank and Park, 1951). At temperatures above T_g , the change toward a new equilibrium conformation occurs instantaneously with the sorbed state, when vapor diffuses into the polymer, and the internal stresses are relieved by rapid chain relaxation. Therefore, above T_g , D is independent of time, but depends only on sorbed penetrant concentration (Crank and Park, 1951). For glassy polymers, where the T_g is higher than room temperature, the rate of conformational change does not occur

instantaneously with sorbed penetrants. Thus, diffusion is expected to be a time-dependent phenomena, where the mass transfer process cannot be described by Fick's law. This anomalous or non-Fickian phenomena can be detected in sorption experiments, where the shape of the sorption curve does not conform to the characteristic features of a Fickian sorption profile. The so-called non-Fickian sorption has been reported in describing the sorption of water by cellulose (Newns, 1956), as well as sorption of organic vapors by cellulose nitrate (Drechsel et al., 1952), cellulose acetate (Mandelkern and Long, 1951) and polystyrenes (Odani, 1961).

Different modes of vapor sorption in polymers usually occur and the diffusion constants are often highly dependent on the concentration of penetrant in the polymer (Rogers, 1985). In general, the permeability rate for vapors is a function of many parameters, including temperature, concentration, the nature of the penetrant and the nature of the polymer.

Factors Affecting the Permeation Process

Temperature

Temperature dependency of the diffusion, solubility, and permeability coefficients, expressed by the Arrhenius equation, are found to fit the experimental data for a variety of permeant/polymer systems, within a limited temperature range. The Arrhenius equations describing the temperature dependency of the respective mass transfer parameters are as follows.

$$D = D_o \exp\left(\frac{-E_D}{RT}\right) \quad (14)$$

$$S = S_o \exp\left(\frac{-\Delta H_s}{RT}\right) \quad (15)$$

$$P = P_o \exp\left(\frac{-E_p}{RT}\right) \quad (16)$$

where D_o , and S_o are pre-exponential terms. E_D and ΔH_s are diffusion activation energy, and heat of solution, respectively. E_p is the apparent activation energy of permeation and is equal to $E_D + \Delta H_s$, when Henry's law is obeyed and the $P=D \times S$ relationship holds. R is the gas constant and T is the absolute temperature. D_o includes both the entropy of activation and the jump length, and would also be expected to increase with the size of the diffusing molecule. The diffusion coefficient increases with increasing temperature, as an increase in temperature provides the energy for a general increase in segmental motion and hole formation, which increases the free volume within the bulk polymer. The solubility coefficient decreases or increases with increasing temperature, depending on the physical state of the penetrants. Values of D , E_D , and D_o for gases in various polymers have been gathered and reported by Crank and Park (Crank and Park, 1968).

The heat of solution may be expressed as the sum of the molar heat of condensation, $\Delta \bar{H}_{cond}$, and the partial molar heat of mixing, $\Delta \bar{H}_1$.

$$\Delta H_s = \Delta \bar{H}_{cond} + \Delta \bar{H}_1 \quad (17)$$

The value of $\Delta \bar{H}_1$ can be related to the Hildebrand solubility of the permeant and the

polymer.

$$\Delta \bar{H}_1 \approx \Delta \bar{E}_1 = \bar{v}_1 (\delta_1 - \delta_2)^2 \phi_2^2 \quad (18)$$

The solubility parameters δ_1 and δ_2 are the square roots of the cohesive energy densities of the penetrant and polymer. \bar{v}_1 is the partial molar volume of the penetrant and ϕ_2 is the volume fraction of the polymer in the mixture. For permanent gases, such as H_2 , He, O_2 , and N_2 , where their critical point is much lower than room temperature, the value of $\Delta \bar{H}_{cond}$ would be very small, and ΔH_s is governed by $\Delta \bar{H}_1$, which is a small positive value. Thus, the solubility coefficient usually shows a slight increase with increasing temperature. For condensable organic permeants, the value of ΔH_s depends mostly on the value of $\Delta \bar{H}_{cond}$, which is generally negative. Thus, for organic vapors, solubility coefficients generally decrease, as the temperature increases (Rogers, 1985; Delaussus, 1985).

The Arrhenius relationship of diffusion and solubility coefficients versus temperature is not observed at the glass transition temperature, because the rate of change of free volume changes at the glass temperature (Mears, 1954). The glass transition temperature, T_g , is defined as the temperature that marks the freezing of micro-brownian motion of chain segments of 20 to 50 carbon atoms in length. According to Frisch (1965) diffusion occurs by localized activated jumps from one pre-existing cavity to another. When the size of the penetrants is much less than the average hole size in the polymer, the glass temperature has no effect on the diffusion process. However, as the size of the penetrant increases, or the hole size decreases, a change in the slope of the Arrhenius plot

at the glass transition temperature occurs, with a lower energy of activation for a polymer in the glassy state. The restraints of segmental mobility of the polymer makes the diffusion process more dependent, not only on the size and shape of the penetrant molecule, but also more dependent on concentration (Rogers, 1985). At temperatures well above T_g , $\log D$ increases linearly with diffusant concentration, the slope being smaller as the temperature is raised. As the temperature is lowered toward the T_g , the Arrhenius plot becomes curved downward at low concentrations and a linear relationship is not observed (Mears, 1958a; Kishimoto and Matsumoto, 1959). Below the T_g of a polymer, not enough energy is provided to produce the micro-Brownian motion and the chains are fixed in a specific conformation, related to processing conditions. The kinetics of sorption of organic vapors by polymers is almost invariably complicated by various non-Fickian anomalies that occur at temperatures below T_g and up to at least 10-15°C above T_g (Fujita, 1968).

Concentration

For the permeation of gases and small organic vapors, where solubility in the polymer is very limited, the diffusion and solubility coefficients can be thought of as being constant. For organic vapors, where the size is larger, the permeant is more soluble in polymers. These highly soluble permeants are capable of swelling and plasticizing the polymeric structure, leading to an increased mobility of both polymer chain segments and penetrant molecules. Thus, an increase in solubility, with increasing penetrant size, usually results in an increase in the concentration dependence of S , D , and therefore P

(Roger, 1985).

In systems where the concentration of sorbed vapor is small, or the temperature sufficiently high such that sorption follows Henry's law, the dependence of the diffusion coefficient on sorbed penetrant concentration or vapor activity has usually been empirically represented by the following equations.

$$D = D(0) \exp(\gamma c) \quad (19)$$

$$D = D(0) \exp(\alpha a) \quad (20)$$

where c is sorbed concentration and a is the vapor activity, p/p_s . $D(0)$ is D at zero penetrant concentration. γ and α are the characteristic parameters of the system at the given temperature (Roger, 1985).

At high vapor activity, where the sorption process does not conform to Henry's law, a number of penetrant/polymer combinations involving the sorption of organic vapors follow the Flory-Huggins equation, in the simple form (Suwandi and Stern, 1973).

$$S = S(0) \exp(\sigma c) \quad (21)$$

where $S(0)$ is S at zero penetrant concentration and σ is the characteristic parameter of the system at the given temperature.

D can be written as a function of sorbed concentration that obeys the Flory Huggins equation.

$$D = D(0) \exp \left[\frac{\gamma c}{\exp(\sigma c)} \right] \quad (22)$$

At low concentration, when Henry's law is obeyed, $\sigma = 0$ and equation 22 is reduced to equation 19. When the system follows Flory-Huggin sorption, $\sigma \rightarrow 1$ and by expanding the exponential term in σc and neglecting higher order terms equation 22 can be written as

$$D = D(0) \exp \left[\frac{\alpha c}{(1 + \sigma c)} \right] \quad (23)$$

Taken as $\sigma=1$, D can be expressed in terms of penetrant volume fraction, ϕ_1 , as shown in equation 24

$$D = D(0) \exp(\alpha' \phi_1) \quad (24)$$

where ϕ_1 is equal to $\frac{c_1}{(1 + c_1)}$. γ , α , and α' measure the effectiveness with which equal amounts of various penetrants plasticise a polymer to facilitate segmental mobility and, hence, to increase the rate of diffusion of the penetrant. The values are expected to be higher for any systems that cause a decrease in polymer segmental mobility, for instance, a decrease in temperature, an increase in solvating power of the penetrant, an increase in polymer-polymer interaction, etc. (Rogers, 1985).

Nature of Penetrant

At a given temperature the more easily condensable vapors are more soluble in a given polymer. Larger size penetrants condense easier and are more soluble in a polymer matrix. Thus, the linear relationship between the solubility coefficient and either the boiling point temperature, critical temperature or other parameters that measure the ease of condensibility of penetrants have been observed by many investigators (Van Amerongen, 1950, 1964; Barrer and Skirrow, 1948; Strandburg et al., 1991). The increase in the size of a penetrant in a series of chemically similar structures, generally increases solubility and decreases the diffusion coefficients. Shimoda et al. reported that the permeability, diffusion, and solubility coefficients in PE relate linearly with increasing carbon atoms for n-alkanes, aliphatic ethyl esters, n-aldehydes, and n-alcohols up to 10 carbon atoms (Shimoda et al., 1987). The dependence of the solubility coefficient, on increasing the number of carbon atoms, is higher than that of the diffusion coefficient. Thus, the permeability coefficient increases with an increase in the carbon number. A study by Berens and Hopfenberg (1982) showed that diffusion coefficients of simple gases and organic vapors, up to C₆, in a series of glassy polymers, PVC, PS, and PMMA, decreases exponentially and the diffusion activation energy (E_D) increases linearly, with increasing average diameter of “spherical” penetrant molecules. The diffusivity of elongated or flattened molecules is higher by a factor of up to 10^3 , relative to spherical compounds with similar molecular weight, suggesting that elongated molecules tend to align and transport along their long dimension through a polymer membrane. For rubbery polymers, however, several investigators have observed that the diffusion of a series of organic vapors in natural rubbers is much higher and much less dependent upon molecular size than in glassy polymers (Fujita, 1968). The results of sorption studies of

gases and vapors by PVC, as reported by Beren (1990) show that the difference in diffusivity between the glassy and rubbery state of PVC can vary by as much as 1 order of magnitude for small gas molecules and as much as 12 times for plasticizers of size 8 to 10 \AA . Also, the same studies suggest that the activation energy is constant and independent of penetrant size but varies with different kinds of rubbery polymers.

Nature of Polymer

The barrier properties of polymeric materials are determined by the chemical structure of the chain and the systems morphology. A symmetrical, regular structure, with strong cohesive energy between the polymer chains, allows efficient chain packing, which minimizes the free volume within the polymer matrix and thus reduces sorption and diffusion processes. The two properties can be manipulated through the parameters derived from the chemical structure, such as degree of polarity, inter-chain forces, and chain stiffness.

The crystalline region obtained with regular molecular structures increases packing efficiency of the polymer chains, so that the crystalline regions can be regarded as impermeable, relative to the amorphous region (Shimoda et al., 1987). Several investigators have shown that sorption and diffusion processes vary with amorphous phase content in semi-crystalline polymers by the following equations (Michaels, 1961).

$$S = S_a \phi_a \quad (25)$$

$$D = D_a \phi_a^m \quad (26)$$

where S_a is the solubility coefficient and D_a is the diffusion coefficient for a completely amorphous polymer. ϕ is the amorphous volume fraction in a polymer. The parameter m is constant and varies among different polymers. It has been reported as varying from about 0.3 for polyethylene to about unity for PET (Michaels et al., 1959 and 1963).

The effect of the crystalline region on the diffusion process is related to polymer morphology, mainly the tortuosity and immobilization effects. Since the penetrant diffuses around the amorphous region, its average path length is higher than the nominal dimensions of the polymer membrane and this extra path length is referred to as the tortuosity effect. Also, the tie molecules between crystallites and other chains anchored to the crystal would reduce the mobility of the amorphous phase. Reducing polymer chain mobility, reduces hole formation and thus the diffusion rate. The tortuosity and immobilization effect on diffusion in a semicrystalline polymer can be expressed as

$$D = \frac{D_a}{\tau\beta} \quad (27)$$

where τ and β are tortuosity and immobilization factors, respectively. These two effects are experimentally found to decrease the diffusion rate but not the sorption in the amorphous region of a semicrystalline polymer (Weinkauff et al., 1990).

Polymer morphology can be improved to a higher molecular order by orientation of polymer films, resulting in improved barrier properties. Orientation is a process of stretching the polymer film above the glass transition temperature, in order to rearrange

and align the polymer chains in the direction in which it is stretched. The more ordered morphology obtained usually resulted in a decrease in free volume and sorption sites, which resulted in a substantial decrease in the diffusion coefficient and a smaller decrease in the solubility coefficient. For instance, an eighty percent decrease in the diffusion coefficient and less than a forty percent decrease in the solubility coefficient has been observed for carbon dioxide permeation in oriented polystyrene (Weinkauff et al., 1990). The effect of orientation on diffusion is greater in crystallizable polymers than those observed in noncrystallizable polymers, because the deformation in crystallizable polymers causes additional stress-induced crystallization and orientation of the remaining amorphous phase, which tend to increase the tortuosity. In general, the degree of orientation achieved and its effects on barrier properties of polymers depends on the draw ratio and mode of deformation mechanism (Choy et al., 1984)

Permeation of Binary Mixtures

A number of permeability studies have been reported for single component organic vapor/polymer systems (Rogers et al., 1960; Gilbert et al., 1983; Neibergall et al., 1978; Zobel, 1982; Baner et al., 1986; and Hernandez et al., 1986). However, only a limited number of studies have been reported on the permeation of multi-component mixtures of organic liquids and vapors through barrier membranes (DeLassus et al., 1988; Huang et al., 1968; Mickelson et al., 1985; and Hensley et al., 1991). The importance of multi-component mixture permeation is such that it would be more representative of an actual product/package system, where the product aroma profile contains numerous

volatile components at relatively low concentrations.

Studies on the permeability of permanent gas mixtures through various rubbery films by Pye et al.(1976), Stannett et al.(1957) and Meyer et al.(1957), indicated that there was no effect of one penetrant gas on the permeation of another in the mixture. The rate of the permeation of a gas mixture was equal to the sum of the rates of its constituents.

Studies reported dealing with the permeation and diffusion of organic liquid mixtures through barrier polymer films showed that varying degrees of interaction can occur between the components of the mixture and the polymer. For example, the permeation studies of binary organic liquid mixtures of varying composition by Michelson et al. (1985) led the authors to generalize three possible modes of interaction occurring with organic mixtures. First, the mixture may decrease the lag time or breakthrough time of the components. Second, a component that does not permeate as a pure liquid may be transported through the membrane by another component, when present in the mixture. Third, the collective permeation rate for the mixture may be higher than the transmission rate of either pure component of the mixture. Huang et al. (1986) conducted extensive studies on the permeation of various binary organic liquid mixtures through polyethylene (PE) and made three observations regarding the effect of molecular size, shape, and chemical nature of the permeants to the permeation of binary organic mixtures. First, for a given binary mixture containing two members of a homologous series, the lower molecular weight member permeates preferentially. Second, with similar molecular weight and chemical nature in the mixture, molecules with smaller cross sections will permeate at a faster rate than the other. Third, when the mixture contains molecules with a large difference in chemical nature, permeation is not

as affected by their size and shape, but depends more on the chemical nature of the molecule, as can be measured by the solubility parameter. Molecules with a solubility parameter closer to that of the polymer tend to permeate at a higher rate than the other molecules in the mixture. Furthermore, the effect of temperature on the permeation rate of the binary mixture is such that the selectivity of the membrane to the constituents of the mixture is decreased as the temperature is increased. When the temperature rises, increasing the free volume within the polymer matrix, more of the less diffusive molecules can therefore diffuse through the membrane (Huang et al., 1968).

The higher permeation rate of the mixture relative to the sum of permeation rates of the pure components, is attributed to the combined internal plasticizing and solubility effects. The results of permeation and sorption experiments involving d-limonene and ethyl acetate binary mixtures through OPP film, by Hensley et al.(1991) and Nielson and Giacin (1994), led the authors to propose that d-limonene, a more soluble compound in the film, plasticizes the film, which increases the free volume and therefore increases diffusion of its co-permeant, ethyl acetate. While the solubility coefficient of the two compounds in the mixture was not affected by the presence of the co-permeant, the observed increase in total permeation of the mixture was proposed to be the result of increased internal mobility of ethyl acetate caused by plasticization of the OPP film by d-limonene. Similarly, carbon dioxide under high pressure is found to plasticize certain glassy polymers and influence the transport of low molecular weight penetrants in glassy polymers (Berens, 1989). In the polyvinyl chloride (PVC)/CO₂/dimethyl phthalate (DMP) system, liquid carbon dioxide was found to increase the sorption of DMP in PVC from 1%wt to 40% wt in less than one third the time taken for PVC to absorb 1% DMP in

single component sorption. Thus, high-pressure carbon dioxide has practical potential use in incorporating low molecular weight additives into polymers. In the absence of plasticization, the sorption and permeability of a gas in a glassy polymer will be depressed, relative to its pure gas values, by the presence of a second gas (Koros, 1989). The competitive sorption model explains the behavior by which different gas molecules in a mixture compete for sorption sites within the polymer matrix, resulting in suppressing overall permeability.

The effect of mixture composition on the transport process of the individual components can be expressed by the permeation ratio θ , which is defined as the ratio of the sum of permeation rates for components A and B in the mixture, Q , to the sum of permeation rates of pure components A and B, Q^o .

$$\theta = \frac{Q}{Q^o} \quad (28)$$

The permeation ratios for the individual components can be expressed as

$$\theta_A = \frac{q_A}{Q_A} \quad (29)$$

$$\theta_B = \frac{q_B}{Q_B} \quad (30)$$

where θ_A and θ_B are the permeation ratios of components A and B, q_A and q_B are the permeation rates of components A and B in the binary mixture, and Q_A and Q_B are the permeation rates of pure components A and B, respectively.

Thus, the permeation ratio should be equal to unity when a binary organic liquid mixture exhibits ideal permeation behavior. The value of the permeation ratio may be higher or lower than unity for non-ideal permeation. If the permeation ratio of a system is higher than unity, the system can be said to exhibit a permeation enhancement effect, while a value lower than unity indicates a permeation depression effect.

Permeation Measurement Procedure and Technique

The experimental methods for measurement of S , D and P can be divided into permeation and sorption experiment categories, which have been described by a number of investigators (Stannett et al., 1972, Zobel, 1982, Baner et al., 1986, Hernandez et al., 1986). The permeation test methods are based on static state (quasi-isostatic) and dynamic permeation (isostatic) procedures, both of which use different mathematical treatments to find P and D . When the solubility coefficient follows Henry's law, S can be determined from the relationship $S=P/D$. The agreement between the solubility coefficient of gases and vapors in polymers measured by equilibrium sorption and permeation experiments is good at test temperatures above the polymer glass transition temperature (Meares, 1958; Barr, 1996). Barr (1996) reported that the solubility coefficients for ethyl acetate in low density polyethylene, linear low density polyethylene, and ionomer, determined by a gravimetric procedure, was approximately 25 to 30% lower than the values obtained from isostatic permeability techniques. Because the methods of calculating the solubility coefficient values by the two procedures are inherently different this agreement is considered to be within acceptable limits. Since the isostatic

permeation test method will be employed in the present study, the system and the mathematical treatment will be briefly described here, while other methods can be found elsewhere (Hernandez et al., 1986).

The design of the isostatic test system is that permeation data for an organic vapor or gas through a polymer membrane is continuously collected from the initial time zero to steady state conditions, as a function of temperature and penetrant concentration. A constant, desired concentration of penetrant is maintained in the high concentration cell chamber, while a constant flow of carrier gas in the lower cell chamber removes any permeated penetrant and conveys it through to the detector. The detector utilized must be able to give a good response to the kind of permeant tested. Since a flame ionization detector gives a good signal to noise ratio for most organic vapors, it is commonly used in the commercial isostatic test apparatus. The lower concentration cell chamber is maintained at zero penetrant concentration and thus a constant penetrant concentration gradient is achieved during the entire test run. At pre-selected time intervals the concentration of penetrant from the lower cell chamber is determined, and the transmission rate is monitored continuously until steady state is attained. The permeability coefficient at steady state is then calculated as

$$P = \frac{\Delta Q l}{\Delta t A p} \quad (31)$$

where $\Delta Q / \Delta t$ is the transmission rate at steady state, l is the thickness of the film, A is the exposed area of the film, and p is the penetration concentration gradient.

The diffusion coefficient is determined using the solution of Fick's first law of

diffusion given by Pasternak, et al. (1970).

$$\frac{\left(\frac{\Delta M}{\Delta t}\right)_t}{\left(\frac{\Delta M}{\Delta t}\right)_\infty} = \left(\frac{4}{\sqrt{\pi}}\right) \left(\frac{l^2}{4Dt}\right)^{1/2} \exp\left(\frac{-l^2}{4Dt}\right) \quad (32)$$

where $(\Delta M / \Delta t)_t$ and $(\Delta M / \Delta t)_\infty$ are the transmission rate of the penetrant at time t and at steady state, respectively, t is the time and l is the thickness of the film. For each value of $(\Delta M / \Delta t)_t / (\Delta M / \Delta t)_\infty$, a value of $l^2/4Dt$ can be calculated by using a Newton-Raphson method (Chapra and Canale, 1985). The method is briefly described in appendix D. By plotting the reciprocal of these calculated values, $4Dt/l^2$, against time, a straight line is obtained and the diffusion coefficient, D , is calculated by

$$D = \frac{(slope) \times l^2}{4} \quad (33)$$

Another approach to determine a first approximation of D is given by the expression derived by Ziegel, et. al. (Ziegel et. al., 1969).

$$D = \frac{l^2}{7.199t_{0.5}} \quad (34)$$

where $t_{0.5}$ is the time to reach a rate of transmission $(M/t)_t$ equal to half the steady state $(M/t)_\infty$ value.

The most common error involving permeation experiments is usually caused by the failure to obtain the true steady state transmission rate, and inaccuracy of thickness determination. According to equations 33 and 34, these two factors thus constitute a

variation in the estimation of D.

Dynamic Purge and Trap/Thermal Desorption Technique

The dynamic purge and trap/thermal desorption technique is another approach to determine the permeation rate. The technique involves the use of adsorbents to trap and concentrate the permeated penetrant at steady state. The vapors concentrated in the adsorbent trap are subsequently recovered by the desorption system and transferred to a gas chromatograph for analysis. The amount recovered per trapping time is treated as the permeation rate. Since quantification of the amount of vapor permeated is achieved by gas chromatography, the permeation rate of constituents in a gas mixture can be quantified, if the corresponding peaks of the constituents can be separated by a gas chromatography column.

The application of a dynamic purge and trap/thermal desorption procedure coupled with the MAS 2000TM Permeation Test System was developed and performed by Chang (1996). Validation of the method was obtained by comparing the permeance values for α -pinene through a PVdC coated OPP film, determined by the dynamic purge and trap/thermal desorption technique, with the values obtained from the MAS 2000TM Permeation Test System operated in the continuous flow isostatic method. The permeability values obtained by the two procedures were found to be in good agreement. The permeance of α -pinene vapor through a series of high barrier composite membranes, which could not be tested by the normal isostatic procedure, was determined by the dynamic purge and trap/thermal desorption procedure (Chang, 1996). The lowest

detection sensitivity of the dynamic purge and trap/thermal desorption procedure was found to be 0.2 ng/hr which is three to four orders of magnitude less than the continuous flow isostatic procedure. The increased detection sensitivity of the method provides the ability to determine the permeation rate of aroma/flavor permeation rates through high barrier films, where the conventional techniques fail.

MATERIALS AND METHODS

Materials and Equipment

Films:

PVdC-coated OPP film, BICOR 70 HBS-2, one-side sealable, one-side high barrier
PVdC-coated OPP film (Mobil Chemical Co.)

Total Thickness: 0.7 mil

Biaxially oriented polypropylene film (Mobil Chemical Co.)

Thickness 2 mil

Density : 890 kg/m³

Percent Crystallinity: 45.7% determined by differential scanning calorimetry
analysis

Level of Elongation: 420% machine direction

800% cross machine direction

Hildebrand Solubility Parameter: 8.3 (cal/cc)^{1/2} poor H-bonding
(taken from Van Krevelen, 1976)

Permeants:

d-limonene (Aldrich Chemical Co., Milwaukee, WI)

| | |
|---------------------------------|--------------------------------------------------------------------------------------|
| Molecular Structure | (C ₁₀ H ₁₆) |
| Density at 25 °C | 0.840 g/cc |
| Molecular Weight | 136.24 |
| Boiling Range | 175.5-176 °C |
| Hildebrand Solubility Parameter | 8.21 (cal/cc) ^{1/2} poor H-bonding (taken from Halek and Luttmann, 1991) |
| Molar Volume | 162 cc/mol |
| Refractive Index | 1.4730 |
| %Purity | 97% |

Ethyl Butyrate (Aldrich Chemical Co., Milwaukee, WI)

| | |
|---------------------|--------------------------------------------------------------------------------------------------|
| Molecular Structure | (CH ₃ CH ₂ CH ₂ CO ₂ C ₂ H ₅) |
|---------------------|--------------------------------------------------------------------------------------------------|

| | |
|---------------------------------|-------------------------------------------------------------------------------------|
| Density at 25 °C | 0.878 g/cc |
| Molecular Weight | 116.16 |
| Boiling Range | 120 °C |
| Hildebrand Solubility Parameter | 8.5 (cal/cc) ^{1/2} moderate H-bonding (taken from Nielsen et al., 1992) |
| Molar Volume | 132.3 cc/mol |
| Refractive Index | 1.3920 |
| %Purity | 99% |

Ethyl Acetate (Aldrich Chemical Co., Milwaukee, WI)

| | |
|---------------------------------|------------------------------------------------------------------------------------|
| Molecular Structure | (CH ₃ CO ₂ C ₂ H ₅) |
| Density at 25 °C | 0.894 g/cc |
| Molecular Weight | 88.11 |
| Boiling Range | 77.1 °C |
| Hildebrand Solubility Parameter | 9.11 (cal/cc) ^{1/2} moderate H-bonding (taken from Van Krevelen, 1976) |
| Molar Volume | 98.56 cc/mol |
| Refractive Index | 1.37 |
| %Purity | 99.9 % |

Solvent:

Carbon Tetrachloride (Mallinckrodt, Inc., Paris, Kentucky)

| | |
|---------------------|---------------------|
| Molecular Structure | (CCl ₄) |
| Density at 25 °C | 1.585 g/cc |
| Molecular Weight | 153.84 |
| Boiling Range | 76.3-76.8 °C |

Thermal Desorption Apparatus:

Dynatherm 890/891 thermal desorption unit (Supelco Inc., Bellefonte, PA)

CarbotrapTM 300 multi-bed thermal desorption tubes, 6 mm O.D. x 4 mm I.D. x 11.5 cm length (Supelco Inc., Bellefonte, PA)

Gas Chromatograph:

Hewlett Packard model 5890A interfaced with HP 3395 integrator
(Avondale, PA),

Gas Chromatography Column:

Fused Silica Capillary Column
SPB™-5, 30 meters long, 0.32 mm ID, 1.0 µm film thickness
(Supelco Inc., Bellefonte, PA)

Permeation Test Apparatus:

MAS2000™ Organic Permeation Detection System
(Testing Machines Inc., Amityville, N.Y.)

Water Bath

Blue M Magni Whirl (Blue M, A Unit of General Signal, Blue Island, IL)

250 ml Gas Washing Bottle

(Fisher Scientific, Pittsburgh, PA)

Needle Valves

Nupro 'M' series (Nupro Co., Willoughby, OH)

Swagelok Fitting

(Supelco Inc., Bellefonte, PA)

Electronic Mass Flow Meter

Model Top-Trak 821 (Sierra Instruments, Carmel Valley, CA)

Syringe

500 ml gas-tight syringe (Hamilton Co, Reno, Nevada)
5 µl syringe (Hamilton Co, Reno, Nevada)

Methods

Calibration Curves of d-Limonene, Ethyl Butyrate, and Ethyl Acetate by Gas Chromatography Analysis: Preparation and Testing

The vapor activities of the respective permeant vapors evaluated with the MAS2000TM Organic Permeation Detection system were determined by gas chromatography analysis. Standard solutions of the respective test compounds in carbon tetrachloride were prepared by a serial dilution procedure and calibration curves for the respective permeants were constructed according to the following analytical conditions.

Gas Chromatography Condition:

Injection temperature 220°C
Detector temperature 250°C
Head pressure 10 psi
Total flow port (split vent) 27.8 ml/min
Septum purge (purge vent) 2.76 ml/min
Helium flow rate 1 ml/min

Temperature Programming

Two sets of temperature programming conditions were employed, one for d-limonene and ethyl butyrate analysis and the other was for analysis of ethyl acetate. Both programming runs utilized two temperature cycles in order to reduce the total run time.

For d-limonene and ethyl butyrate

Initial oven temperature 50°C
Initial time 2 min
Rate 7°C/min
Final temp 110°C

Final time 0 min
Rate A^(a) 30°C/min
Final temp A^(a) 200°C
Final time A^(a) 3 min
Total run time 16.58 min.

(a) the second temperature programming cycle

For ethyl acetate

Initial temperature 40°C
Initial time 5 min
Rate 7°C/min
Final temp 110°C
Final time 0 min
Rate A^(a) 30°C
Final temp A^(a) 200°C
Final time A^(a) 3 min
Total run time 21 min

(a) the second temperature programming cycle

The above conditions gave retention times for ethyl acetate, ethyl butyrate, and d-limonene of 2.25, 3.95, and 8.94 min, respectively. The quantity of permeant detected was determined by multiplying the standard concentration (v/v) times the volume injected (1 µl), which is then multiplied by the density of the permeant, to give quantity injected. The quantity injected plotted versus the corresponding area response gave the calibration curves which established the linearity and sensitivity of the assay procedure for the respective permeants. The reciprocal of the slope is taken as the calibration factor in grams per area unit. These calibration factors were used to set the vapor activities for the MAS2000TM Organic Detection System. The calibration curves for the test compounds are found in Appendix A.

In order to check the accuracy of the calibration curves determined for the test compounds, their actual saturated vapor pressures were experimentally determined and compared to the literature values. Approximately three ml of each test compound were separately stored in 5 ml septa seal glass vials at 23°C and allowed to equilibrate for at least 48 hours. The vials were sealed with Teflon-faced silicone septum and aluminum crimp cap. A 500 µl gastight syringe was used to withdraw a 50 µl gas sample from the headspace of the septa seal vial and injected directly into the gas chromatograph. The area response was then converted to grams of permeant injected through its calibration factor. The vapor in the vial was assumed to have reached equilibrium and behave as an ideal gas. Therefore, the ideal gas law was used to determine the saturation vapor pressure of each compound at 23°C, by substitution into equation 35.

$$P = \frac{CF \times AU \times R \times T}{MW \times V} \quad (35)$$

where P = partial pressure [mmHg]
 CF = calibration factor [g/AU]
 AU = Area Response from GC [AU]
 R = gas constant, 6.236×10^7 [mmHg µl /mol K]
 MW = molecular weight of compounds [g/mol]
 V = gas sample volume [µl]

The experimentally determined saturated vapor pressures were then compared with the interpolated values obtained from Perry's Chemical Handbook (1984). The accuracy of the calibration factors for d-limonene, ethyl butyrate, and ethyl acetate was within 10% between experiment and literature saturation vapor pressure values.

Saturated Vapor Pressure in mmHg at 23°C

| | Experiment ^(a) | Perry's Chemical Handbook ^(b) | % difference |
|----------------|---------------------------|------------------------------------------|--------------|
| d-limonene | 2.34 | 2.32 | 0.73% |
| Ethyl butyrate | 14.23 | 15.34 | 7.23% |
| Ethyl acetate | 79.82 | 82 | 2.65% |

^(a) *average of 10 samples.*

^(b) *values were interpolated by polynomial function to the fifth power.*

Because of the wide variation in the saturation vapor pressure of the various penetrants, at the respective temperatures of test, the partial pressure gradient for the permeability experiments was expressed as vapor activity. This allowed for barrier performance to be compared at a standard driving force for the permeants evaluated. Vapor activity values were calculated by:

$$a = \frac{p}{p_s} \quad (36)$$

where p = partial vapor pressure
 p_s = saturated vapor pressure

Calibration Curves for Dynamic Purge and Trap/Thermal Desorption Procedure

The choice of adsorbents to efficiently trap the components in the mixture and the desorption conditions to ensure a complete recovery of penetrants is important. The Carbotrap 300™ adsorbent tube from Supelco was selected for the present study because its multi-bed adsorbent design allows trapping of various organic compounds with different size and different functional groups. Also, its sampling capacity within

trapping time in the present study is sufficient and the recovery of trapped penetrants is near quantitative. Problems may arise when preparing a standard calibration curve by this procedure, as some solvents do not desorb instantaneously during the thermal desorption process. This leads to a broad solvent peak with a tailing baseline. Only the desorption of carbon tetrachloride solvent from Carbotrap 300TM was found to give a satisfactory flat baseline, with accurate and precision peak areas for the trapped penetrants, following their desorption.

To establish the linearity and sensitivity of the thermal desorption procedure, standard calibration curves for the respective test compounds were prepared. A 1 μ l sample of standard solutions of limonene, ethyl butyrate, and ethyl acetate of known concentration in carbon tetrachloride, was directly injected onto the sorption tube. The sorption tube was then inserted into a heating chamber of the thermal desorption unit, which is interfaced directly to the column of the gas chromatograph for quantification. The gas chromatography column is the same as that described previously for vapor activity determination. The test compounds, which are sorbed onto the trap, are desorbed by heating and then separated into the individual components, according to the following analytical conditions.

Thermal desorption unit condition

Tube desorption chamber temperature 370°C

Valve compartment temperature 250°C

Transfer line temperature 250°C

Tube preparation chamber temperature 350°C

Desorption time 8 min

Preparation time 30 min.

Desorption carrier gas flow rate at flow check port 9 ml/min

Preparation carrier gas flow rate at side port 15 ml/min

Gas chromatography condition:***For d-limonene and ethyl butyrate***

Initial temperature 50°C
Initial time 5 min
Rate 10°C/min
Final temperature 200°C
Final time 3 min
Total run time 23 min.

For d-limonene and ethyl acetate

Initial temperature 35°C
Initial time 5 min
Rate 10°C/min
Final temperature 200°C
Final time 3 min
Total run time 24.50 min

The gas chromatographic conditions gave retention times for ethyl butyrate and d-limonene of 6.8 and 11.4 min, respectively. The second set of conditions gave retention times for ethyl acetate and d-limonene of 3.41 and 12 min, respectively. Again, plotting grams of permeant introduced onto the sorption trap against its corresponding area response provided a series of calibration curves. The reciprocal of the slope was taken as the calibration factor for quantification. The calibration profiles for each test compound are shown in appendix B. After 8 min. of desorption time, the tube is cleaned to remove any residual compounds by heating at 350°C for 30 min.

Permeability Test System

Permeability studies were carried out with a MAS 2000TM Organic Permeation

Detection System, which was modified with a device for trapping permeated organic vapors employing a dynamic purge and trap technique. The MAS2000TM Organic Permeation Detection System is based on an isostatic permeation test procedure. This system allows for the continuous collection and measurement of the permeation rate of the organic vapor through a polymer membrane, from the initial time zero to steady state conditions. The MAS 2000TM system incorporates a flame ionization detector (FID), and precisely controls the cell temperature (range from ambient to 100°C) and all gas flow rates (nitrogen as carrier, air, and hydrogen as fuel). An IBM 486SX computer system with a very user friendly software package was interfaced to the system to control many of the test parameters. The computer can also activate and deactivate the gas flow direction, cell opening/closing, as well as display data, while recording all pertinent instrument parameters. All permeation data can be stored in the computer hard drive, and LOTUS 1-2-3 is used to recall the permeation data to calculate the respective mass transfer parameters and give the transmission rate profile curve.

In order to determine the permeability of binary organic vapor mixtures, the test unit employed in the present study incorporated a dynamic purge and trap system to allow accumulation of the permeated vapor. In the original MAS2000TM system, the permeated vapor is directly conveyed to a flame ionization detector (FID) for quantification. However, in the modified system, a bypass line was inserted to convey the permeated vapor to a sorption trap. The trapping system was designed to ensure that the low concentration cell chamber is continuously flushed with the carrier gas and the permeated vapor is conveyed to the trapping tube attached. The sorption trap was connected to the exit port of the bypass line, which is incorporated on the instrument

chassis, via a ¼" thumb wheel swagelok fitting for easy removal. Figure 4 shows a schematic of the permeation test and trap system. The glass thermal desorption tubes, Carbotrap™ 300, were employed as adsorption traps, which were prepacked by Supelco Inc. The trapping tubes contain 300 mg of Carbotrap C adsorbent, 200 mg of Carbotrap B adsorbent, and 125 mg of Carbosieve S-III adsorbent.

Permeability Measurements

The permeability studies were carried out at 50°C for OPP and 60°C for PVdC-coated OPP. A minimum of three different concentrations were run for each test compound as a pure vapor and a minimum of six different binary mixture combinations of varying composition were run, except for ethyl acetate. For ethyl acetate, three binary mixture combinations with limonene through OPP were studied. Tests for each vapor activity evaluated were carried out in duplicate.

Prior to initiating a test run, the test film was conditioned at 60°C \pm 1°C for 6 hours, to desorb any residual monomer, or other low molecular weight volatiles from the film, which could interfere with detection of permeated vapor. For each test run, a sample film approximately 6" x 6 ½" was cut, mounted on a paperboard film holder with tape, and then placed in the permeability cell. The area of the test film was 0.0081 m² (12.6 in²).

A constant concentration of permeant vapor for the high concentration cell chamber was produced by bubbling nitrogen through the liquid permeant, with the flow rate equal to 30 ml/min. The liquid permeant is contained in a vapor generator consisting

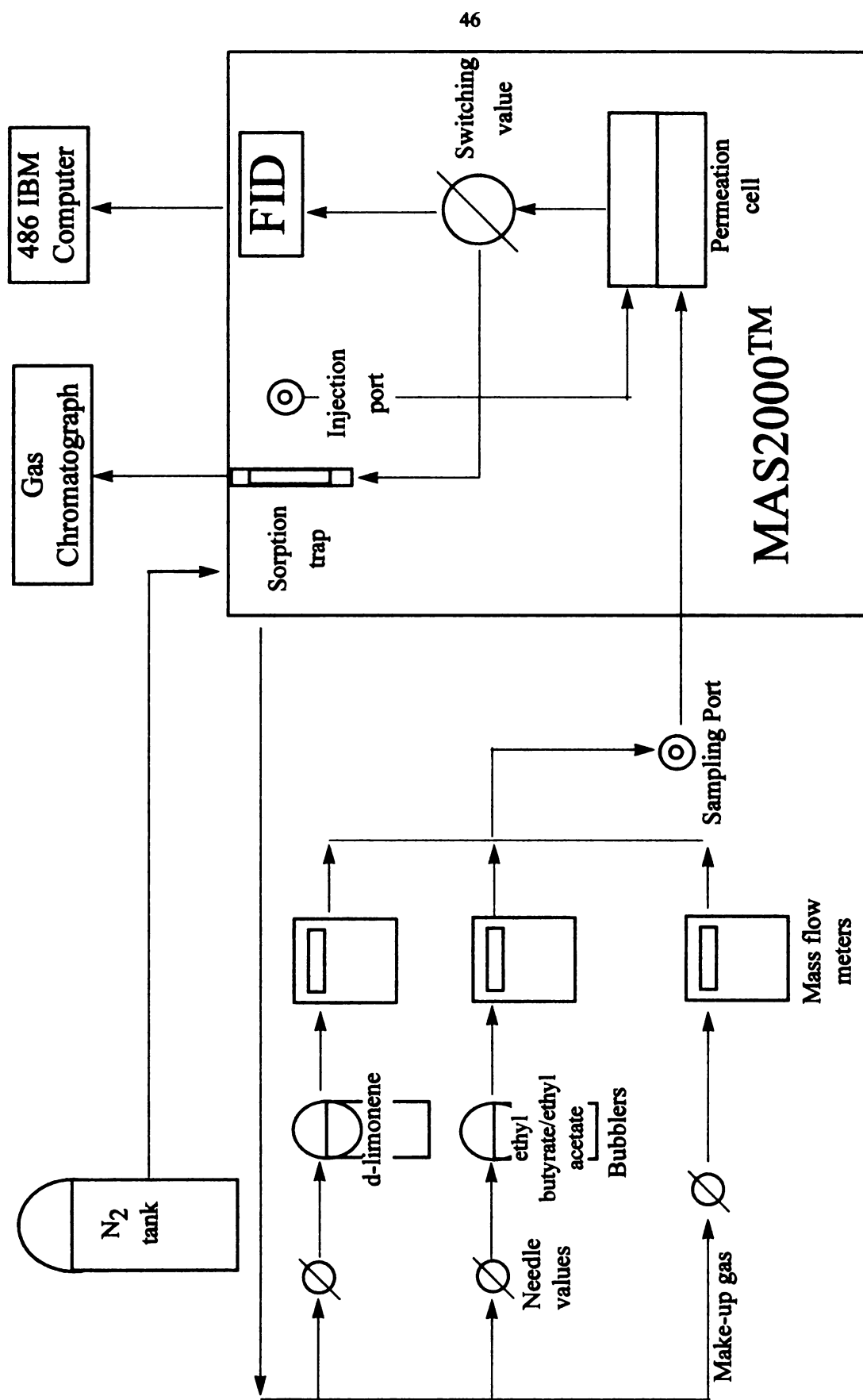


Figure 4. Schematic Diagram of Permeation Test and Trap Apparatus

of a 250 ml gas washing bottle. The gas washing bottles were placed in a constant temperature water bath and the temperature maintained at $23 \pm 1^\circ\text{C}$, throughout.

In order to obtain a wide range of vapor concentration levels, the permeant vapor stream was mixed with another stream of pure carrier gas (nitrogen). Flow meters and needle valves were used to adjust the flows and to indicate constant flow rates.

For studies involving the permeation of binary mixtures, separate vapor streams were generated and mixed to provide a series of binary vapor mixtures of varying vapor activity values.

The vapor activity was correlated linearly with the flow of carrier gas through the bubbler as shown in appendix C. The digital mass flow meters were used to select vapor activity levels required and to monitor a constant flow throughout the test run.

In order to provide an accurate measurement of the permeant vapor concentration or activity, a gas sampling port was installed between the dispensing manifold and the test cell. To determine the specific vapor concentration, a 50 μl sample was withdrawn from the sampling port with a 500 μl gas-tight syringe, and injected directly into the gas chromatograph for quantification. The GC analysis conditions were the same as that for determining the saturated vapor pressure.

The computer software monitors the transmission rate by recording and plotting the signal output in picoamps against time, until it reaches a steady state. The picoamp signal is converted to transmission rate by calibrating a known amount of vapor against the integration value in picoamp per second from the area of picoamp versus time plot. The calibration procedure is done by manually introducing a known amount of vapor through the injection port of the MAS2000TM. The average calibration factor determined

from different vapor activity levels was then used to quantify the transmission rate of the respective permeants through the film. The permeability constant and diffusion coefficient are determined manually from raw data of the MAS2000™.

| Organic Vapors | Average calibration factor* picogram/pamp x sec |
|----------------|----------------------------------------------------|
| Ethyl acetate | 331.14 |
| Ethyl butyrate | 278.571 |
| d-limonene | 152.42 |

* Average value determined from three vapor activity levels.

Dynamic Purge and Trap/Thermal Desorption Procedure

Once the operational parameters of gas flow rates, temperature, vapor pressure, and signal base line became stable, the permeation tests were started. In conducting a permeability run, the test film is initially exposed under isostatic conditions at the required test temperature and permeant concentration and the permeation process continually monitored until a steady state transmission rate is attained. After attaining a steady state rate of transmission, the switching valve was activated and the system was operated in the accumulation or dynamic purge and trap mode for a predetermined time interval. The trapping time for the low barrier OPP film was 30 seconds, while the trapping time for the high barrier PVdC coated OPP film was 3 minutes. The sorbant tube was then removed and immediately replaced by a new trapping tube and the permeated vapor again accumulated for quantification. This sample collection procedure was repeated in triplicate. The sorbant tube removed from the permeability test system

was then transferred to a thermal desorption unit, which thermally desorbs any organic volatiles from the sorbant tube and transfers them to the gas chromatograph for quantification. The sorbed volatiles were desorbed by heating for 8 minutes at 370°C with the valve and transfer line held at 250°C to maintain the desorbed compounds in the vapor phase, while being transferred to the gas chromatograph. Helium was used as a carrier gas through the thermal desorption unit at a flow rate of 9 ml/minute at 40 psi. After sample desorption, the sorbant tubes were conditioned at 350°C for 30 minutes prior to re-use. The trapping and subsequent thermal desorption of volatiles allows their effective release, undiluted, and allows monitoring of otherwise undetectable levels of penetrant concentration.

After each test run, the switching valve in the MAS2000TM was checked for any possible residual volatiles that might have been retained from the previous run. There was no indication of residual volatiles retained by the switching valve on testing, thus, cleaning of the switching valve was not carried out in the present experiment.

Analysis of Test Permeant by Thermal Desorption/Gas Chromatography Procedure

Gas chromatographic (GC) analysis was carried out with a Hewlett-Packard Model 5890 gas chromatograph, equipped with a flame ionization detector and interfaced to a Hewlett-Packard Model 3395 integrator (Avondale, PA), for quantification of permeated vapor. The GC conditions were the same as that for determining the respective calibration curves. The permeance or permeability constant was determined by substitution into

$$P = \frac{CFxAU}{txA\Delta p} \quad (37)$$

where P* = permance [kg / sec m² Pa]

AU = area unit response from integrator [AU]

A = exposed area of the film

CF = dynamic purge and trap/thermal desorption calibration factor

t = trapping time [sec]

Δp = vapor pressure gradient [Pa]

**permeability coefficient is calculated by multiplying permeance by the film thickness*

RESULTS AND DISCUSSION

Comparison between MAS2000™ Isostatic Test Procedure and Dynamic Purge and Trap/Thermal Desorption Procedure

Estimation of the Detection Sensitivity Limit Between the Two Procedures

The lowest detection limit for the dynamic purge and trap/thermal desorption procedure depends upon the trapping time and the gas chromatographic output signal for each particular permeant. Applying the dynamic purge and trap/thermal desorption procedure, Chang (1996) reported that the lowest signal output from the gas chromatograph, with good precision and accuracy, was assumed to be around 5,000 area response units. The longest trapping time in the present study is 3 min. Thus, the minimum measurable transmission rate of limonene is calculated as follows.

$$\frac{5000 AU}{180 \text{ sec}} \times \frac{5.26 \times 10^{-14} \text{ g}}{AU} \times \frac{3600 \text{ sec}}{1 \text{ hr}} \times \frac{1000 \text{ mg}}{1 \text{ g}} = 5.26 \times 10^{-6} \frac{\text{mg}}{\text{hr}} \quad (38)$$

The 5.26×10^{-14} g/AU is the calibration factor of limonene determined by the thermal desorption procedure (Appendix B).

Operating the MAS2000™ Organic Permeation Detection System by the isostatic procedure, the calibration factor in pg/pamp sec was the average value determined at the respective vapor activity levels for each permeant. Assuming that 0.5 pamp is the lowest

detection signal, since it was the lowest signal output obtained for limonene permeability through PVdC coated OPP that was accurate and repeatable, the minimum measurable transmission rate of limonene is calculated as follows.

$$\frac{152.42 \text{ pg}}{\text{pamp sec}} \times 0.5 \text{ pamp} \times \frac{1 \text{ mg}}{10^9 \text{ pg}} \times \frac{3600 \text{ sec}}{1 \text{ hr}} = \frac{2.74 \times 10^{-4} \text{ mg}}{\text{hr}} \quad (39)$$

Table 1. Estimated lowest measurable transmission rate between the two procedures

| Organic Vapors | MAS2000™ Isostatic Mode | Dynamic Purge and Trap/Thermal Desorption Procedure ^(a) |
|----------------|-------------------------------------|--------------------------------------------------------------------------|
| limonene | $2.74 \times 10^{-4} \text{ mg/hr}$ | $5.26 \times 10^{-6} \text{ mg/hr}$ |
| Ethyl butyrate | $1.00 \times 10^{-3} \text{ mg/hr}$ | $1.14 \times 10^{-5} \text{ mg/hr}$ |

^(a) Values are based on a 3 minutes trapping time

Based on this analysis, the sensitivity of the transmission rate measured by the dynamic purge and trap/thermal desorption procedure is two orders of magnitude greater than the MAS2000™ isostatic procedure for both limonene and ethyl butyrate (see Table 1). Chang (1996) also reported similar finding for permeability studies involving the permeability of α -pinene through high barrier polymer membranes.

Comparison of Permeability Values Between the MAS 2000™ Isostatic Test Procedure and the Dynamic Purge and Trap/Thermal Desorption Procedure

A comparison of the permeability coefficient values obtained for d-limonene, ethyl butyrate, and ethyl acetate by the isostatic and dynamic purge and trap/thermal desorption procedures for OPP film is shown in Tables 2, 3, and 4, respectively. Tables 5 and 6 summarize the permeance values for d-limonene and ethyl butyrate through PVdC

coated OPP film. For better illustration the data is presented graphically in Figures 5 and 6, where the permeability parameter (i.e. permeability coefficient or permeance) values, obtained by the respective procedures, are plotted as a function of vapor activity.

Table 2. Permeability coefficient, $\text{kg m/m}^2 \text{ s Pa} \times 10^{-15}$, of limonene through OPP film (50°C) determined by the two procedures ^(a)

| Vapor activity ^(b) | Vapor Pressure (Pa) | MAS2000™ | Dynamic Purge and Trap/TD Procedure | % deviation from MAS2000™ |
|-------------------------------|---------------------|--------------|-------------------------------------|---------------------------|
| 0.3 | 93 | 4.15+/- .37 | 3.67+/- .15 | 11.57% |
| 0.2 | 62 | 4.54+/- .15 | 3.34+/- .017 | 26.43% |
| 0.13 | 41 | 3.65+/- .071 | 3.24+/- .031 | 11.23% |
| 0.05 | 16 | 3.30+/- .42 | 2.68+/- .40 | 18.79% |

^(a) All values are the average of duplicate runs.

^(b) Vapor activity values were determined at room temperature (24°C).

Table 3. Permeability coefficient, $\text{kg m/m}^2 \text{ s Pa} \times 10^{-15}$, of ethyl butyrate through OPP film (50°C) determined by the two procedures ^(a)

| Vapor activity ^(b) | Vapor Pressure (Pa) | MAS2000™ | Dynamic Purge and Trap/TD Procedure | % deviation from MAS2000™ |
|-------------------------------|---------------------|--------------|-------------------------------------|---------------------------|
| 0.2 | 404 | 1.83+/- .19 | 2.07+/- .30 | 13.11% |
| 0.12 | 241 | 1.47+/- .039 | 1.56+/- .012 | 6.12% |
| 0.04 | 73 | 1.53+/- .13 | 1.41+/- .25 | 7.84% |

^(a) All values are the average of duplicate runs.

^(b) Vapor activity values were determined at room temperature (24°C).

Table 4. Permeability coefficient, $\text{kg m/m}^2 \text{ s Pa} \times 10^{-16}$, of ethyl acetate through OPP film (50°C) determined by the two procedures ^(a)

| Vapor activity ^(b) | Vapor Pressure (Pa) | MAS2000™ | Dynamic Purge and Trap/TD Procedure | % deviation from MAS2000™ |
|-------------------------------|---------------------|--------------|-------------------------------------|---------------------------|
| 0.2 | 3287.5 | 6.34+/- .14 | 6.40+/- .28 | 0.95% |
| 0.12 | 1093 | 4.91+/- .079 | 5.29+/- .33 | 7.74% |
| 0.04 | 404 | 4.21+/- .46 | 4.68+/- .26 | 11.16% |

^(a) All values are the average of duplicate runs.

^(b) Vapor activity values were determined at room temperature (24°C).

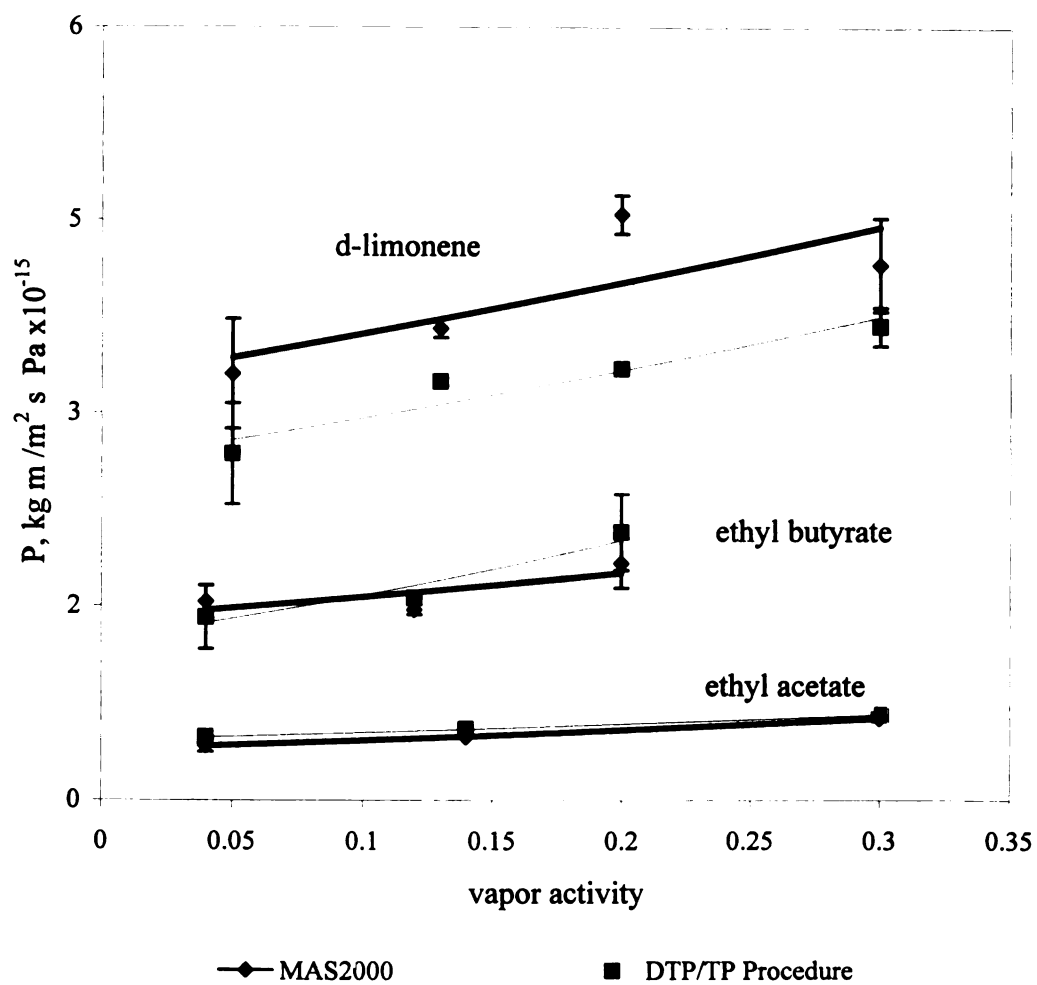


Figure 5. Comparison of permeability of organic vapors through OPP film by MAS2000TM and DTP/TP procedures (50°C)

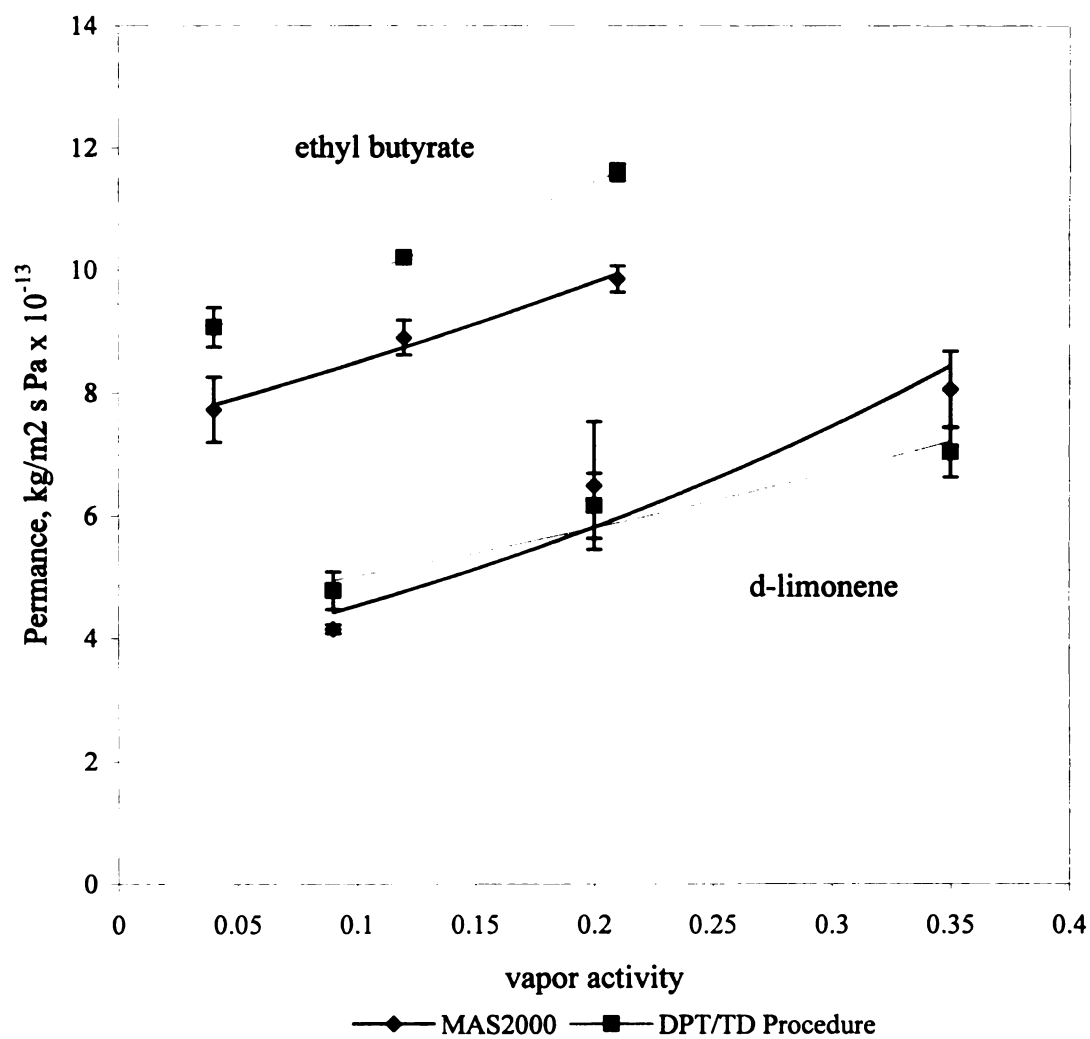


Figure 6. Comparison between MAS2000TM and DPT/TD procedures: organic vapor permeation through PVdC coated OPP film (60°C)

Table 5. Permeance, $\text{kg}/\text{m}^2 \text{ s Pa} \times 10^{-13}$, of limonene through PVdC coated OPP film (60°C) determined by the two procedures ^(a)

| Vapor activity ^(b) | Vapor Pressure (Pa) | MAS2000 TM | Dynamic Purge and Trap/TD Procedure | % deviation from MAS2000 TM |
|-------------------------------|---------------------|-----------------------|-------------------------------------|----------------------------------------|
| 0.35 | 108 | 8.06+/- .62 | 7.04+/- .41 | 12.66% |
| 0.2 | 68 | 6.49+/-1.0 | 6.16+/- .53 | 5.08% |
| 0.09 | 28 | 4.15+/- .071 | 4.78+/- .31 | 15.14% |

^(a) All values are the average of duplicate runs.

^(b) Vapor activity values were determined at room temperature (24°C).

Table 6. Permeance, $\text{kg}/\text{m}^2 \text{ s Pa} \times 10^{-13}$, of ethyl butyrate through PVdC coated OPP film (60°C) determined by the two procedures ^(a)

| Vapor activity ^(b) | Vapor Pressure (Pa) | MAS2000 TM | Dynamic Purge and Trap/TD Procedure | % deviation from MAS2000 TM |
|-------------------------------|---------------------|-----------------------|-------------------------------------|----------------------------------------|
| 0.21 | 436 | 9.85+/- .21 | 11.6+/- .14 | 17.77% |
| 0.12 | 251 | 8.90+/- .28 | 10.2+/- .028 | 14.61% |
| 0.04 | 73 | 7.73+/- .53 | 8.90+/- .86 | 15.14% |

^(a) All values are the average of duplicate runs.

^(b) Vapor activity values were determined at room temperature (24°C).

As shown by the results presented in Tables 2 through 6 and from Figures 5 and 6, there was good agreement between the permeability values obtained by the two test methods for the respective permeant/barrier films systems studied, which considered permeants of various chemical structure, as well as low and high barrier films. The % deviation between the permeability values obtained from the dynamic purge and trap/thermal desorption procedure, as compared with the MAS2000TM isostatic procedure, was less than 20%, except for the permeability of limonene through OPP at a = 0.2, which gave a 26% deviation between the respective permeability coefficient values. The average % deviation between the permeability values obtained by the two procedures for limonene, ethyl butyrate, and ethyl acetate was 14%, 12%, and 7%, respectively. Because of the procedure differences between the isostatic and dynamic

purge and trap/thermal desorption techniques, this agreement is considered to be within acceptable limits.

The average % deviation between the permeability values obtained by the two test procedures was 12%. Thus, establishing the suitability of the proposed dynamic purge and trap/thermal desorption method for measuring permeation rates of binary organic vapor mixtures through barrier films.

The variation between the permeability values obtained by the two procedures can be attributed to a number of factors, such as errors introduced by the gas chromatography procedures and to calibrating both the MAS 2000TM system and the thermal desorption unit. Fluctuation in temperatures and film thickness can also contribute to the observed variation. With respect to the dynamic purge and trap/thermal desorption procedure, variation in trapping time, incomplete trapping during sample collection and incomplete desorption of the trapped volatiles during the desorption process can also introduce sources of error.

Effect of Vapor Activity on the Organic Vapor Diffusion and Permeability Analyzed by Isostatic Permeability Test Procedure

Isostatic permeability studies were carried out to determine the effect of vapor activity on permeability, diffusion, and solubility coefficient values for d-limonene, ethyl acetate, and ethyl butyrate through OPP and PVdC OPP films. The permeability tests were conducted at 50°C for the OPP film and at 60°C for the PVdC coated OPP film at three different vapor activity levels for each respective penetrant, except for the limonene/OPP system, where four vapor activity levels were evaluated. Under these

experimental conditions, the time required for the permeants to reach steady state through the OPP film ranged from 6 hours for ethyl acetate and ethyl butyrate to 8 hours for d-limonene. A steady state rate of permeation through PVdC coated OPP film was achieved within 12 hours for ethyl butyrate and 20 hours for d-limonene, under the experimental conditions.

The diffusion coefficient values reported were the best estimated diffusion coefficient values (D_{est}) based upon the sum of squares technique. The sum of squares method selects the diffusion coefficient which gives the least differences between the experimental transmission rate curve and the theoretical transmission rate curve, obtained by the relation of Fick's first law, as given by Pasternak et al. (1970) (see equation 32). Mathematically the method sums the squares of the differences between experimental and calculated transmission rate values at each point of the transmission rate profile curve. A plot of the corresponding sum of squares values versus diffusion coefficient is then used to determine the least sum of squares diffusion coefficient value. Since the PVdC coated OPP film investigated in the present study is a coated structure, permeance values were calculated to describe the barrier properties of the total structure and the diffusion coefficient values reported were apparent diffusion coefficients, representative of the specific structure. Assuming that the relationship $P = D \times S$ is valid, the solubility coefficients can also be determined. Permeability, diffusion, and solubility coefficient values determined for limonene, ethyl butyrate, and ethyl acetate through the respective polymer membranes, as a function of vapor activity, are summarized in Tables 7-11.

Table 7. Permeability and diffusion coefficients for limonene through the two test films ^(a)

| OPP film (50°C) | | | | PVdC OPP film(60°C) | | | |
|-----------------------|------------------------|----------------------------------------------------|--------------------------------------------------|-----------------------|------------------------|--------------------------------------------------|----------------------------------------------|
| Vapor activity (b) | Vapor Pressure (Pa) | P, kg m/m ² s Pa x 10 ⁻¹⁵ | D, m ² /sec x10 ⁻¹⁴ (c) | Vapor activity (b) | Vapor Pressure (Pa) | P, kg/ m ² s Pa x10 ⁻¹³ | D, m ² /sec x10 ⁻¹⁵ |
| 0.3 | 93 | 4.15+/- .37 | 5.88+/- .18 | 0.35 | 108 | 8.06+/- .62 | 2.73+/- .035 |
| 0.2 | 62 | 4.54+/- .15 | 5.38+/- .18 | 0.2 | 68 | 6.49+/- 1.0 | 2.33+/- .46 |
| 0.13 | 41 | 3.65+/- .071 | 5.05+/- .071 | 0.09 | 28 | 4.15+/- .071 | 2.25+/- .35 |
| 0.05 | 16 | 3.30+/- .42 | 5.13+/- .18 | | | | |

^(a) All values are average of duplicate runs.

^(b) Vapor activity values were determined at room temperature (24°C).

^(c) D determined by the sum of squares method

Table 8. Solubility coefficient values for limonene and the estimated % sorbed (v/v) in the two test films

| OPP film (50°C) | | | | PVdC OPP film(60°C) | | | |
|-------------------------------|------------------------|-------------------------------------------|-------------------|-------------------------------|------------------------|-------------------------------------------|-------------------|
| Vapor activity ^(a) | Vapor Pressure (Pa) | S, kg/m ³ Pa ^(b) | % sorbed (v/v) | Vapor activity ^(a) | Vapor Pressure (Pa) | S, kg/m ³ Pa ^(b) | % sorbed (v/v) |
| 0.3 | 93 | .071 | 0.79% | 0.35 | 108 | .0052 | 0.07% |
| 0.2 | 62 | .084 | 0.62% | 0.2 | 68 | .0050 | 0.04% |
| 0.13 | 41 | .072 | 0.35% | 0.09 | 28 | .0033 | 0.01% |
| 0.05 | 16 | .064 | 0.12% | | | | |

^(a) Vapor activity values were determined at room temperature (24°C).

^(b) S determined by $P=D \times S$ relationship.

Table 9. Permeability and diffusion coefficients for ethyl butyrate through the two test films ^(a)

| | | OPP film (50°C) | | PVdC OPP film(60°C) | |
|-----------------------|------------------------|----------------------------------------------------|--------------------------------------------------|-------------------------------------------------|--------------------------------------------------|
| Vapor Activity (b) | Vapor Pressure (Pa) | P, kg m/m ² s Pa x 10 ⁻¹⁵ | D, m ² /sec x10 ⁻¹³ (c) | P, kg/s m ² Pa x10 ⁻¹³ | D, m ² /sec x10 ⁻¹⁵ (c) |
| 0.2 | 436 | 1.83+/- .19 | 2.08+/- .035 | 9.85+/- .21 | 11.5+/- 1.4 |
| 0.12 | 251 | 1.47+/- .039 | 2.20+/- 0.00 | 8.90+/- .28 | 9.78+/- .035 |
| 0.04 | 73 | 1.53+/- .13 | 1.95+/- 0.00 | 7.73+/- .53 | 9.88+/- .88 |

^(a) All values are average of duplicate runs.

^(b) Vapor activity values were determined at room temperature (24°C).

^(c) D determined by the sum of squares method.

Table 10. Solubility coefficient values for ethyl butyrate and the estimated % sorbed (v/v) through the two test films ^(a)

| Vapor activity | Vapor Pressure (Pa) | OPP film (50°C) | | PVdC OPP film(60°C) | |
|----------------|---------------------|-------------------------|----------------|-------------------------|----------------|
| | | S, kg/m ³ Pa | % sorbed (v/v) | S, kg/m ³ Pa | % sorbed (v/v) |
| 0.2 | 436 | 0.0088 | 0.40% | 0.0015 | 0.07% |
| 0.12 | 251 | 0.0067 | 0.18% | 0.0016 | 0.05% |
| 0.04 | 73 | 0.0078 | 0.06% | 0.0014 | 0.01% |

^(a) S determined by $P=DxS$ relationship

Table 11. Permeability, diffusion and solubility coefficient values and the estimated % permeant sorbed for ethyl acetate through OPP film at 50°C ^(a)

| Vapor activity ^(b) | Vapor Pressure (Pa) | P, kg m/m ² s Pa x 10 ⁻¹⁶ | D, m ² /sec x 10 ⁻¹³ ^(c) | S, kg/m ³ Pa ^(d) | % sorbed (v/v) |
|-------------------------------|---------------------|-------------------------------------------------|-----------------------------------------------------------|----------------------------------------|----------------|
| 0.3 | 3287.5 | 6.34+/-0.14 | 5.58+/-0.11 | 0.0011 | 0.40% |
| 0.14 | 1093 | 4.91+/-0.079 | 5.25+/-0.035 | 0.00094 | 0.11% |
| 0.04 | 404 | 4.21+/-0.46 | 4.38+/-0.18 | 0.00096 | 0.04% |

^(a) All permeability and diffusion values are average of duplicate runs.

^(b) Vapor activity values were determined at room temperature (24°C).

^(c) D determined by sum of squares method.

^(d) S determined by $P=DxS$ relationship

To better illustrate the effect of vapor activity on the permeability of the test films, the results are presented graphically in Figures 5 and 6, where the permeability parameters (permeability coefficient or permeance) are plotted as a function of vapor activity. Figures 7 and 8 plot the diffusion coefficient values of each permeant through OPP and PVdC coated OPP films as a function of permeant vapor activity. The relationship between the solubility coefficient values for the respective permeant/barrier membrane systems, as a function of vapor activity, is presented graphically in Figures 9 and 10, respectively.

A single factor statistical analysis, using Minitab software, was performed to determine whether the experimentally obtained permeability, diffusion and solubility

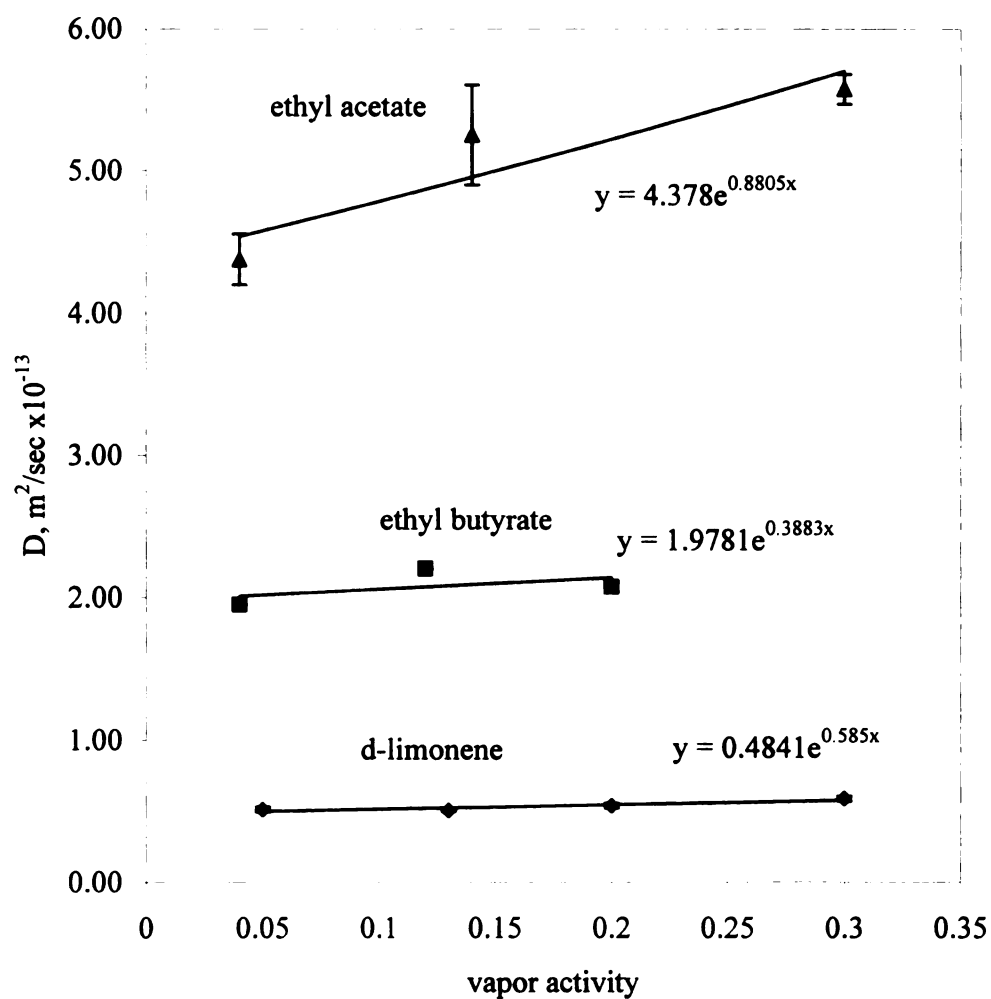


Figure 7. Diffusion coefficient of organic vapors through OPP film as a function of vapor activity (50°C)

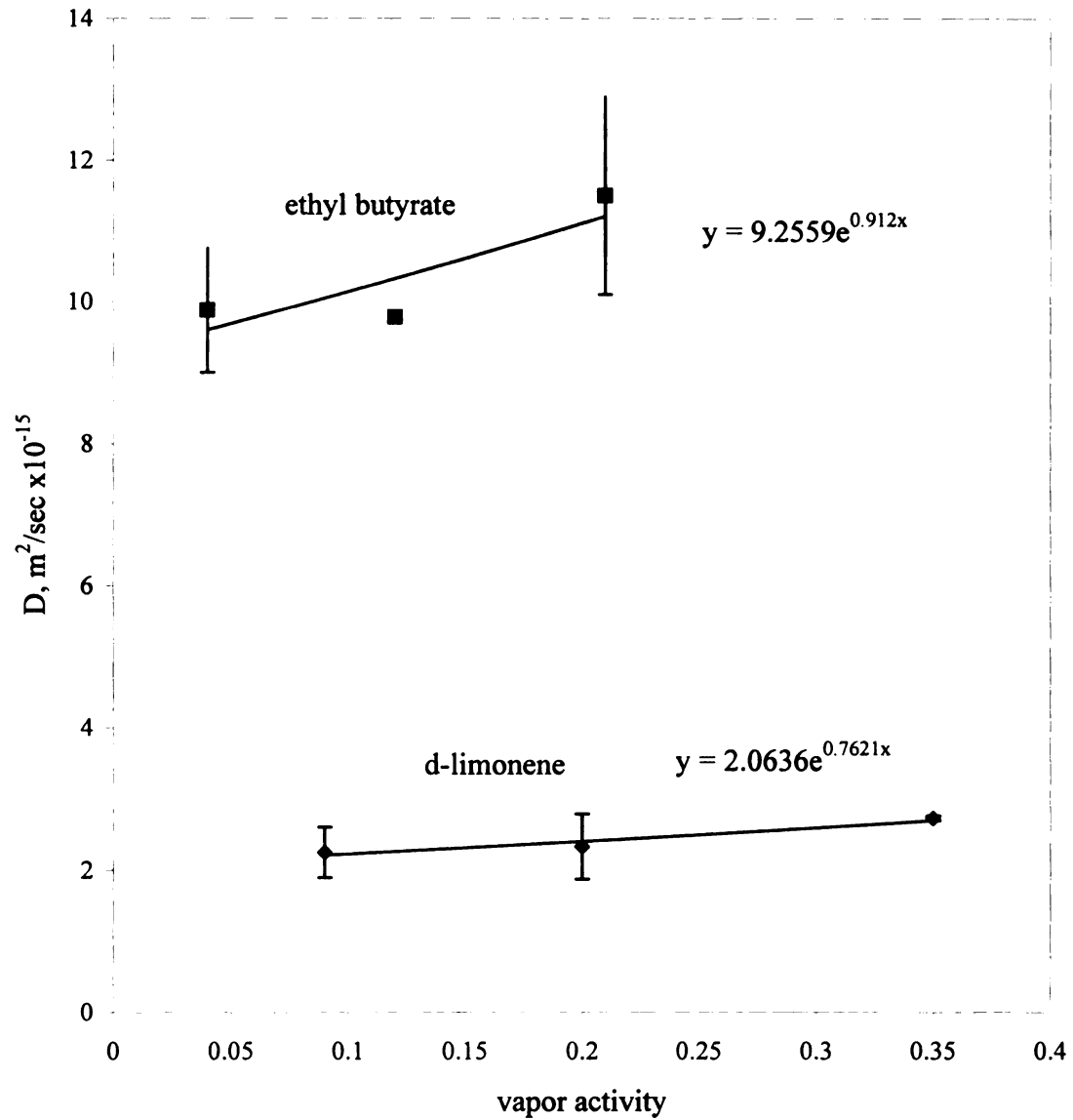


Figure 8. Apparent diffusion coefficient of organic vapors through PVdC coated OPP as a function of vapor activity

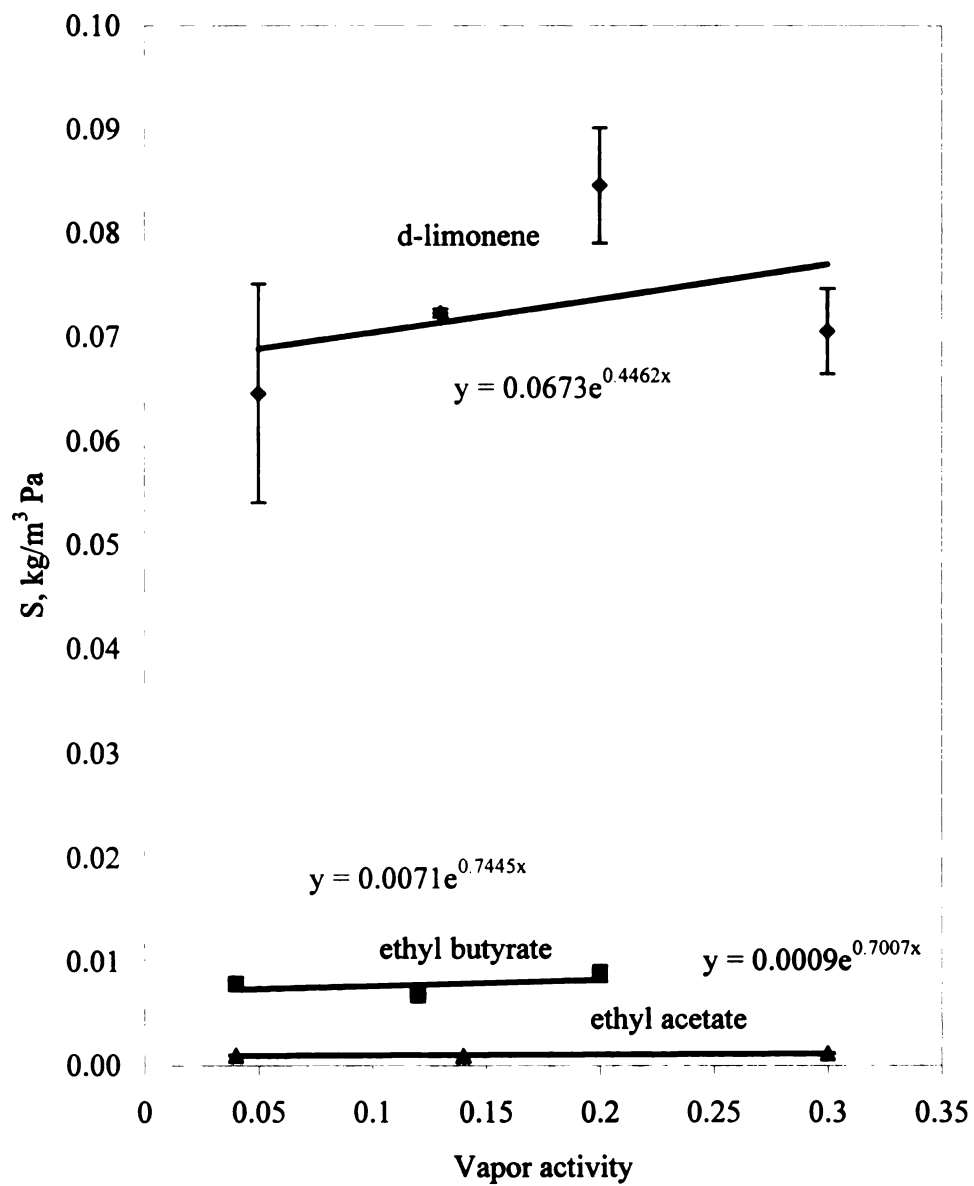


Figure 9. Solubility coefficient of organic vapors in OPP film as a function of vapor concentration (50°C)

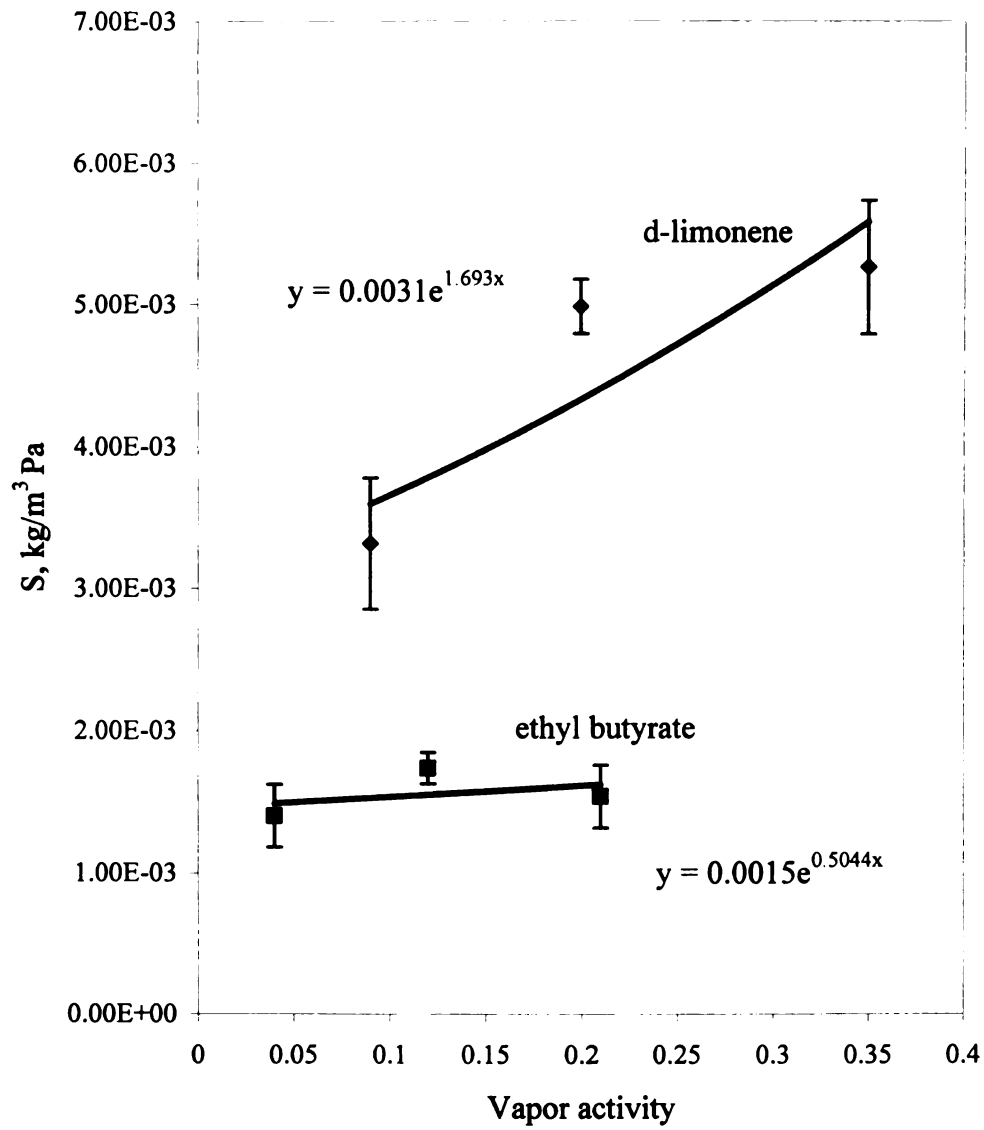


Figure 10. Solubility coefficient of organic vapors in PVdC coated OPP film as a function of vapor concentration

coefficient values differed significantly over the vapor activity ranges evaluated. The significant level of test is at alpha 0.05. A detailed description of the statistical analysis performed is presented in appendix E. The analysis indicated a statistically significant effect of vapor concentration on the diffusion coefficients obtained for OPP film and the respective permeants. However, there was no statistically significant effect of vapor concentration on the diffusion coefficient values determined for the PVdC coated OPP film. The effect of vapor concentration on the solubility coefficient for the respective permeants and the test films evaluated was not statistically significant, except for the limonene/PVdC coated OPP film permeant/polymer system. The permeants showed a statistically significant effect of vapor concentration on the permeability values obtained for both OPP and PVdC coated OPP (permeability coefficient or permeance), except for the ethyl butyrate/OPP system.

Even though there was a statistically significant effect of vapor concentration on the diffusion coefficient for selected permanent/ film systems, the effect is small. According to equation 20 in the literature review, the slope of the plot of the diffusion coefficient vs vapor activity, which is defined as α , measures the plasticizing effect that each sorbed penetrant has on the polymer chains.

$$D = D(0) \exp(\alpha a) \quad (20)$$

The maximum value of α found in the present study is less than 1. The small value of α suggests that there was no plasticization of polymer chains by the permeants at the test conditions.

The respective solubility coefficient values and the estimated % permeant sorbed (v/v) for each permeant in OPP and PVdC coated OPP films are summarized in Tables 8, 10, and 11. Figures 9 and 10 show a plot of the solubility coefficients for each permeant in the OPP and PVdC films, as a function of vapor activity. The overall % permeant sorbed by either film is less than 1%, on a volume/volume basis. The observed transport behavior suggests that the sorption of the permeants at the test temperatures and the concentration range evaluated does not result in strong penetrant/polymer interaction and thus swelling of the polymer matrix. The transport process therefore appears to behave like that of a permanent gas, where the permeant driving force concentration has little or no effect on the permeability values.

In the present study, the effect of permeant size and its chemical nature on the diffusion and sorption processes follows that predicted by mass transfer theory. In OPP film the diffusion coefficient is highest for the lowest molecular weight permeant, ethyl acetate and lowest for the highest molecular weight permeant, limonene. This is illustrated graphically in Figure 11, where $\log D_0$, the diffusion coefficient at zero penetrant concentration through OPP film at 50°C, is plotted against the penetrant molar volume. The diffusion coefficient decreases by nearly one order of magnitude as the penetrant molar volume increases by approximately 150%. Diffusion of the permeants through PVdC coated OPP also behave in a similar way.

The Hildebrand solubility parameters (δ) values for the permeants and OPP, calculated by the component group contributions method of Hofryzer and Van Krevelen (1976), are presented in Table 12. The solubility parameters of d-limonene and polypropylene are equivalent, while the difference for ethyl butyrate and OPP is 0.2, and

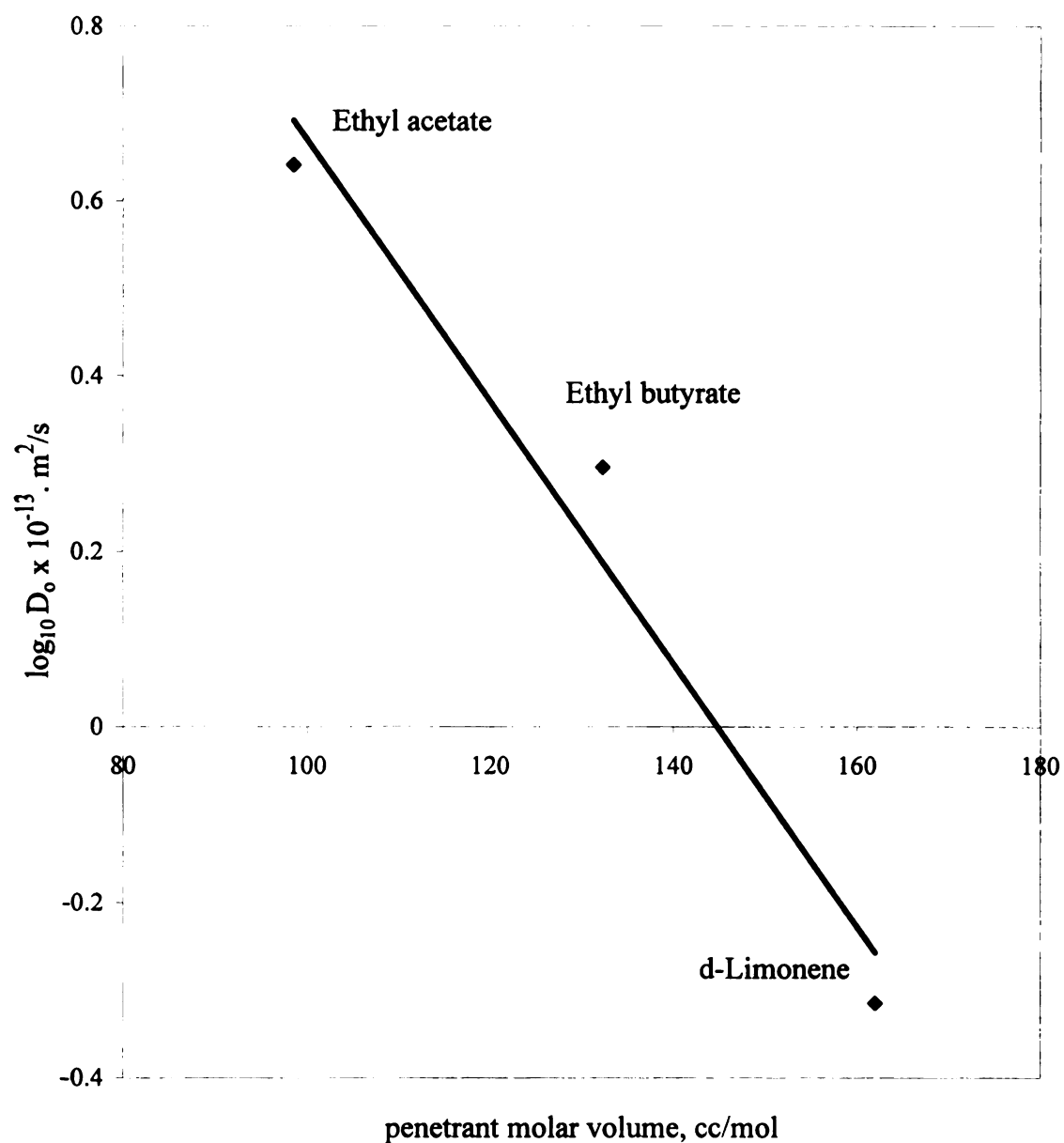


Figure 11. Diffusivities of organic vapors through OPP at 50°C as a function of penetrant molar volume

the difference between the solubility parameter values of ethyl acetate and polypropylene is 0.6. Both ethyl acetate and ethyl butyrate have moderate polar bonding force contribution, while polypropylene and d-limonene have no polar bonding force contribution. This would predict limonene to have the highest solubility coefficient in OPP and PVdC coated OPP film, where the bulk of the film is OPP, followed by ethyl butyrate and ethyl acetate, respectively. Experimental solubility data for OPP and PVdC coated OPP films agreed well with the trend of the estimated values of the solubility parameters. The solubility coefficient of limonene is the highest in both films because of the similar nonpolar structures of limonene and polypropylene, which tend to maximize solubility, as compared to the relatively polar ethyl acetate and ethyl butyrate structures. Moreover, when comparing ethyl acetate and ethyl butyrate, two permeants of similar chemical structure, the solubility coefficient in OPP film for the higher molecular weight permeant, ethyl butyrate, is greater than that of ethyl acetate, the lower molecular weight permeant. As the size of the permeant molecule increases, the diffusion coefficient decreases and the solubility coefficient increases. Many investigators have observed a similar trend (Zobel, 1982; Hotchkiss et al., 1988).

Table 12. The Hildebrand solubility parameters (δ) values

| Permeant/Polymer | Hildebrand Solubility Parameters, (cal/cc) ^{1/2} | Polar-bonding character |
|------------------|-----------------------------------------------------------|-------------------------|
| PP | 8.3 ^(a) | Poor |
| d-Limonene | 8.21 ^(b) | Poor |
| Ethyl acetate | 9.11 ^(a) | Moderate |
| Ethyl butyrate | 8.5 ^(c) | Moderate |

^(a) Values taken from Van Krevelen, 1976

^(b) Value taken from Halek and Luttmann, 1991

^(c) Value taken from Nielsen et al., 1992

The Effect of Binary Mixtures Composition on Co-permeant Permeability

The effect of a co-permeant on the permeability of binary mixtures through the OPP film and the PVdC coated OPP film was studied by determining the permeation rate of the constituents of the binary mixture for a series of binary mixtures of varying composition using a dynamic purge and trap/thermal desorption procedure. The results are summarized in Tables 13, 14, 15, and 16. Tables 13 and 14 summarize the permeability coefficient values for d-limonene and ethyl butyrate as both single permeants and in binary mixtures through OPP film at 50°C. Table 13 also summarizes permeability coefficient values for limonene/ethyl acetate binary mixtures. Tables 15 and 16 summarize permeance values for d-limonene and ethyl butyrate, as both single permeants and in binary mixtures, through PVdC coated OPP at 60°C. As shown in Tables 13 and 15, the permeability runs were carried out at limonene vapor activity levels of $a=0.3$, 0.2, 0.13, and 0.05 for the OPP film and at vapor activity levels of $a=0.2$ and 0.13 for the PVdC coated OPP film. For the respective limonene vapor activity levels, three different ethyl butyrate vapor activity levels were studied, except for the limonene vapor activity of $a = 0.3$ in OPP film, where only two ethyl butyrate vapor activity levels were evaluated. For better illustration, the results from Tables 13 and 15 are presented graphically in Figures 12 and 13, where d-limonene permeability rates are plotted as a function of ethyl butyrate vapor activity. It follows from Tables 13 and 15 and from the graphical presentation (Figures 12 and 13) that at the concentration levels evaluated, ethyl butyrate did not appear to affect the transport characteristics of limonene vapor

Table 13. The permeability coefficient, $\text{kg m/s m}^2 \text{ Pa} \times 10^{-15}$, of limonene through OPP film (50°C) as a single permeant and in binary mixtures with ethyl butyrate and ethyl acetate ^(a) ^(b) ^(c)

| Limonene | | Single permeant | co-permeant with ethyl butyrate vapor activity of | | |
|----------------|---------------------|-----------------|---------------------------------------------------|-------------------|------------------|
| Vapor activity | Vapor Pressure (Pa) | | a = 0.2 (404 Pa) | a = 0.12 (241 Pa) | a = 0.04 (73 Pa) |
| 0.3 | 93 | 3.67+/-0.15 | | 3.95+/-0.11 | 3.59+/-0.21 |
| 0.2 | 62 | 3.34+/-0.017 | 4.32+/-0.67 | 3.93+/-0.35 | 3.56+/-0.13 |
| 0.13 | 41 | 3.24+/-0.031 | 3.66+/-0.15 | 3.65+/-0.09 | 3.47+/-0.29 |
| 0.05 | 16 | 2.68+/-0.40 | 3.30+/-0.28 | 3.12+/-0.01 | 3.30+/-0.06 |
| Limonene | | Single permeant | co-permeant with ethyl acetate vapor activity of | | |
| Vapor activity | Vapor Pressure (Pa) | | a = 0.3 | a = 0.14 | a = 0.04 |
| | | | 3287.5 Pa | 1093 Pa | 404 Pa |
| 0.2 | 62 | 3.34+/-0.017 | 4.2+/-0.0064 | 3.65+/-0.0042 | 3.52+/-0.00 |

^(a) All values are average of duplicate runs.

^(b) All values were determined by dynamic purge and trap/thermal desorption procedure.

^(c) All vapor activity levels are determined at room temperature.

Table 14. The permeability coefficient, $\text{kg m/s m}^2 \text{ Pa} \times 10^{-15}$, of ethyl butyrate through OPP film (50°C) as a single permeant and in binary mixture with limonene ^(a) ^(b) ^(c)

| Ethyl butyrate | | Single permeant | co-permeant with limonene vapor activity of | | | |
|----------------|---------------------|-----------------|---------------------------------------------|-----------------|------------------|------------------|
| vapor activity | Vapor Pressure (Pa) | | a = 0.3 (93 Pa) | a = 0.2 (62 Pa) | a = 0.13 (41 Pa) | a = 0.05 (16 Pa) |
| 0.2 | 404 | 2.07+/-0.30 | | 2.24+/-0.46 | 1.80+/-0.099 | 1.92+/-0.127 |
| 0.12 | 241 | 1.56+/-0.012 | 1.95+/-0.15 | 1.70+/-0.15 | 1.55+/-0.035 | 1.62+/-0.078 |
| 0.04 | 73 | 1.41+/-0.25 | 2.10+/-0.24 | 1.68+/-0.071 | 1.65+/-0.29 | 1.75+/-0.071 |

^(a) All values are average of duplicate runs.

^(b) All values were determined by dynamic purge and trap/thermal desorption procedure.

^(c) All vapor activity levels are determined at room temperature.

through either OPP or PVdC coated OPP films. For the respective ethyl

butyrate/limonene vapor activity combinations evaluated, the permeability coefficient for

Table 15. The permeance, $\text{kg/s m}^2 \text{ Pa} \times 10^{-13}$, of limonene through PVdC coated OPP film (60°C) as a single permeant and in binary mixtures with ethyl butyrate ^{(b) (c) (d)}

| Limonene | | Single permeant | Co-permeant with ethyl butyrate vapor activity of | | |
|----------------|-------------------|----------------------------|---------------------------------------------------|-------------------|------------------|
| Vapor activity | Vapor Pressure Pa | | a = 0.2 (436 Pa) | a = 0.12 (251 Pa) | a = 0.04 (73 Pa) |
| 0.2 | 62 | 6.16+/- .53 | 6.50+/- .318 | 5.24+/- .332 | 4.64+/- .9 |
| 0.13 | 41 | 4.78+/- .31 ^(a) | 4.73+/- .643 | 5.02+/- .594 | 5.59+/- .11 |

^(a) Value based upon limonene vapor activity of $a = 0.09$

^(b) All values are average of duplicate runs

^(c) All values were determined by dynamic purge and trap/thermal desorption procedure.

^(d) All vapor activity levels are determined at room temperature

Table 16. The permeance, $\text{kg/s m}^2 \text{ Pa} \times 10^{-12}$, of ethyl butyrate through PVdC coated OPP film (60°C) as a single permeant and in binary mixtures with d-limonene ^{(a) (b) (c)}

| Ethyl butyrate | | Single permeant | Co-permeant with limonene vapor activity of | |
|----------------|-------------------|-----------------|---------------------------------------------|------------------|
| Vapor activity | Vapor Pressure Pa | | a = 0.2 (62 Pa) | a = 0.13 (41 Pa) |
| 0.2 | 436 | 1.16+/- .014 | 1.40+/- .0071 | 1.36+/- .028 |
| 0.12 | 251 | 1.02+/- .0028 | 1.13+/- .064 | 1.04+/- .18 |
| 0.04 | 73 | 0.89+/- .086 | 1.04+/- .0021 | 1.16+/- .14 |

^(a) All values are average of duplicate runs.

^(b) All values were determined by dynamic purge and trap/thermal desorption procedure.

^(c) All vapor activity levels are determined at room temperature.

limonene remained constant and was statistically equivalent to the permeability

coefficient value obtained for pure limonene vapor, at similar activity levels.

Tables 14 and 16 summarize the results of permeability studies carried out to evaluate the effect of d-limonene on the permeability of ethyl butyrate. Permeability studies were carried out at ethyl butyrate vapor activity levels of $a=0.2$, $a=0.14$ and 0.04 for both OPP and PVdC coated OPP films. Three to four different limonene vapor activity levels for the OPP film and two different limonene vapor activity levels for the

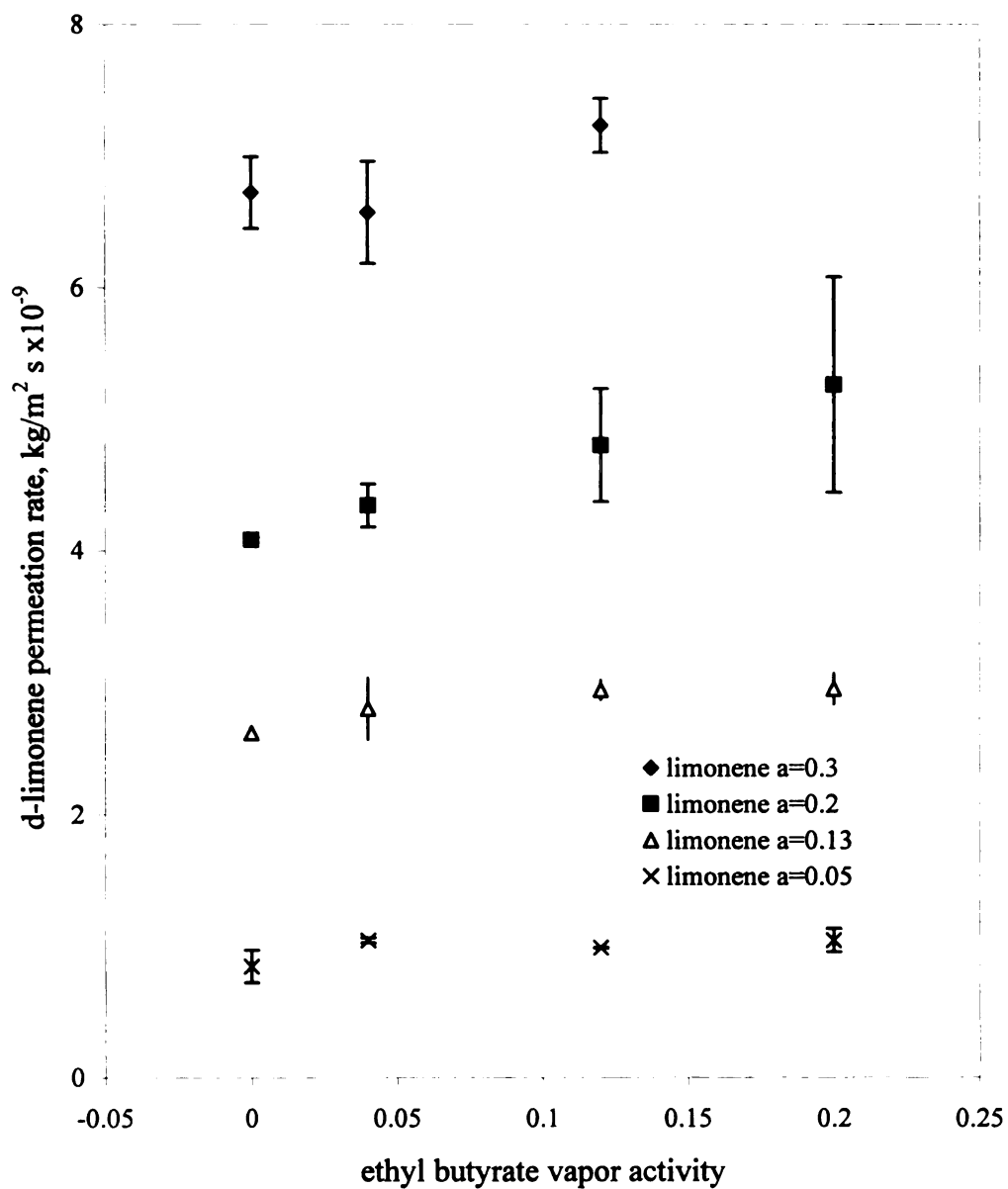


Figure 12. Effect of ethyl butyrate on the permeation rate of d-limonene through OPP as a function of binary mixture composition (50°C)

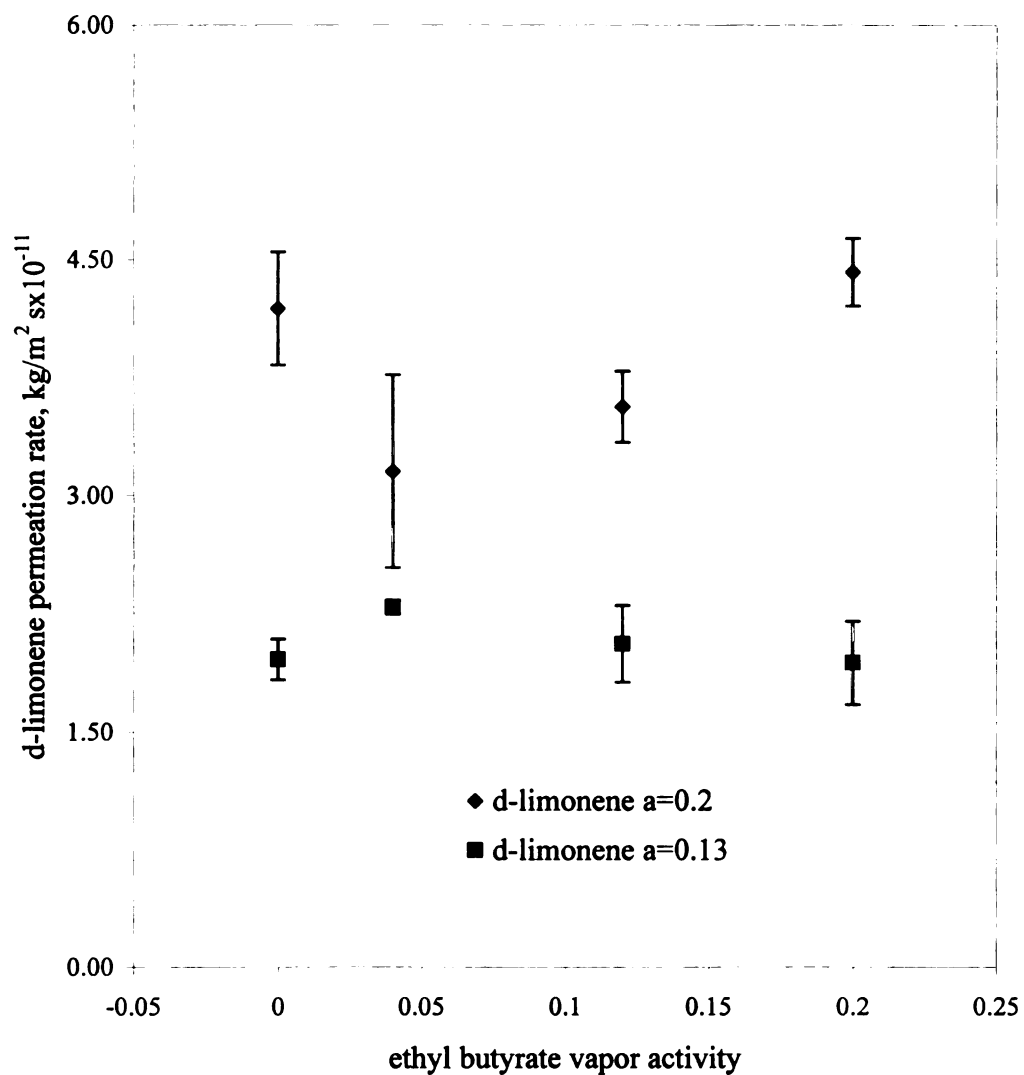


Figure 13. Effect of ethyl butyrate on permeation rate of d-limonene through PVdC/OPP film as a function of binary mixture composition (60°C)

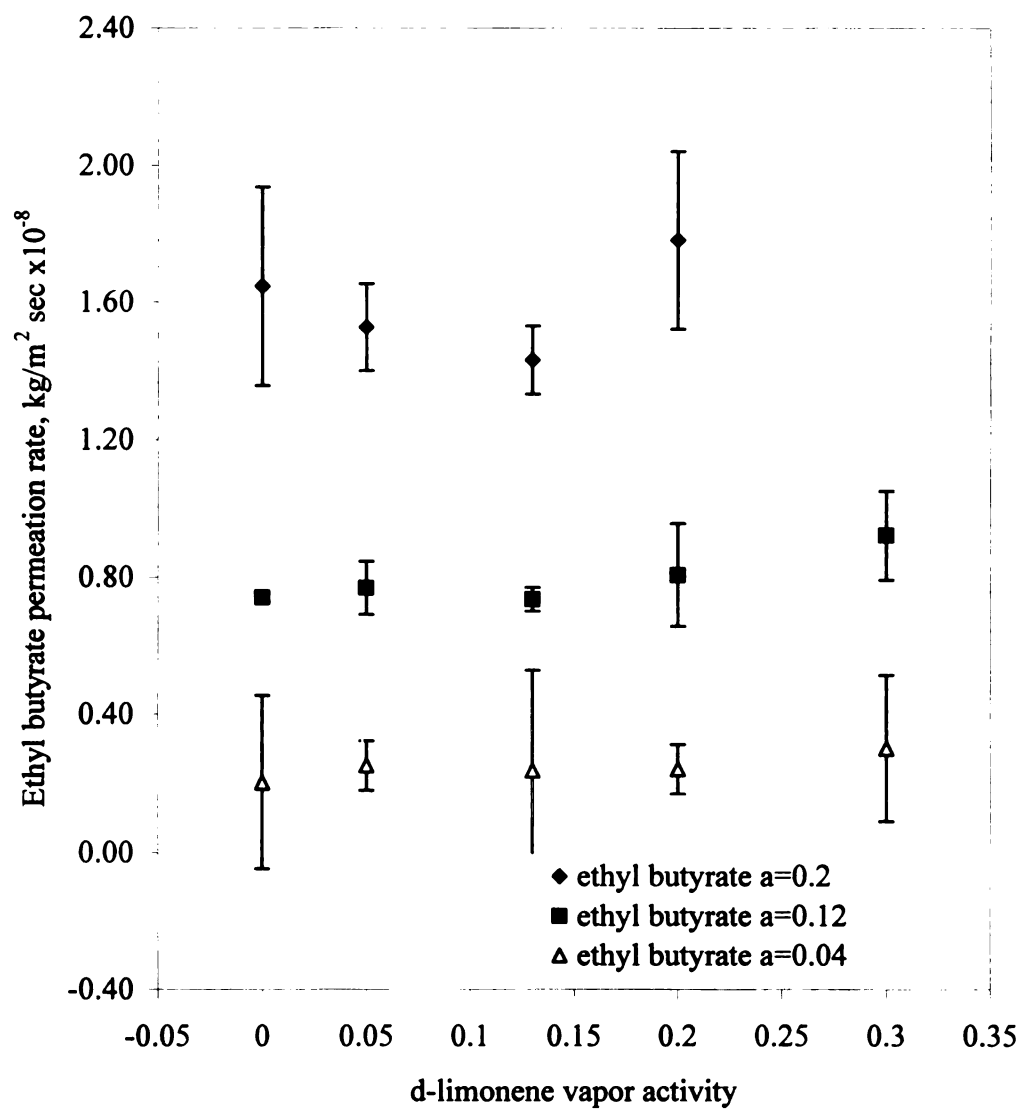


Figure 14. Effect of d-limonene on the permeation rate of ethyl butyrate through OPP as a function of binary mixture composition (50°C)

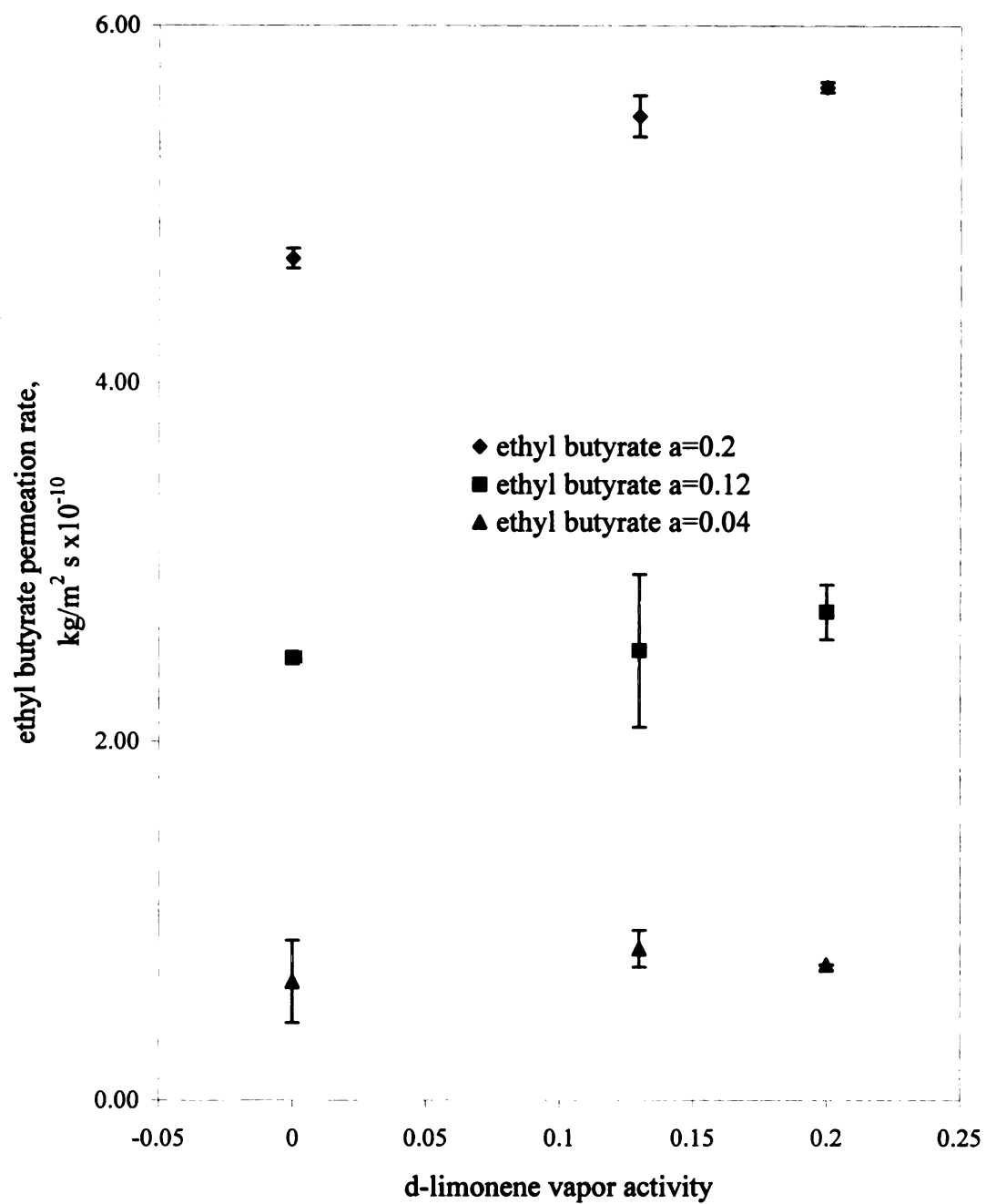


Figure 15. Effect of d-limonene on the permeation rate of ethyl butyrate through PVdC/OPP film as a function of binary mixture composition (60°C)

PVdC coated OPP film were evaluated for the respective ethyl butyrate vapor activity levels. Limonene did not appear to influence the permeability of ethyl butyrate vapor through either OPP or PVdC coated OPP films, at the concentrations evaluated. Statistical analysis indicated that the permeability of one binary mixture composition through OPP film and two mixture compositions through PVdC coated OPP films showed a statistically significant increase in ethyl butyrate permeability in the presence of limonene. In general, for the respective binary vapor mixtures studied, d-limonene does not appear to affect the transport characteristics of ethyl butyrate vapor, as compared to the permeability values obtained for ethyl butyrate as a single permeant, run at comparable vapor activity levels. The results summarized in Tables 14 and 16 are presented graphically in Figures 14 and 15, where ethyl butyrate permeability rates are plotted as a function of d-limonene vapor activity.

By direct measurement of the permeation rates (Tables 13 to 16) it was found that the permeability values for d-limonene and ethyl butyrate were not affected by the presence of a co-permeant, over the range of vapor activity levels studied. This is illustrated graphically in Figure 16, where the transmission rate profile curves for ethyl butyrate ($a = 0.04$) and d-limonene ($a = 0.05$), determined as pure single component vapors and as a binary mixture (ethyl butyrate $a = 0.04$ /d-limonene $a = 0.05$) through OPP, are superimposed. As shown, the total permeation rate of the binary mixture is equal to the sum of the permeation rates of the individual permeants.

Similar results were obtained for the permeability of ethyl butyrate/ limonene binary mixtures through PVdC coated OPP film, as illustrated in Figure 17, where the transmission rate profile curves for the pure permeants (ethyl butyrate $a = 0.21$ and d-

Table 19. The permeability coefficient, $\text{kg m/s m}^2 \text{ Pa} \times 10^{-16}$, of ethyl acetate through OPP film (50°C) in single permeant and in binary mixture with limonene ^(a) ^(b) ^(c)

| Ethyl acetate | | Single permeant | Co-permeant with limonene vapor activity of $a=0.2$ (62 Pa) |
|----------------|-------------|-----------------|-------------------------------------------------------------------|
| Vapor activity | Pressure Pa | | |
| 0.3 | 3287.5 | 6.40+/-0.28 | 8.99+/-0.31 |
| 0.14 | 1093 | 5.29+/-0.33 | 6.71+/-0.042 |
| 0.04 | 404 | 4.68+/-0.26 | 4.82+/-0.28 |

^(a) All values are average of duplicate runs.

^(b) All values were determined by dynamic purge and trap/thermal desorption procedure.

^(c) All vapor activity levels are determined at room temperature.

While statistical analysis showed a significant difference, at a confidence level of 95%, between the permeability of pure ethyl acetate and for ethyl acetate in the binary mixtures described above, the effect of the co-permeant (i.e. limonene) was minimal when compared to the synergistic effect of d-limonene on the permeability of ethyl acetate vapor reported by Hensley et al. (1991), who found that limonene as a co-permeant increased the permeability of ethyl acetate through OPP film by as much as 40 times.

To account for the observed dramatic increase in the permeability coefficient for ethyl acetate in the presence of limonene as a co-permeant, Nielson and Giacin (1994) proposed a co-penetrant dependency of the diffusion coefficient, due in part to co-penetrant induced relaxation effects occurring within the polymer matrix. The absorption of organic vapors can result in polymer swelling and thus change the conformation of the polymer chains. These conformation changes are not instantaneous, but are controlled by the retardation times of polymer chains. If these times are long, stresses may be set up which relax slowly. Thus, the absorption and diffusion of organic vapors can be accompanied by concentration as well as time-dependent processes within the polymer

bulk phase, which are slower than the micro-Brownian motion of polymer chain segments which promote diffusion (Mears, 1965).

Thus, the previously reported dramatic increase in the permeability of ethyl acetate through OPP in the presence of limonene may be attributed to co-penetrant induced relaxation effects occurring during the diffusion of ethyl acetate/limonene binary mixtures through the oriented polypropylene film investigated. Such relaxation processes, which occur over a longer time-scale than diffusion, may be related to a structural reordering of the free volume elements in the polymer. Thus, providing additional sites of appropriate size and frequency of formation, which promote diffusion and account for the observed increase in the permeation rate of ethyl acetate in the presence of limonene as a co-permeant.

In comparing the results of the permeability studies of ethyl acetate/limonene binary mixtures through OPP film reported by Hensley et al. (1991) with the results of the present study, it should be noted that Hensley et al. carried out the permeability studies at ambient temperature (i.e. $23 \pm 1^\circ\text{C}$), while the present studies was carried out at 50°C . The results of their two studies suggest that the effect of limonene on the permeability of a co-permeant in binary mixtures at high temperature is minimized. At high temperature, the sorption of limonene might not be at a level required to cause changes in polymer chain conformation. The estimated solubility values of d-limonene by OPP film in the present study ranges from 0.064 to $0.084 \text{ kg/m}^3 \text{ Pa}$. The values are four times less than the value of $0.33 \text{ kg/m}^3 \text{ Pa}$ reported by Nielson and Giacini (1994). Therefore, such co-permeant induced relaxation mechanism as proposed by Nielson and Giacini (1994) might not have occurred in oriented polypropylene at the present test

temperature of 50°C. Thus, a substantial increase in the permeation rates of the co-permeants, ethyl acetate and ethyl butyrate, in the presence of limonene were not observed in the present study.

Statistical Analysis of Binary Mixture Permeability Studies

For each concentration level of limonene and ethyl butyrate, statistical analysis, using single factor ANOVA, was performed on MINITAB to determine whether there was a difference between the permeation rate of the pure permeant and the permeant in a binary mixture. If such a difference was detected at 95% confidence interval, a Dunnett pairwise comparison test was further performed to determine which pairwise comparison between the permeability of a permeant in a binary mixture and the permeability of the pure permeant, at similar concentration level, is significant at the 95% confidence level. For all limonene vapor activity levels evaluated in both OPP and PVdC coated OPP films, the addition of ethyl butyrate did not result in a statistically significant increase or decrease in permeability values of d-limonene, with a confidence level of 95%. Further, the addition of ethyl acetate to limonene vapor at an activity level of $a=0.20$ did not significantly change the permeability of limonene through OPP film, at a confidence level of 95%. The addition of limonene to ethyl butyrate vapor resulted in a significant increase in the permeability of ethyl butyrate with a 95% confidence level, only at one mixture composition for OPP film and two binary mixture compositions for PVdC coated OPP film. The binary mixture compositions are limonene $a=0.3$ /ethyl butyrate $a=0.12$ for OPP; limonene $a=0.2$ /ethyl butyrate $a=0.21$ and limonene $a=0.13$ /ethyl butyrate $a=0.21$

for PVdC coated OPP film.

For comparing ethyl acetate permeability coefficients through OPP film as a single vapor vs. the permeability of ethyl acetate in binary mixtures with limonene vapor activity of $a=0.2$, a two sample t-test was performed to determine whether the permeability values at each respective vapor activity level are significantly different at a 95% confidence level. Of the three ethyl acetate/ limonene mixture compositions, two mixture compositions showed that the ethyl acetate permeability coefficients are significantly different at 95% confidence level. They are limonene $a=0.2$ /ethyl acetate $a=0.30$ and limonene $a=0.2$ /ethyl acetate $a=0.14$. Appendix F summarizes details of statistical analysis utilized in the present study.

SUMMARY AND CONCLUSIONS

The dynamic purge and trap/thermal desorption procedure developed was found to increase the sensitivity of the permeability values by as much as two orders of magnitude, as compared to the isostatic permeation test procedure employed by the MAS2000TM Permeation Test System. Both procedures showed good agreement between the permeability values obtained, with the % deviation between the permeability values obtained being less than 20%. The average % deviation between the permeability values obtained by the two procedures for limonene, ethyl butyrate, and ethyl acetate was 14%, 12%, and 7%, respectively. While the MAS2000TM Permeation Test System lacks the ability to detect the constituents of a binary mixtures, the dynamic purge and trap/thermal desorption procedure developed, proved to be an effective analytical procedure to study the permeability of multi-component organic vapor mixtures through polymer membranes.

This study was designed to determine the effect of varying concentrations of organic vapors alone, and in binary mixtures on the barrier properties of an oriented polypropylene film and a high barrier PVdC coated oriented polypropylene film. The permeability tests were carried out at 50°C for OPP and 60°C for PVdC coated OPP film. The results obtained indicated that the permeants; ethyl butyrate, ethyl acetate and d-limonene showed minimal concentration dependency for the mass transfer parameters, permeability coefficient and permeance constant, and D, within the vapor activity ranges

studied, for the two test membranes. The effect of a co-permeant on the permeability of binary mixtures through OPP film and the PVdC coated OPP film was studied by determining the permeation rate of the constituents of the binary mixture for a series of binary mixtures of varying composition using the dynamic purge and trap/thermal desorption procedure. When combined in a series of binary mixtures, the constituents of the mixtures showed little propensity of altering the transport properties of the co-permeant. For the respective ethyl butyrate/limonene vapor activity combinations evaluated, the permeability values for limonene remained constant and were statistically equivalent to the permeability values obtained for pure limonene vapor at similar activity levels.

The results of permeability studies carried out to evaluate the effect of d-limonene on the permeability of ethyl butyrate showed that limonene did not influence the permeability of ethyl butyrate vapor through either OPP or PVdC coated OPP films at the vapor concentrations evaluated, as compared to the permeability values for the ethyl butyrate as a single permeant, run at comparable vapor activity levels.

Similar results were obtained for the permeability of d-limonene/ethyl acetate binary mixtures through OPP film and while statistical analysis showed a significant difference, at a confidence level of 0.05%, between the permeability coefficient of ethyl acetate and for ethyl acetate in selected binary mixtures evaluated (see Appendix F), the effect of the co-permeant (i.e. limonene) was minimal.

FUTURE STUDY

A number of additional studies can be proposed to develop a better understanding of the factors influencing the permeability of multi-component vapor mixtures. With limonene, which is known to plasticize polymers having a similar chemical structure such as OPP, it is interesting to determine how molecular size, geometry, or the chemical nature of the co-permeant contributes to the effect of d-limonene on the permeability of the co-permeant. Other permeants, such as oxygen and carbon dioxide, which have a smaller molecular size than organic compounds, should also be affected by limonene in the mixture as well. While the results from this study suggest that there was a minimal effect of co-permeant on the permeability of the respective constituents of limonene/ethyl acetate binary mixtures at an elevated temperature, it is not fully understood what the relationship is between temperature and the effect of limonene as a co-permeant on the permeability of binary vapor mixtures. It is therefore proposed that a study be carried out to evaluate the effect of temperature on the permeability of binary vapor mixtures, such as d-limonene/ethyl acetate. The proposed studies would be carried out at constant vapor pressures, with the temperature of test ranging from ambient (i.e. 23°C) to 50°C. It has been proposed, based on the studies of Hensley et al. (1991) and Nielson and Giacini (1994), that the plasticization of OPP by d-limonene leads to an increase in free volume within the polymer bulk phase and thus an increase in the rate of diffusion of a co-permeant. It is not clear whether such plasticization would occur in the crystalline or

amorphous regions of the polymer matrix. By varying the % crystallinity of the test film and conducting permeability studies with binary vapor mixtures, a better understanding of how % crystallinity influences the co-permeant effect of limonene may be gleaned. The proposed studies can all be carried out using the dynamic purge and trap/thermal desorption procedure coupled with the MAS2000TM Permeability Test System, as described in the present study. The data from these studies might help develop or test a mathematical model to accurately predict the permeation characteristics of multi-component organic vapor mixtures through polymer based packages. Such a model, or actual experimental data, would help in the design of an aroma barrier package system for packaging a product whose quality is based solely upon maintaining its original aroma profile.

APPENDICES

Appendix A

Gas Chromatograph Calibration Procedure

A stock solution of 500 ppm (v/v) is prepared by dissolving 5 μ l of d-limonene, ethyl butyrate, and ethyl acetate into a 10 ml volumetric flask filled with carbon tetrachloride to make 10 ml of 500 ppm stock solution. Standard solutions of ethyl butyrate and d-limonene, with concentrations of 20, 40, 100, and 200 ppm (v/v), were prepared by diluting from the stock solution according to the following table.

Table 20. The solution of ethyl butyrate and d-limonene in CCl₄

| Conc, ppm (v/v) | #ml stock solution d-limonene | #ml stock solution ethyl butyrate | #ml CCl ₄ | Total volume |
|-----------------|-------------------------------|-----------------------------------|----------------------|--------------|
| 20 | .4 | .4 | 9.2 | 10 |
| 40 | .8 | .8 | 8.4 | 10 |
| 100 | 2 | 2 | 6 | 10 |
| 200 | 4 | 4 | 2 | 10 |

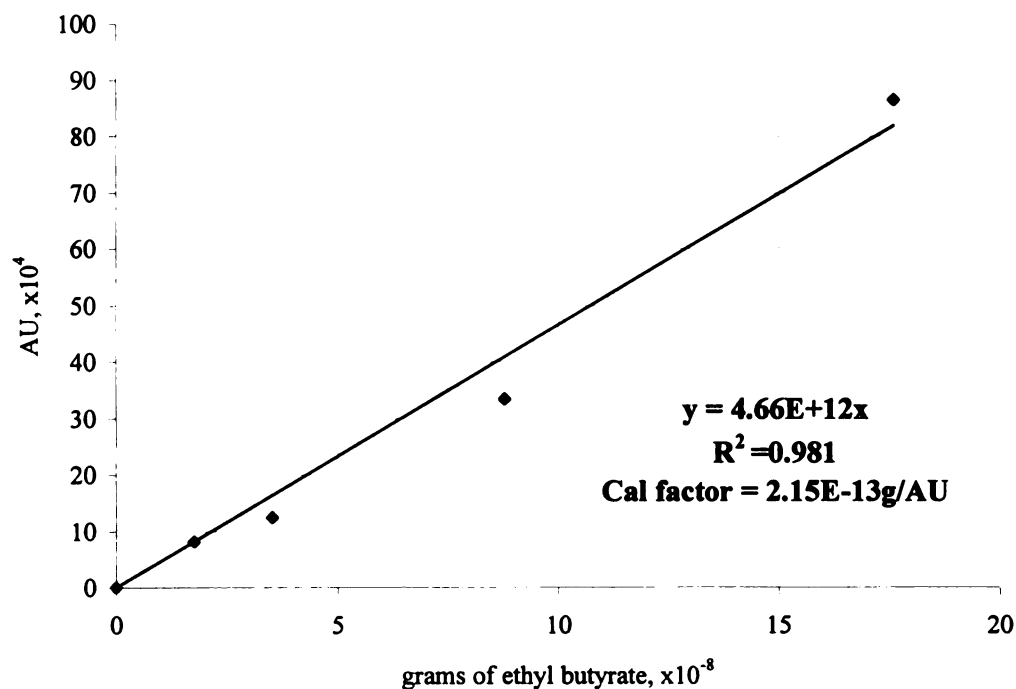
The ethyl acetate solution was separately prepared by diluting from its stock solution in a similar fashion.

Table 21. Calibration Data of Ethyl Butyrate and d-limonene by Gas chromatograph.

| Conc, (v/v) | grams of ethyl butyrate, $\times 10^{-8}$ | area response, AU, $\times 10^4$ | grams of d-limonene, $\times 10^{-8}$ | area response, Au, $\times 10^5$ |
|-------------|-------------------------------------------|----------------------------------|---------------------------------------|----------------------------------|
| 20 | 1.8 | 8.2 | 1.7 | 1.4 |
| 40 | 3.5 | 12.5 | 3.4 | 2.5 |
| 100 | 8.8 | 33.4 | 8.4 | 6.4 |
| 200 | 17.6 | 86.5 | 16.8 | 14.8 |

Table 22. Calibration Data of Ethyl Acetate by Gas Chromatograph.

| Con, (v/v) | grams of ethyl acetate, $\times 10^{-8}$ | Area response, AU, $\times 10^4$ |
|------------|---------------------------------------------|-------------------------------------|
| 20 | 1.8 | 9.8 |
| 40 | 3.6 | 16.7 |
| 100 | 9.0 | 36.7 |
| 200 | 18.0 | 82.7 |

**Figure 17. Calibration curve of ethyl butyrate for setting vapor activity.**

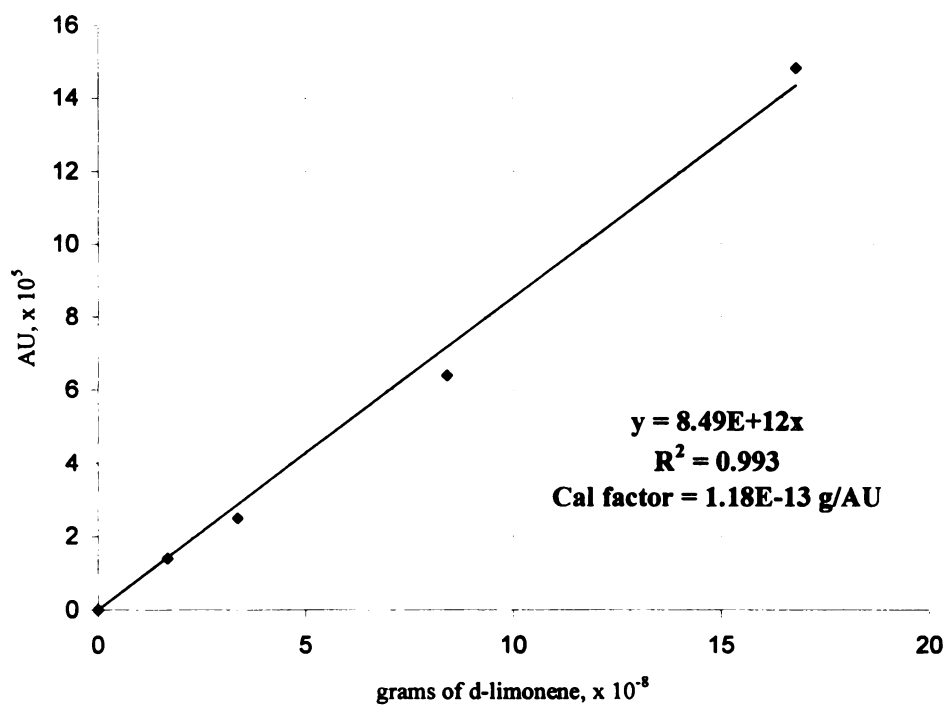


Figure 18. Calibration curve of d-limonene for setting vapor activity

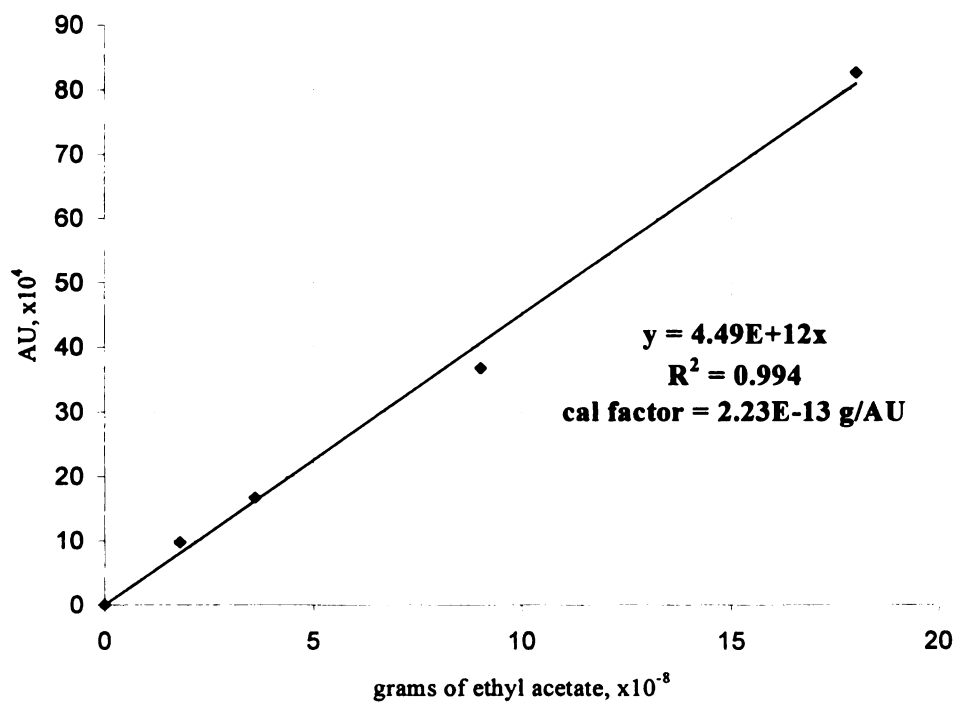


Figure 19. Calibration curve of ethyl acetate for setting vapor activity.

Appendix B

Dynamic Purge and Trap/Thermal Desorption Calibration Procedure

The same solutions prepared for vapor activity setting were used to generate calibration curves for the desorption thermal/desorption procedure. The following tables show the calibration profile for each test compound.

Table 23. Calibration data of ethyl butyrate and d-limonene for dynamic purge and trap/thermal desorption procedure.

| Conc, (v/v) | grams of ethyl butyrate, $\times 10^{-8}$ | area response, AU, $\times 10^5$ | grams of d-limonene, $\times 10^{-8}$ | area response, Au, $\times 10^5$ |
|-------------|-------------------------------------------|----------------------------------|---------------------------------------|----------------------------------|
| 40 | 3.5 | 3.0 | 3.4 | 6.0 |
| 100 | 8.8 | 8.2 | 8.4 | 15.1 |
| 200 | 17.6 | 15.5 | 16.8 | 31.8 |
| 500 | 44.0 | 38.6 | 42.1 | 80.2 |

Table 24. Calibration data of ethyl acetate for dynamic purge and trap/thermal desorption procedure.

| Con, (v/v) | grams of ethyl acetate, $\times 10^{-8}$ | Area response, AU, $\times 10^5$ |
|------------|------------------------------------------|----------------------------------|
| 20 | 1.8 | 1.4 |
| 40 | 3.6 | 2.4 |
| 100 | 9.0 | 6.2 |
| 200 | 18.0 | 10.1 |

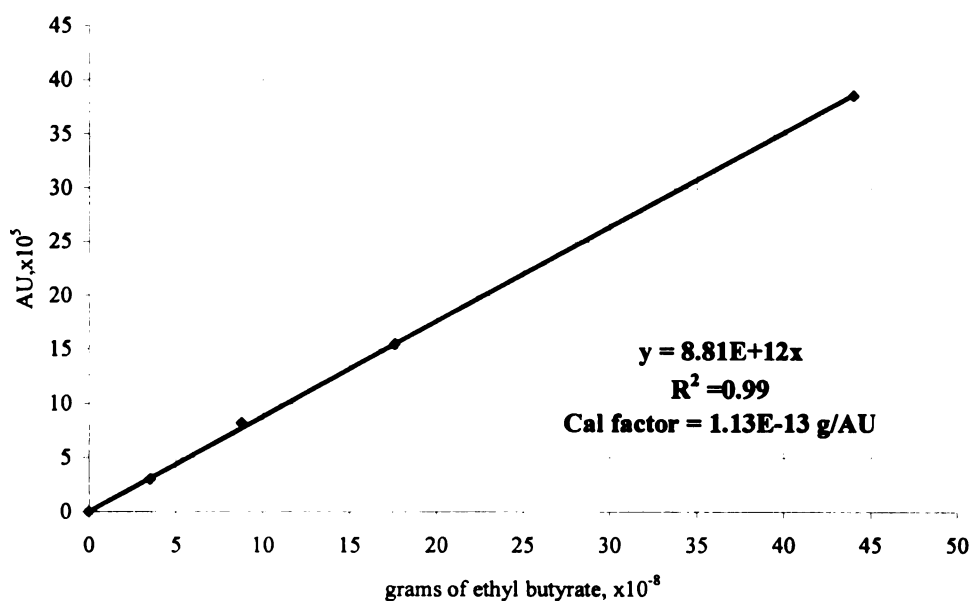


Figure 20. Calibration curve of ethyl butyrate for dynamic purge and trap/thermal desorption procedure.

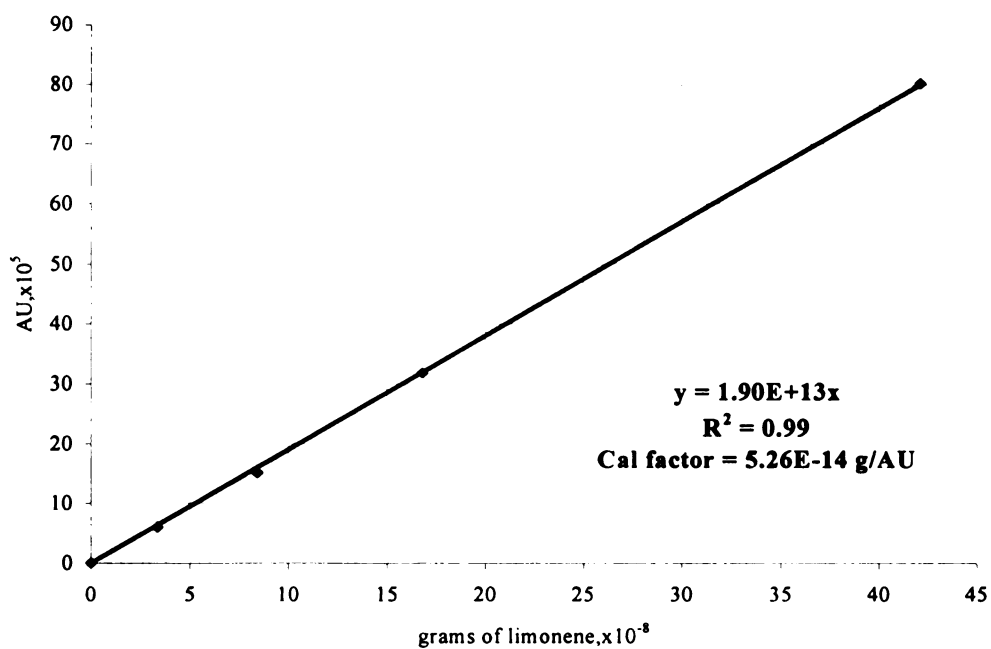


Figure 21. Calibration curve of d-limonene for dynamic purge and trap/thermal desorption procedure.

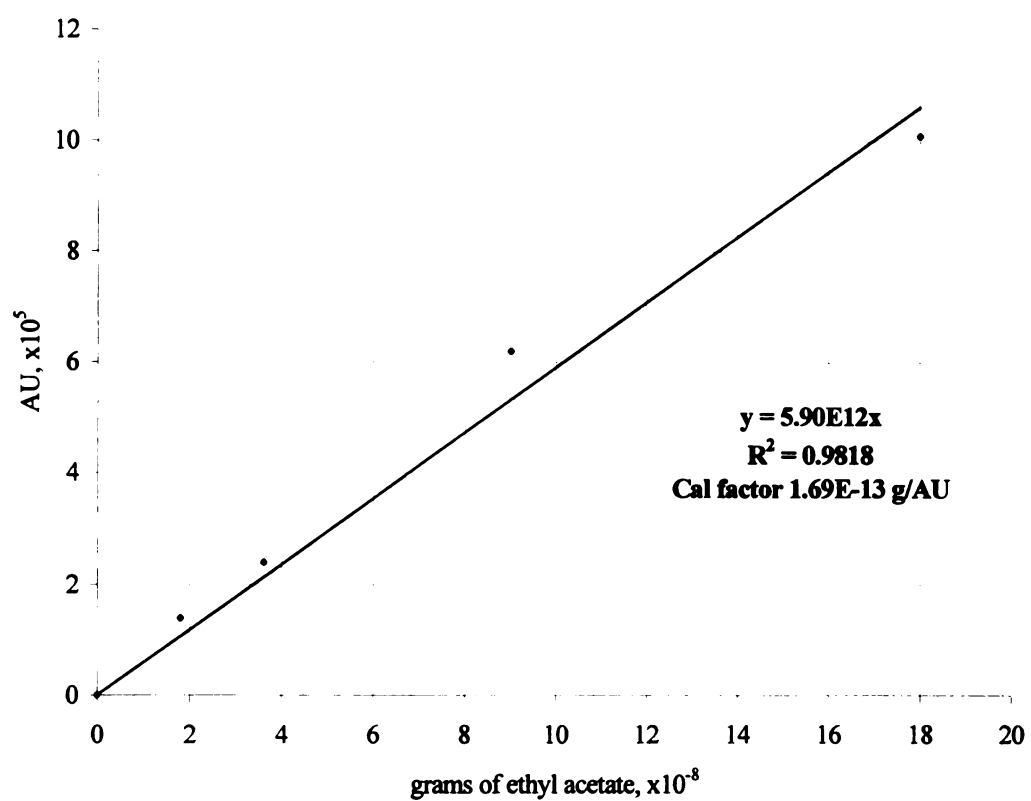


Figure 22. Calibration curve of ethyl acetate for dynamic purge and trap/thermal desorption procedure.

Appendix C

Calibration Curve of Carrier Gas Flow Rate Versus Permeant Vapor Activity

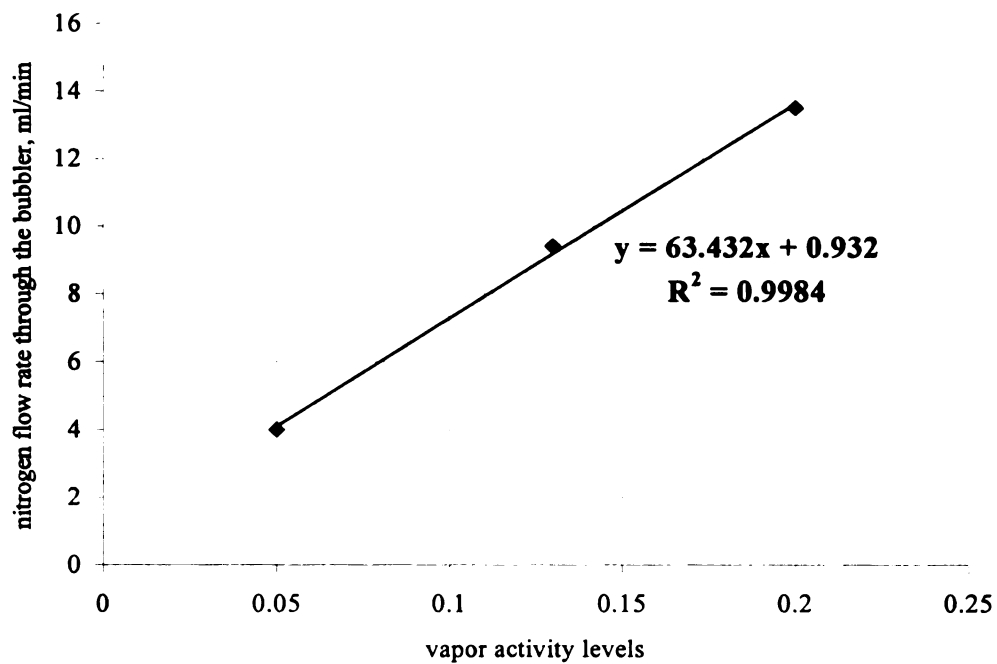


Figure 23. Calibration curve of carrier gas flow rate versus limonene vapor activities

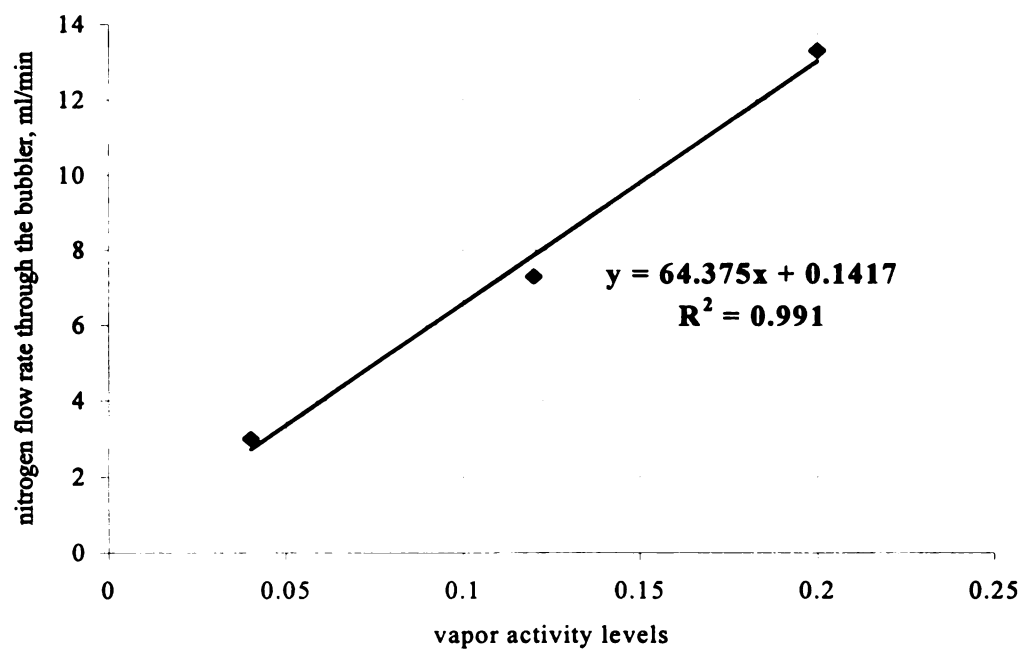


Figure 24. Calibration curve of carrier gas flow rate versus ethyl butyrate and ethyl acetate vapor activities

Appendix D

Method of Calculating $l^2/4Dt$ for each Value of $(\Delta M/\Delta t)_t/(\Delta M/\Delta t)_\infty$ from Equation 32

Equation 32 can be written as

$$A = X^{1/2} \exp(-X)$$

where

$$A = \frac{\sqrt{\pi}}{4} \frac{\left(\frac{\Delta M}{\Delta t} \right)_t}{\left(\frac{\Delta M}{\Delta t} \right)_\infty}$$

And

$$X = \frac{l^2}{4Dt}$$

To solve for value of X for each value of $(\Delta M/\Delta t)_t/(\Delta M/\Delta t)_\infty$ a Newton-Rawson method was employed. Equation 32 can be rewritten as

$$G = X^{1/2} \exp(-X) - A$$

With G being equal to zero, the iteration process is described by

$$X^{(k+1)} = X^{(k)} - \frac{G(k)}{\exp[-X^{(k)}] \left\{ \frac{1}{2} [X^{(k)}]^{-1/2} - [X^{(k)}]^{1/2} \right\}}$$

where $x^{(k+1)}$ is the k+1 iteration step for x value.

Appendix E

Statistical Analysis of P, D, and S as a Function of Permeant Vapor Activity

ANOVA for d-limonene permeability coefficient through OPP (50°C) as a function of vapor activity.

| Source | DF | SS | MS | F | P |
|---------|----|------|-------|---------|---------|
| Between | 3 | 1.8 | 0.6 | 7.00101 | 0.04535 |
| Error | 4 | 0.34 | 0.085 | | |
| Total | 7 | 2.1 | | | |

- MS and SS $\times 10^{-30}$

ANOVA for d-limonene diffusion coefficient through OPP (50°C) as a function of vapor activity.

| Source | DF | SS | MS | F | P |
|---------|----|------|------|---------|---------|
| Between | 3 | 83.0 | 28.0 | 11.2532 | 0.02028 |
| Error | 4 | 9.9 | 2.5 | | |
| Total | 7 | 93.0 | | | |

- MS and SS $\times 10^{-30}$

ANOVA for d-limonene solubility coefficient through OPP (50°C) as a function of vapor activity.

| Source | DF | SS | MS | F | P |
|---------|----|---------|---------|---------|---------|
| Between | 3 | 0.00042 | 0.00014 | 3.56415 | 0.12564 |
| Error | 4 | 0.00016 | 0.00004 | | |
| Total | 7 | 0.00058 | | | |

ANOVA for ethyl butyrate permeability coefficient through OPP (50°C) as a function of vapor activity.

| Source | DF | SS | MS | F | P |
|---------|----|----------|--------|---------|---------|
| Between | 2 | 0.15167 | 0.0758 | 4.22635 | 0.13407 |
| Error | 3 | 0.053831 | 0.0179 | | |
| Total | 5 | 0.2055 | | | |

- MS and SS $\times 10^{-30}$

ANOVA for ethyl butyrate diffusion coefficient through OPP (50°C) as a function of vapor activity.

| Source | DF | SS | MS | F | P |
|---------|----|-------|------|----|---------|
| Between | 2 | 625 | 312 | 75 | 0.00275 |
| Error | 3 | 12.5 | 4.17 | | |
| Total | 5 | 637.5 | | | |

- MS and SS $\times 10^{-30}$

ANOVA for ethyl butyrate solubility coefficient through OPP (50°C) as a function of vapor activity.

| Source | DF | SS | MS | F | P |
|---------|----|--------|-------|---------|---------|
| Between | 2 | 4.5946 | 2.3 | 6.61576 | 0.07946 |
| Error | 3 | 1.0417 | 0.347 | | |
| Total | 5 | 5.6364 | | | |

- MS and SS $\times 10^{-6}$

ANOVA for ethyl acetate permeability coefficient through OPP (50°C) as a function of vapor activity.

| Source | DF | SS | MS | F | P |
|---------|----|---------|---------|---------|---------|
| Between | 2 | 0.0472 | 0.024 | 30.6257 | 0.01026 |
| Error | 3 | 0.00234 | 0.00078 | | |
| Total | 5 | 0.0495 | | | |

- MS and SS $\times 10^{-30}$

ANOVA for ethyl acetate diffusion coefficient through OPP (50°C) as a function of vapor activity.

| Source | DF | SS | MS | F | P |
|---------|----|-------|-------|---------|--------|
| Between | 2 | 1.54 | 0.77 | 13.7985 | 0.0307 |
| Error | 3 | 0.168 | 0.056 | | |
| Total | 5 | 1.71 | | | |

- MS and SS $\times 10^{-26}$

ANOVA for ethyl acetate solubility coefficient through OPP (50°C) as a function of vapor activity.

| Source | DF | SS | MS | F | P |
|---------|----|-------|------|---------|---------|
| Between | 2 | 4.83 | 2.4 | 8.27714 | 0.06009 |
| Error | 3 | 0.876 | 0.29 | | |

Total 5 5.71

- MS and SS $\times 10^{-8}$

ANOVA for d-limonene permance through PVdC coated OPP (60°C) as a function of vapor activity.

| Source | DF | SS | MS | F | P |
|---------|----|-----|------|---------|---------|
| Between | 2 | 15 | 7.7 | 15.8519 | 0.02542 |
| Error | 3 | 1.5 | 0.49 | | |
| Total | 5 | 17 | | | |

- MS and SS $\times 10^{-26}$

ANOVA for d-limonene diffusion coefficient through PVdC coated OPP (60°C) as a function of vapor activity.

| Source | DF | SS | MS | F | P |
|---------|----|-----|-----|---------|---------|
| Between | 2 | 2.6 | 1.3 | 1.15926 | 0.42364 |
| Error | 3 | 3.4 | 1.1 | | |
| Total | 5 | 6 | | | |

- MS and SS $\times 10^{-31}$

ANOVA for d-limonene solubility coefficient through PVdC coated OPP (60°C) as a function of vapor activity.

| Source | DF | SS | MS | F | P |
|---------|----|------|------|---------|---------|
| Between | 2 | 4.4 | 2.2 | 13.8897 | 0.03043 |
| Error | 3 | 0.48 | 0.16 | | |
| Total | 5 | 4.9 | | | |

- MS and SS $\times 10^{-6}$

ANOVA for ethyl butyrate permance through PVdC coated OPP (60°C) as a function of vapor activity.

| Source | DF | SS | MS | F | P |
|---------|----|-------|-------|---------|---------|
| Between | 2 | 4.53 | 2.27 | 16.7511 | 0.02356 |
| Error | 3 | 0.406 | 0.135 | | |
| Total | 5 | 4.94 | | | |

- MS and SS $\times 10^{-26}$

ANOVA for ethyl butyrate diffusion coefficient through PVdC coated OPP (60°C) as a function of vapor activity.

| Source | DF | SS | MS | F | P |
|---------|----|------|-------|---------|---------|
| Between | 2 | 3.75 | 1.88 | 2.02201 | 0.27794 |
| Error | 3 | 2.78 | 0.928 | | |
| Total | 5 | 6.53 | | | |

- MS and SS $\times 10^{-30}$

**ANOVA for ethyl butyrate solubility coefficient through PVdC coated OPP (60°C)
as a function of vapor activity.**

| Source | DF | SS | MS | F | P |
|---------|----|------|-------|---------|---------|
| Between | 2 | 1.14 | 0.572 | 1.56024 | 0.34317 |
| Error | 3 | 1.1 | 0.366 | | |
| Total | 5 | 2.24 | | | |

- MS and SS $\times 10^{-7}$

Appendix F

Statistical Analysis of Binary Mixture Permeability Studies

ANOVA for d-limonene permeability coefficient at $a=0.3$ vs d-limonene permeability coefficient in the binary mixture with ethyl butyrate (OPP film)

| Source | DF | SS | MS | F | P |
|---------|----|--------|--------|------|-------|
| Between | 2 | 0.1416 | 0.0708 | 2.66 | 0.216 |
| Error | 3 | 0.0799 | 0.0266 | | |
| Total | 5 | 0.2215 | | | |

- MS and SS $\times 10^{-30}$

ANOVA for d-limonene permeability coefficient at $a=0.2$ in single vapor vs d-limonene permeability coefficient in the binary mixture with ethyl butyrate and in the binary mixture with ethyl acetate (OPP film)

| Source | DF | SS | MS | F | P |
|---------|----|--------|--------|------|-------|
| Between | 6 | 1.6188 | 0.2698 | 3.15 | 0.080 |
| Error | 7 | 0.6003 | 0.0858 | | |
| Total | 13 | 2.2191 | | | |

- SS and MS value $\times 10^{-30}$

ANOVA for d-limonene permeability coefficient at $a=0.13$ vs d-limonene permeability coefficient in the binary mixture with ethyl butyrate (OPP film)

| Source | DF | SS | MS | F | P |
|---------|----|--------|--------|------|-------|
| Between | 3 | 0.2277 | 0.0759 | 2.63 | 0.186 |
| Error | 4 | 0.1154 | 0.0288 | | |
| Total | 7 | 0.3431 | | | |

- SS and MS value $\times 10^{-30}$

ANOVA for d-limonene permeability coefficient at $a=0.05$ vs d-limonene permeability coefficient in the binary mixture with ethyl butyrate (OPP film)

| Source | DF | SS | MS | F | P |
|---------|----|--------|--------|------|-------|
| Between | 3 | 0.5180 | 0.1727 | 2.93 | 0.163 |

| | | | |
|-------|---|--------|--------|
| Error | 4 | 0.2355 | 0.0589 |
| Total | 7 | 0.7535 | |

• SS and MS value $\times 10^{-30}$

ANOVA for ethyl butyrate permeability coefficient at $\alpha=0.2$ vs ethyl butyrate permeability coefficient in the binary mixture with d-limonene (OPP film)

| Source | DF | SS | MS | F | P |
|---------|----|--------|--------|------|-------|
| Between | 3 | 0.2127 | 0.0709 | 0.87 | 0.526 |
| Error | 4 | 0.3254 | 0.0814 | | |
| Total | 7 | 0.5382 | | | |

• SS and MS value $\times 10^{-30}$

ANOVA for ethyl butyrate permeability coefficient at $\alpha=0.12$ vs ethyl butyrate permeability coefficient in the binary mixture with d-limonene (OPP film)

| Source | DF | SS | MS | F | P |
|---------|----|--------|--------|------|-------|
| Between | 4 | 0.2162 | 0.0541 | 5.25 | 0.049 |
| Error | 5 | 0.0514 | 0.0103 | | |
| Total | 9 | 0.2677 | | | |

• SS and MS value $\times 10^{-30}$

Comparison Mean Difference

Critical Values = 0.348×10^{-15}

| Pure ethyl butyrate Vapor activity | Ethyl butyrate in binary mixture with d-limonene vapor activity of | Permeability coefficient difference $\times 10^{-15}$ | Dunnett's test |
|---------------------------------------|-----------------------------------------------------------------------------|-------------------------------------------------------------|----------------|
| 0.12 | 0.3 | 0.3900 | * |
| 0.12 | 0.2 | 0.1400 | |
| 0.12 | 0.13 | -0.0100 | |
| 0.12 | 0.05 | 0.0600 | |

* Significant at 95% CI

ANOVA for ethyl butyrate permeability coefficient at $\alpha=0.04$ vs ethyl butyrate permeability coefficient in the binary mixture with d-limonene (OPP film)

| Source | DF | SS | MS | F | P |
|---------|----|--------|--------|------|-------|
| Between | 4 | 0.4972 | 0.1243 | 2.96 | 0.132 |
| Error | 5 | 0.2097 | 0.0419 | | |
| Total | 9 | 0.7068 | | | |

- SS and MS value $\times 10^{-30}$

ANOVA for d-limonene permeance at $\alpha=0.2$ vs d-limonene permeance in the binary mixture with ethyl butyrate (PVdC coated OPP film)

| Source | DF | SS | MS | F | P |
|---------|----|--------|--------|------|-------|
| Between | 3 | 4.3398 | 1.4466 | 4.45 | 0.092 |
| Error | 4 | 1.2994 | 3.2485 | | |
| Total | 7 | 5.6392 | | | |

- SS and MS value $\times 10^{-26}$

ANOVA for d-limonene permeance at $\alpha=0.13$ vs d-limonene permeance in the binary mixture with ethyl butyrate (PVdC coated OPP film)

Analysis of Variance for .13b

| Source | DF | SS | MS | F | P |
|---------|----|-------|-------|------|-------|
| Between | 3 | 0.938 | 0.313 | 1.43 | 0.359 |
| Error | 4 | 0.876 | 0.219 | | |
| Total | 7 | 1.815 | | | |

- SS and MS value $\times 10^{-26}$

ANOVA for ethyl butyrate permeance at $\alpha=0.21$ vs ethyl butyrate permeance in the binary mixture with d-limonene (PVdC coated OPP film)

| Source | DF | SS | MS | F | P |
|---------|----|----------|----------|-------|-------|
| Between | 2 | 0.064300 | 0.032150 | 91.86 | 0.002 |
| Error | 3 | 0.001050 | 0.000350 | | |
| Total | 5 | 0.065350 | | | |

- SS and MS $\times 10^{-24}$

Comparison Mean Difference

Critical Values = 0.387×10^{-13}

| Pure ethyl butyrate Vapor activity | Ethyl butyrate in binary mixture with d-limonene vapor activity of | Permeance difference $\times 10^{-12}$ | Dunnnett's test |
|---------------------------------------|-----------------------------------------------------------------------------|-------------------------------------------|-----------------|
| 0.21 | 0.2 | .24 | * |
| 0.21 | 0.13 | .34 | * |

* Significant at 95% CI

ANOVA for ethyl butyrate permeance at $a=0.12$ vs ethyl butyrate permeance in the binary mixture with d-limonene (PVdC coated OPP film)

| Source | DF | SS | MS | F | P |
|---------|----|--------|--------|------|-------|
| Between | 2 | 0.0119 | 0.0060 | 0.52 | 0.640 |
| Error | 3 | 0.0344 | 0.0115 | | |
| Total | 5 | 0.0463 | | | |

• SS and MS $\times 10^{-24}$

ANOVA for ethyl butyrate permeance at $a=0.04$ vs ethyl butyrate permeance in the binary mixture with d-limonene (PVdC coated OPP film)

| Source | DF | SS | MS | F | P |
|---------|----|--------|--------|------|-------|
| Between | 2 | 0.0192 | 0.0096 | 0.80 | 0.528 |
| Error | 3 | 0.0362 | 0.0121 | | |
| Total | 5 | 0.0554 | | | |

• SS and MS $\times 10^{-24}$

Two sample t-test for comparing ethyl acetate permeability coefficient in pure vapor vs the permeability coefficient in binary mixture with limonene vapor activity level $a=0.2$.

Comparing Mean Difference

| Pure ethyl acetate Vapor activity | Ethyl acetate in binary mixture with d-limonene vapor activity of | $ t_o $ | p-value | Significant at 95% confidence level |
|--------------------------------------|----------------------------------------------------------------------------|---------|---------|----------------------------------------------|
| 0.30 | 0.20 | 8.83 | 0.013 | * |
| 0.14 | 0.20 | 6.12 | 0.026 | * |
| 0.04 | 0.2 | 0.51 | 0.66 | |

BIBLIOGRAPHY

BIBLIOGRAPHY

Adamson, A.W., and Gast, A.P., Physical chemistry of Surfaces. 6th Edition, John Wiley & Sons, Inc. (1997).

Baner, A.L., Hernandez, R.J., Jayaraman, K., and Giacin, J.R., "Isostatic and quasi-isostatic methods for determining the permeability of organic vapors through barrier membranes". In: Current Technologies in Flexible Packaging, ASTM STP 912 (1986).

Barr, C., A comparison of solubility coefficient values determined by gravimetric and isostatic permeability techniques. M.S. Thesis. Michigan State University, East Lansing, MI (1996).

Barrer, R. M., and Skirrow, G., J. Polym. Sci. 3: 564 (1948).

Berens, A.R., and Hopfenberg, H.B., "Diffusion of organic vapors at low concentrations in glassy PVC, polystyrene, and PMMA". Journal of Membrane Science. 10:283 (1982).

Berens, A. R.; Huvar, G.S.; Korsmeyer, R.W., U.S. Patent 4 820 752, April 11, (1989).

Berens, A. R., "Transport of plasticizing penetrants in glassy polymers". Ed. Koros, W. J., In: Barrier Polymers and Structures, Chapter 4, American Chemical Society, Washington, DC (1990).

Brandrup, J. Ed., Polymer Handbook. 2nd Edition, John Wiley & Sons, Inc. (1975).

Chapra, S.C. and Canale, R.P., Numerical Methods for Engineers, McGraw-Hill Book Company (1985).

Chang, Y., Organic vapor permeability of high barrier polymer membranes by a dynamic purge and trap/thermal desorption procedure. M.S. Thesis. Michigan State University, East Lansing, MI (1996).

Choy, C. L., Leung, W. P., and Ma, T.L., "Sorption and diffusion of toluene in highly oriented polypropylene". Journal of Polymer Science, Polymer Physics Edition. 22: 707-719 (1984).

- Crank, J. *The Mathematics of Diffusion*. 2nd Edition, Claredon Press, Oxford, England (1975).
- Crank, J. and Park, G.S., *Diffusion in Polymers*, Academic Press, New York, NY (1968).
- Crank, J., and Park, G. S., *Trans. Faraday Soc.* 47: 1072 (1951).
- DeLassus, P. T., "Transport of unusual molecules in polymer films". *Polymers, Laminations, and Coating Conference*. 445-449 (1985).
- DeLassus, P.T., Tou, J.C, Babinec, M.A., Rulk, D.C., Karp, DB.K., Howell, B.A., *Food and Packaging Interactions*, ACS Symposium Series 365, Ed J.H. Hotchkiss, Chapter 2:11 (1988).
- Drechsel, P., Hoard, J.L., and Long, F. A. J., *Polym. Sci.* 10: 241 (1953).
- Fick, A., *Annln Phys.* 110: 59 (1855).
- Frisch, H.L., *J. Polym. Sci. B.* 2: 13 (1965).
- Fujita, H., "Organic vapors above the glass transition temperature". Ed. Crank, J., and Park, G.S., In: *Diffusion in Polymers*, Chapter 3, Academic Press, New York, NY (1968).
- Fujita, H., "Diffusion in polymer-diluent systems". *Fortsch-Hochpolym-Forsch*, 3:1 (1961).
- Gilbert, S.G., Hatzidimitriu, e., Lai, C., and Passy, N., "Studies on barrier properties of polymeric films to various organic aromatic vapors". *Instrumental Analysis of Food*, 1:405 (1983).
- Halek, G. W. and Luttmann, J. P., Sorption behavior of citrus-flavor compounds in polyethylenes and polypropylenes: Effects of permeant functional groups and polymer structure. In: "Food and Packaging Interactions", Chapter 12, American Chemical Society, Washington, D.C. 212-226 (1991).
- Hensley, T. M., The permeability of binary organic vapour mixtures through a biaxially oriented polypropylene film. M.S. Thesis. Michigan State University, East Lansing, MI (1991).
- Hernandex, R.J., Giacin, J.R., and Baner, A.L., "The evaluation of the aroma barrier properties of polymer films". *J. of Plastic Film and Sheeting*. 2(5): 187 (1986).
- Hotchkiss, J.H., "An overview of food and packaging interactions". In: *Food and Packaging Interactions*, Chapter 1, American Chemical Society, Washington, DC (1988).

- Huang, R.Y.M., Lin, V.J.C., "Separation of liquid mixtures by using polymer membranes. I. Permeation of binary organic liquid mixtures through polyethylene". *Journal of Applied Polymer Science*. 12:2615 (1968).
- Kishimoto, A. and Matsumoto, K. J., *Phys.Chem.* 63: 1529 (1959).
- Koros, W. J., and Story, B.J., "Comparison of three models for permeation of CO₂/CH₄ mixtures in poly(phenylene oxide)". *Journal of Polymer Science: Part B: Polymer Physics*. (28) 1927-1948 (1989).
- Koros, W. J., "Barrier polymers and structures: Overview". In: *Barrier Polymers and Structures*, Chapter 4, American Chemical Society, Washington, DC 1990.
- Koszinowski, J., and Piringer, O., "Food/Package compatibility and migration". *Journal of Plastic Film and Sheeting*, 3:96 (1987).
- Li, N.N., Long, R.B., Henley, E.J., "Membrane separation processes". *Industrial and Engineering Chemistry*. 57(3):18 (1965).
- Mandelkern, L., and Long, F. A. J., *Polym. Sci.* 6: 457 (1951).
- Meares, P., *J. Am. Chem. Soc.* 76: 3415 (1954).
- Meares, P., *Trans. Faraday Soc.* 54: 40 (1958).
- Mears, P., *J. Polym. Sci.* 27: 391 (1958a).
- Mears, P., "Polymers: structure and bulk properties". Van Nostrand & Co. LTD, London (1965).
- Meyer, F.A., Roger, C., Stannett, V., and Szwarc, M., "Studies in the gas and vapor permeability of plastic films and coated papers, part III.J. The permeation of mixed vapor and gases". *TAPPI* 40: 142 (1957).
- Michaels, A.S., and Parker, R.B., *J. Polym. Sci.* 41: 53 (1959).
- Michaels, A.S., and Bixler, H. J., *J. Polym. Sci.* 50: 393 (1961).
- Michaels, A.S., and Vieth, W.R., and Barrie, J.A., *J. Polymer Sci.* 13: 1, 13 (1963).
- Michelson, R.L., Roder, M.M., Berardinelli, S.P., "Permeation of chemical protective clothing by three binary solvent mixtures". National Institute for Occupational Safety and Health Division of Safety Research. 944 Chestnut Ridge Road, Morgantown, WV 26505. (1985).
- Newns, A.C., *Trans. Faraday Soc.* 52: 1533 (1956).

Niebergall, W., Jumeid, A., and Blochl, W., "The aroma permeability of packaging films and its determination by means of a newly developed measuring apparatus". *Lebensm-Wiss U. Technol.* 11(1):1 (1978).

Nielson, T.J., Jagerstad, I.M., Oste, R.E., and Wesslen, B.O., "Comparative absorption of low molecular aroma compounds into commonly used food packaging polymer films". *Journal of Food Science.* 57(2): 490 (1992).

Nielson, T. J., and Gicain J. R., "The sorption of limonene/ethyl acetate binary vapour mixtures by a biaxial oriented polypropylene film". *Packaging Technology and Science.* 7, 247-258 (1994).

Odani, H., Hayashi, J., and Tamura M., *Bull. Chem. Soc. Jpn.* 34: 817 (1961).

Pasternack, R.A., Schimsheimer, J.F., Heller, J., "A dynamic approach to diffusion and permeation measurements". *J. Polymer Sci. Part A-2.* 8: 467 (1970).

Perry's Chemical Engineers' Handbook, 6th edition, McGraw-Hill (1984)

Pye, D.G., Hoehn, H.H., Panar, M., "Measurement of gas permeability of polymers. II Apparatus for determination of permeabilities of mixed gases and vapors". *Journal of Applied Polymer Science.* 20: 287 (1976).

Rogers, C.E., Stannet, W., and Szwarc, M., "The sorption, diffusion and permeation of organic vapors in polyethylene". *J. Polymer Sci.* 45: 61 (1960).

Rogers, C.E., "Permeation of gases and vapours in polymers". Ed. Comyn, J., In: *Polymer Permeability*, Chapter 2, Elsevier Applied Science Publishers, N.Y. (1985).

Rohan, T.A., "What constitutes flavour?" *Food Manuf.*, 45: 42-44,66 (1970).

Rudin, A., "Polymer mixtures". In: *The Elements of Polymer Science and Engineering: an Introductory Text for Engineers and Chemists*, Chapter 12, Academic Press, Inc., California, (1982).

Salame, M., "The use of barrier polymers in food and beverage packaging". *Journal of Plastic Film & Sheeting*, 2: 321-334 (1986).

Salame, M., *Barrier Materials: An In-Depth Review and Comparative Analysis*, Polysultants Co., CT (1996).

Shimoda, M., Matsui, T., and Osajima, Y., "Effect of the number of carbon atoms of flavor compounds on diffusion, permeation, and sorption with polyethylene films". *Nippon Shokuhin Kogyo Gakkaishi*, 34 (8): 535-539 (1987).

Stannett, V., "Simple gases". Ed. Crank, J. and Park, G. S., In: Diffusion in Polymers, Chapter 2, Academic Press Inc., New York, NY (1968).

Stannett, V., Hopfenberg, H.B., and Petropoulos, J.H., "Diffusion in Polymers" Ed. Baum, C.E., In: Macromolecular Science, Chapter 8, 329 (1972).

Stern, S.A., and Trohalaki, S., "Fundamentals of gas diffusion in rubbery and glassy polymers". Ed. Koros, W. J., In: Barrier Polymers and Structures, Chapter 2, American Chemical Society, Washington, DC 1990.

Strandburg, G., DeLassus, P.T., and Howell, B.A., "Thermodynamics of permeation of flavors in polymers: prediction of solubility coefficients". In: Food and Packaging Interactions, Chapter 12, American Chemical Society, Washington, D.C. (1991).

Suwandi, M.S. and Stern, S.A., "Transport of heavy organic vapors through silicone rubber". Journal of Polymer Science. 11: 663-681 (1973).

Strandburg, G., DeLassus, P.T., and Howell, B.A., "Thermodynamics of permeation of flavors in polymers: prediction of solubility coefficients". In: Food and Packaging Interactions, Chapter 12, American Chemical Society, Washington, D.C. 133-148 (1991).

Van Amerongen, G. J., J. Polym. Sci. 5: 307 (1950).

Van Amerongen, G.J., J. Rubb. Chem. Technol. 37: 1065 (1964).

Van Krevelen, D. W., "Permeation of polymers; the diffusive transport of gases, vapours and liquids in polymers", In: Properties of Polymers, Chapter 18, Elsevier Scientific Publishing Inc., Amsterdam (1976).

Weinberg, D.S., "Polymer liquid interactions. 2. Permeation of multicomponent liquids through barrier polymer films". Coatings and Plastic Preprints. 37(1): 173 (1976).

Weinkauf, D.H. and Paul, D.R., Effects of structural order on barrier properties, Ed. Koros, W. J., In: Barrier Polymers and Structures, Chapter 4, American Chemical Society, Washington, DC 1990.

Ziegel, K.D., Frensdorff, H.K. and Blair, D. E., "Measurement of Hydrogen Isotope Transport in Poly(Vinyl Fluoride) Films by Permeation Rate Method". J. Polymer Sci., Part A-2, 7: 809 (1969).

Zobel, M.G.R., "Measurement of odour permeability of polypropylene packaging films at low odourant levels". Polymer Testing. 33:133 (1982).

MICHIGAN STATE UNIV. LIBRARIES



31293017120043